SANDIA REPORT

SAND2018-13984
Unlimited Release
Printed December 2018

Uncertainty Analysis of Consequence Management (CM) Data Products: Extended Analyses

Lainy D. Cochran, Aubrey C. Eckert-Gallup, Brian D. Hunt, Terry D. Kraus, Sean D. Fournier, Elliott J. Leonard, Mark B. Allen, Matthew D. Simpson, Jessica L. Osuna, Colin E. Okada

Prepared by
Sandia National Laboratories
Albuquerque, New Mexico 87185 and Livermore, California 94550

Sandia National Laboratories is a multimission laboratory managed and operated by National Technology and Engineering Solutions of Sandia, LLC, a wholly owned subsidiary of Honeywell International, Inc., for the U.S. Department of Energy's National Nuclear Security Administration under contract DE-NA0003525.

Issued by Sandia National Laboratories, operated for the United States Department of Energy by National Technology and Engineering Solutions of Sandia, LLC.

Available to DOE and DOE contractors from
U.S. Department of Energy
Office of Scientific and Technical Information
P.O. Box 62
Oak Ridge, TN 37831

Telephone: (865) 576-8401
Facsimile: (865) 576-5728
E-Mail: reports@osti.gov
Online ordering: http://www.osti.gov/scitech

Available to the public from
U.S. Department of Commerce
National Technical Information Service
5301 Shawnee Rd
Alexandria, VA 22312

Telephone: (800) 553-6847
Facsimile: (703) 605-6900
E-Mail: orders@ntis.gov
Online order: https://classic.ntis.gov/help/order-methods/

SAND2018-13984
Printed December 2018
Unlimited Release

Uncertainty Analysis of Consequence Management (CM) Data Products: Extended Analyses

Lainy D. Cochran[1], Aubrey C. Eckert-Gallup[2], Brian D. Hunt[1], Terry D. Kraus[1], Sean D. Fournier[3], Elliott J. Leonard[3], Mark B. Allen[3]

Departments 6631[1], 1544[2], and 0631[3]
Sandia National Laboratories
P.O. Box 5800
Albuquerque, New Mexico 87185-0748

Matthew D. Simpson and Jessica L. Osuna

Lawrence Livermore National Laboratory
National Atmospheric Release Advisory Center
P.O. Box 808, L-103
Livermore, CA 94551

Colin E. Okada

Mission Support and Test Services, Remote Sensing Laboratory
Contractor to US Department of Energy
P.O. Box 98521, M/S RSL-47
Las Vegas, NV 89193-8521

Abstract

The goal of this project, started in FY17, is to develop and execute methods of characterizing uncertainty in data products that are developed and distributed by the DOE Consequence Management (CM) Program. This report presents the results of uncertainty analyses performed in FY18 for additional scenarios of increased complexity, including different time phases and radionuclide source terms.

ACKNOWLEDGMENTS

The authors would like to acknowledge the contributions of Dustin Whitener (SNL) and Richard Schetnan (SNL) for the effort to update Turbo FRMAC© to work with Dakota and the technical input of Keith Eckerman (ORNL), Shaheen Dewji (ORNL), and Warnick Kernan (PNNL). The authors thank Arthur Shanks (SNL) and Jim Phelan (SNL) for the programmatic support that they provided.

This work was funded by the Department of Energy (DOE), National Nuclear Security Administration (NNSA), NA-84 Technology Integration Program.

TABLE OF CONTENTS

LIST OF FIGURES

LIST OF TABLES

EXECUTIVE SUMMARY

Background

This document describes the methods and results of a project performed under the DOE NNSA NA-84 Technology Integration Program to develop and execute methods for characterizing uncertainty in data products that are developed and distributed by the DOE Consequence Management (CM) Program. The FY18 extension project builds on the work completed in FY17 by considering additional scenarios of interest. The ultimate goal of this project is to quantify the uncertainty inherent in data products to ensure that appropriate public and worker protections decisions are supported by defensible analysis.

Purpose and Scope

The goal of the analyses described in this report is to characterize uncertainty in the values used as contours on CM data products. This process does not require the characterization of uncertainty inherent to the situation under analysis; sources of uncertainty such as the type of release, location of release, etc., were held constant for this project in order to allow for the examination of the impact of sources of uncertainty within the analysis process itself.

The scope of this project is limited to the analysis of the uncertainty associated with Public Protection Derived Response Levels (DRLs), which are used to evaluate the radiological impacts to members of the public from exposure to radioactive material. A DRL is a level of radioactivity in the environment that is expected to produce a dose equal to the corresponding Protective Action Guide (PAG), as defined in the 2017 Environmental Protection Agency (EPA) PAG Manual. The data products for which Public Protection DRLs are calculated are used to help decision makers determine where protective actions (e.g., sheltering, evacuation, or relocation of the public) may be warranted. The DRL calculations for the analyses used all Federal Radiological Monitoring and Assessment Center (FRMAC) defaults, as specified in the FRMAC Assessment Manual, Vol. 1.

The FY17 analysis was performed for the Public Protection DRL calculation and considered only Cs-137 and the Early Phase (Total Dose) time phase. The scenarios for FY18 analyses consider different time phases and radionuclide source terms, as well as more complex atmospheric dispersion conditions. The additional time phases include the Early Phase (Avoidable Dose) time phase which excludes dose from the plume and the First Year time phase. The additional radionuclide source terms include Am-241 by itself, and a 1:1 combination of Cs-137 and Am-241.

Uncertainty Quantification Approach

The meaning of the term uncertainty in the context of this report is defined as follows. The true value of a model result (i.e., the true DRL value) is assumed to be fixed but unknown. The variation in the observation of this result (i.e., the approximate DRL calculated from a given Turbo FRMAC© simulation) relative to this fixed value is termed as the uncertainty in the model result. A collection of many Turbo FRMAC© simulations with varying inputs calculated using the principles of Monte Carlo Analysis can be used to quantify this uncertainty.

The project does not seek to quantify model uncertainty; the same models that are currently available in Turbo FRMAC© and were employed for the scenario of interest were used for every

simulation. The current practice for the calculation of quantities such as DRLs for data products is to use a set of constant default input parameter values. These input parameters, though supported by standard-practice, literature, and data, are inherently approximations. In addition, parameters and inputs derived from data collection during an event are uncertain due to a variety of factors including those related to the measurement device and methods, field contamination, etc. The scope of this project seeks to identify and characterize the relationship between the uncertainty in these inputs to the overall uncertainty in CM data products.

A Monte Carlo analysis was used to characterize uncertainty in data products for the purposes of this project. The process of executing a Monte Carlo analysis for the purposes of this project is described as follows. First, the uncertainty in Turbo FRMAC© inputs used in the calculation of DRLs for the study scenario was characterized using probability distributions. These distributions were then sampled many times. A single deterministic Turbo FRMAC© simulation was run for each sample, propagating uncertainty through the model. The final collection of simulation results was then analyzed to characterize overall uncertainty (uncertainty analysis) and to determine the contribution of each variable to the overall uncertainty (sensitivity analysis). The methods used to execute each of these steps, including the tools used and details regarding updates to Turbo FRMAC© required for this analysis, are described in detail in the body of the document.

Sources of Uncertainty & Input Distributions

The first step in characterizing the overall uncertainty in CM data products is to assess the uncertainty in the inputs that are used in to calculate DRLs for these data products. These inputs are assigned a probability distribution that describes the uncertainty that might be expected for a given parameter and that is based on published data and/or expert opinion. Table ES - 1 lists the Public Protection DRL inputs and the probability distributions assigned for this project. In determining the distributions for the Public Protection DRL inputs, the original reference for each input was examined for uncertainty information. Additional references were used when the original references did not provide the needed uncertainty information.

DRL calculations are based on measured or projected concentrations of radionuclides in the environment. Measured values can be provided through multiple sources, including analytical laboratory results (Laboratory Analysis) or field measurements obtained either through Aerial Measuring Systems (AMS) or ground-based monitoring teams (In Situ Deposition). Projections are usually obtained from atmospheric dispersion modelling calculations performed using plume projections from the National Atmospheric Release Advisory Center (NARAC). In order to characterize the uncertainty in data products due to varying sources of radioactivity concentration data, a probabilistic analysis was completed for each activity source. The probabilistic runs for Laboratory Analysis, In Situ Deposition, and AMS used a source term based on activity per area with the same parameter distributions type (Normal) and with the same mean value but with a different standard deviation (SD) based on the uncertainty in each activity source. The runs for NARAC used a distribution for integrated air activity instead of activity per area. Building on the FY17 analyses, the FY18 analyses included a NARAC input distribution that was developed using a more complex NARAC dataset to explore the impact of NARAC atmospheric dispersion uncertainty for a more complex terrain and wind flow environment.

Table ES - 1. Summary of input distributions for the FY18 uncertainty analyses.

Input	Default Value	Distribution Type	Mean	SD	Mode	Lower Bound	Upper Bound	Units
Air Concentration Uncertainty Multiplier – NARAC Simplified*	1	Lognormal+	0.59	3.99				---
Air Concentration Uncertainty Multiplier – NARAC Complex*	1	Lognormal+	4.06	4.69				---
Activity per Area‡	DRL	Normal	DRL	See note		0		$\mu Ci/m^2$
Deposition Velocity	3.00E-3	Triangular			3.00E-3	3.00E-4	3.00E-2	m/s
Breathing Rate – Light Exercise, Adult Male	1.50	Normal	1.75	0.42		0.54	3.00	m^3/hr
Breathing Rate – Activity-Averaged, Adult Male	0.92	Triangular			0.92	0.54	1.50	m^3/hr
Ground Roughness Factor	0.82	Normal	0.82	0.082		0	1	--
Resuspension Coefficient Multiplier§	1	Lognormal+	1	4.2				--
Weathering Coefficient Multiplier§	1	Lognormal+	1	1.2				--
Deposition External Dose Coefficient Multiplier	1	Triangular			0.8	0.5	1.5	--
Cs-137 Inhalation Dose Coefficient Multiplier**	1	Lognormal+	1	1.5		1.67	7.02	--
Am-241 Inhalation Dose Coefficient Multiplier++	1	Lognormal+	1	2		1.38	22.8	--
Plume External Dose Coefficient Multiplier	1	Triangular			0.8	0.5	1.5	--

* This uncertainty multiplier is multiplied by a user-defined air concentration value to sample air concentration with uncertainty.

+ The means and standard deviations (SD) listed for lognormal distributions on this table are the geometric mean and geometric standard deviation, respectively. The lognormal distribution is defined by parameters μ, the mean of the natural logarithm of the data, and σ, the standard deviation of the natural logarithm of the data. Then, the geometric mean (GM) is given by $GM = e^{\mu}$ and the geometric standard deviation (GSD) is given by $GSD = e^{\sigma}$. This treatment is also applied to the lower and upper bounds where applicable.

‡ The uncertainty associated with activity per area is dependent on the quantity being measured and the measurement type. For details, see Section 4.2.

§These multipliers are to be applied only to the coefficients outside the exponentials in the Resuspension and Weathering Factors

** This multiplier is specifically for Cs-137, Lung Clearance Type F, Effective (Whole Body). Ba-137m is present at equilibrium with Cs-137 at the start of the time phase. The uncertainty in the Ba-137m inhalation dose coefficient is neglected because its ingrowth from Cs-137 over the dose commitment period dominates the delivered dose. The Cs-137 inhalation dose coefficient accounts for dose and uncertainty from the ingrowth of Ba-137m. (per communication with Keith Eckerman on May 10, 2017)

++ This multiplier is specifically for Am-241, Lung Clearance Type M, Effective (Whole Body)

Probabilistic Analysis Results

The probabilistic analysis completed for each source of radioactivity concentration data (In Situ, Laboratory Analysis, AMS, NARAC Simplified, and NARAC Complex) used 10,000 Turbo FRMAC© simulations to generate a set of results for each output of interest. This number of simulations was selected because the computational time spent on each simulation is relatively low, allowing for a large number of simulations to be run in a short period of time (on the order of two hours). Bootstrap analysis was applied to determine confidence bounds about the uncertainty analysis results in order to characterize the stability of these results due to the selected number of simulations. This analysis found that the selected number of simulations provided a sufficient, stable characterization of the results.

The probabilistic analysis results were analyzed to characterize the uncertainty in each output, to determine the relationship between the uncertainty in each input to the uncertainty in the output, and to confirm that the selected sample size adequately captures the mean value for each output.

The FY18 analyses yielded 45 sets of results – nine scenarios were run for each of the five sources of radioactivity concentration data. In an effort to keep this report more concise, only the results of interest are presented and are organized topically in this report. The results discussion focuses on the radionuclide-specific Deposition DRLs in particular, as this is the most commonly used quantity for CM data products. The full set of results for all DRLs and Dose Parameters included in Turbo FRMAC© calculations can be requested through the primary author of this report.

The analyses for the additional single-radionuclide scenarios confirmed the FY17 finding that DRL calculations for single-radionuclide source terms are not influenced by the uncertainty associated with the activity per area or integrated air concentration assigned to the radionuclide of interest. The scenarios that considered a 1:1 mixture of Cs-137 and Am-241 showed that this is not necessarily the case for calculations with multiple-radionuclide source terms. An example set of results that reflect this behavior are included in Table ES - 2 and Figure ES - 1. The NARAC Simplified results are not presented for brevity throughout as they were not as uncertain as the more realistic NARAC Complex results.

For each uncertainty analysis considered in this report, the mean result for the Deposition DRL is about the same if not larger than the same result calculated using the default values for all inputs. This indicates that the default DRL is conservative in comparison to the best estimate of the DRL derived from the uncertainty analyses. An example of this is included in the “Mean/Default” column in Table ES - 2. It is important to note that the consistent conservatism of the default Deposition DRL, a quantity frequently used for informing protective action decisions, has been observed only for the scenarios considered in this project. It is possible that a different combination of radionuclides in a different ratio could yield a case where the mean Deposition DRL does not show that the default once-through approach is conservative. It is also important to note that the same “conservative” behavior was not always observed for the Integrated Air DRL results. However, for sake of brevity and because these DRLs are less frequently used operationally, these results are not presented in this report.

Table ES - 2. First Year Cs-137 Deposition DRL (μCi/m²) uncertainty results for 1:1 Cs-137:Am-241 simulations based on different sources of radioactivity concentration data.

Data Source	Default	Mean	5th	50th	95th	Mean/ Default	95th/ 5th
In Situ	3.78	6.713	0.305	3.698	23.491	1.78	77.0
AMS	3.78	7.397	0.284	3.945	26.208	1.96	92.3
Laboratory Analysis	3.78	6.722	0.302	3.690	23.540	1.78	78.1
NARAC Complex	3.78	10.328	0.048	3.656	40.223	2.73	831

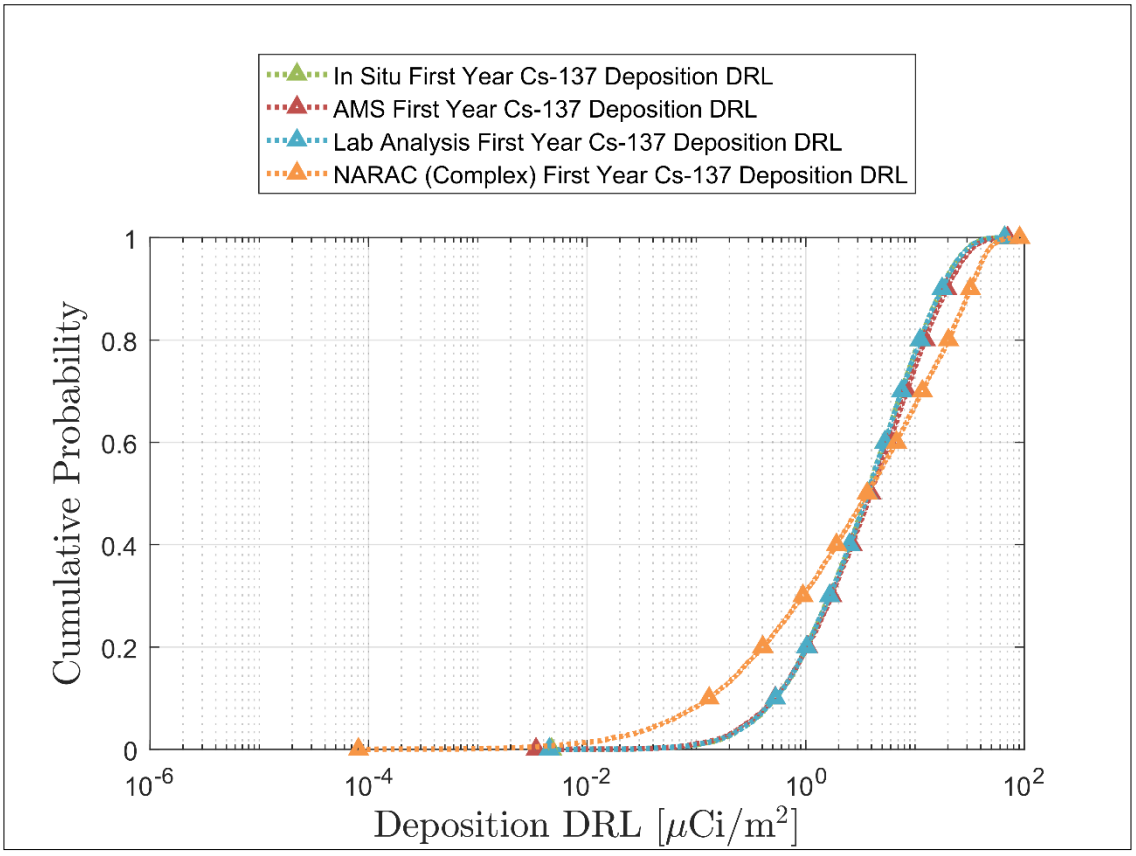

Figure ES - 1. Cumulative probabilities for the First Year Cs-137 Deposition DRL for 1:1 Cs-137:Am-241 simulations based on different sources of radioactivity concentration data.

The sensitivity analysis generally showed that deposition velocity is the most important contributor to DRL uncertainty in the case of a single-radionuclide source term DRL calculation that includes the plume. When the plume is not included, the DRL uncertainty is driven by the inputs to the primary dose pathway. For Cs-137, these are the groundshine inputs and for Am-241, these are the resuspension inhalation inputs. Because the resuspension inhalation inputs were assigned a broader probability distribution than the groundshine inputs, the Am-241 DRLs

are more uncertain. These results can be used to motivate additional studies to better characterize these inputs and in turn reduce the overall uncertainty in the DRL results.

Incorporating Uncertainty Results in Data Products

Several data products are included in this report to illustrate the potential real-world implications of incorporating uncertainty analysis results into data products that inform protective action decisions. An example data product is shown in Figure ES - 2. Each data product has a contour that corresponds to the 5th percentile (magenta), 95th percentile (yellow), and mean (orange) of the Deposition DRL distributions resulting from the uncertainty analyses. The default (red) contour is also included on each data product. The default is the result from a single Turbo FRMAC© simulation using FRMAC Assessment default values for the inputs (i.e., what is currently used for data products).

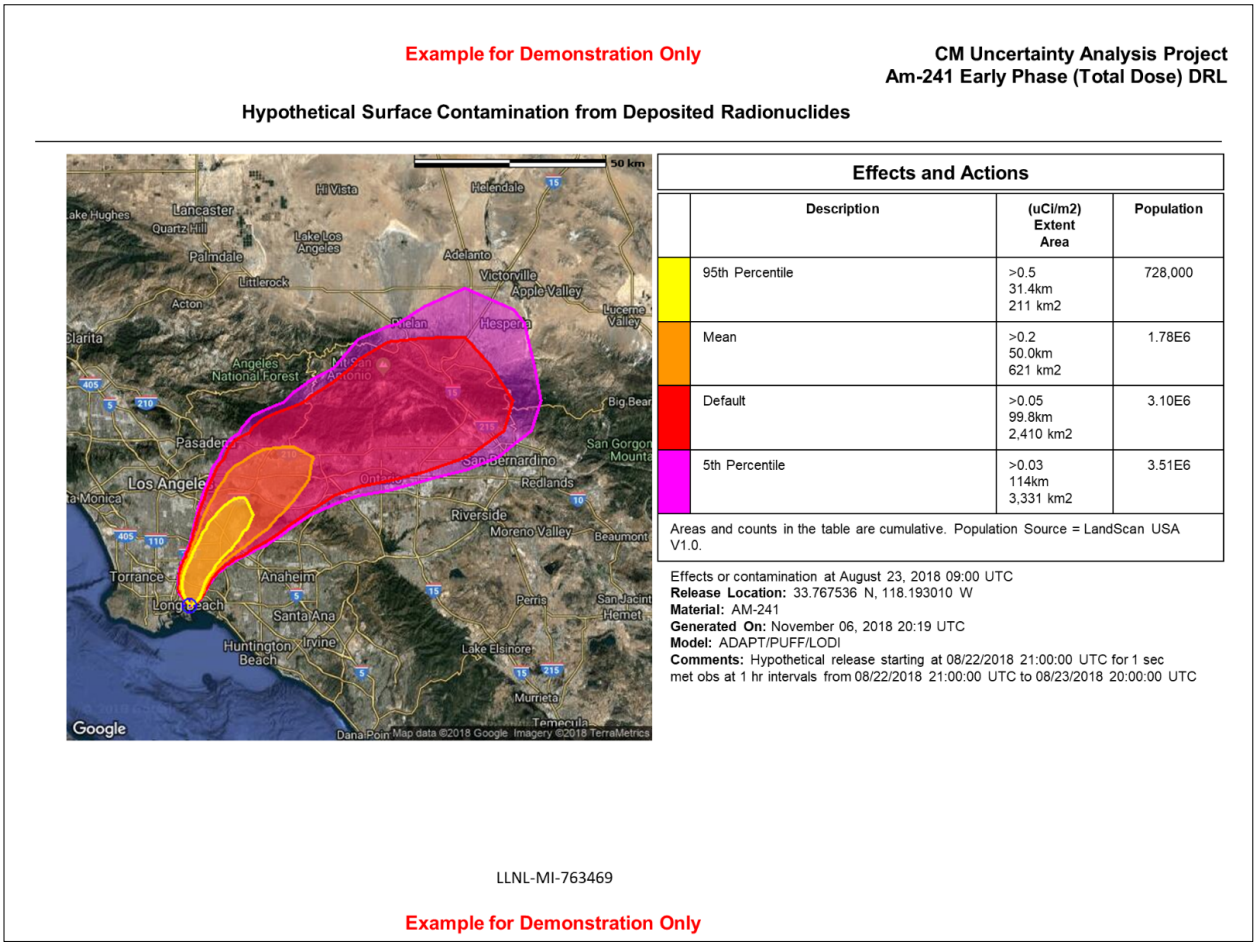

Figure ES - 2. Data product displaying the Early Phase (TD) Am-241 Deposition DRL distribution for In Situ single radionuclide simulations.

The data products can be interpreted as follows. Looking at the magenta contour for the 5th percentile, 95% of the simulation results have a Deposition DRL that is greater than the activity per area used for that contour. This means that 95% of the time, the contour could be drawn inside of the magenta shaded area if the contour was based on the DRL value calculated for a

single simulation selected from the 10,000 samples. Further, 5% of the simulation results have a Deposition DRL that is less than the activity per area used for that contour. This means that 5% of the time the contour could be drawn outside of the magenta shaded area if the contour was based on the DRL value calculated for a single simulation selected from the 10,000 samples. Decision makers may interpret this as meaning that there is a 5% chance that someone outside of the magenta shaded area could receive a dose that exceeds the PAG if a protective action is not taken.

The location of a given percentile from a DRL distribution on a map, whether 5^{th}, 95^{th}, or some other meaningful statistical metric, differs significantly depending on the scenario-specific source term and what is driving the total dose.

Implications & Future Work

The results of this probabilistic analysis show that the uncertainty in CM data products could be large. However, the mean result for the Deposition DRL, which is the most frequently used DRL for public protection data products, is larger than the same result calculated using the default values for all inputs. This indicates that a smaller area would be evacuated using the mean result when compared to the default. This demonstrates that, for the analyses included in this project, the default DRL calculated using the once-through approach is conservative in comparison to the best estimate of the DRL derived from this uncertainty analysis. The sensitivity analysis results point to input variables whose uncertainty impacts uncertainty in simulation results the most. These important variables could be targeted for further study in order to reduce the uncertainty in the data products for which they are used as simulation inputs. It is critical to note that these results have only been generated for a limited set of scenarios; implications of these findings for a wider range of CM scenarios and data products is an important area of future work. The application of the methods and tools developed and used to perform this analysis will be expanded in an extension of this project. As the scenarios studied increase in complexity, the statistical methods and tools used to both generate simulation inputs and to perform uncertainty and sensitivity analysis may need to be adapted to adequately analyze results.

The FY17-18 project demonstrated that probabilistic dose assessment calculations made for scenarios with increased complexity using CM tools are possible; however, the interpretation and use of uncertainty analysis results in the operational public protection context still needs to be addressed. The probabilistic framework developed for this project enables CM to generate DRL values for any percentile of interest for use as contours on CM data products. It is yet to be determined what is considered an acceptable amount of uncertainty in the DRLs used to inform protective action decisions. Additionally, it would be prudent to consider the non-radiological hazards and socioeconomic risks associated with implementing protective actions such as evacuation and relocation. The discussions needed to determine a proposed default approach for using uncertainty analysis results in the public protection decision-making process are also planned for FY19.

NOMENCLATURE

Abbreviation	Definition
AAL	Analytical action level
AD	Avoidable Dose
AGL	Above ground level
Am-241	Americium-241
AMS	Aerial Measuring System
Ba-137m	Metastable barium-137
CDF	Cumulative distribution function
CI	Confidence interval
CM	Consequence Management
Cs-137	Cesium-137
DCNPP	Diablo Canyon Nuclear Power Plant
DOE	Department of Energy
DOPPTEX	Diablo Canyon Tracer Experiment
DP	Dose parameter
DRL	Derived response level
EPA	Environmental Protection Agency
FRMAC	Federal Radiological Monitoring and Assessment Center
GM	Geometric mean
GPS	Global positioning system
GSD	Geometric standard deviation
HPGe	High purity germanium
ICRP	International Commission on Radiological Protection
Lc	Critical level
LHS	Latin Hypercube Sampling
NARAC	National Atmospheric Release Advisory Center
NNSA	National Nuclear Security Administration
NRC	Nuclear Regulatory Commission
ORNL	Oak Ridge National Laboratory
PAG	Protective action guide
PNNL	Pacific Northwest National Laboratory
R^2	Value indicating the amount of output variance explained by a given regression model
RA	Radar altimeter

RN	Radionuclide
ROI	Region of interest
RSL	Remote Sensing Laboratory
RSPD	Radiation Protection Sample Diagnostics
SD	Standard deviation
SNL	Sandia National Laboratories
SOARCA	State-of-the-Art Reactor Consequence Analysis
SRRC	Standardized rank regression coefficient
TD	Total Dose
WRF	Weather Research and Forecast

1. INTRODUCTION

This document describes the methods and results of a project performed under the DOE NNSA NA-84 Technology Integration Program. This project, started in FY17, established a methodology for characterizing uncertainty in data products that are developed and distributed by the DOE Consequence Management (CM) Program. The FY18 extension project builds on the work completed in FY17 [1] by considering additional scenarios.

This project required collaboration with subject matter experts across a wide range of CM skill sets in order to quantify the uncertainty from each area of the CM process and to understand how variations in these uncertainty sources contribute to the aggregated uncertainty present in data products. The ultimate goal of this project is to quantify the uncertainty inherent in data products to ensure that appropriate public and worker protections decisions are supported by defensible analysis.

The scope of this project is limited to the analysis of the uncertainty associated with Public Protection Derived Response Levels (DRLs), which are used to evaluate the radiological impacts to members of the public from exposure to radioactive material. A DRL is a level of radioactivity in the environment that is expected to produce a dose equal to the corresponding Protective Action Guide (PAG), as defined in the 2017 Environmental Protection Agency (EPA) PAG Manual [2]. The data products for which Public Protection DRLs are calculated are used to help decision makers determine where protective actions (e.g., sheltering, evacuation, or relocation of the public) may be warranted.

Assessment Scientists use the Turbo FRMAC© software [3] to estimate the projected dose following a radiological release to the environment. This projected dose is then used to create a data product (typically a map) which is used by decision makers to make appropriate protective action decisions. These calculations performed by Turbo FRMAC© rely on data which may be collected from one of several methods: analytical results from laboratories, results from Aerial Measuring Systems (AMS), or field measurements made by ground-based monitoring teams. Source term data can also be generated using computer models. The results of the Assessment calculations are then used to create contours on a data grid developed using National Atmospheric Release Advisory Center (NARAC) atmospheric dispersion predictions.

In FY17, a probabilistic framework was developed to characterize the CM process and the interrelated nature of error and uncertainty propagation that contributes to the overall uncertainty in data products. This framework was applied to additional, more complex release scenarios and data products in FY18. The results of probabilistic runs for these scenarios were analyzed using statistical methods to characterize their uncertainty and to quantify the importance of uncertainty in simulation inputs to the uncertainty in simulation outputs. The goal of this project is to develop the methods that could be used to execute a probabilistic analysis for data products; this project does not seek to provide specific and final information regarding the uncertainty in data products as a whole. Therefore, the results presented in this report should be considered examples derived from a proof of concept of simulation methods and should not be explicitly applied or used to draw conclusions about the full range of potential uncertainties in data products.

This report is organized as follows. Chapter 2 describes the study scenarios for the FY18 analyses. Chapter 3 presents the uncertainty quantification methods that were applied to develop

a probabilistic framework and describes the methods that were used in the statistical post-processing of simulation outputs. Chapter 4 details the probability distributions that were selected for the new inputs introduced for the FY18 analyses and provides a referential basis for each of these distribution selections. Chapter 5 provides the results of the probabilistic analysis conducted for the study scenarios. Chapter 6 summarizes the methods and results presented in the report and provides information about future areas of study.

2. STUDY SCENARIOS

The goal of this analysis is to characterize uncertainty in the CM data product development process. This does not require the characterization of uncertainty inherent to the situation under analysis; sources of uncertainty such as the type of release, location of release, etc., were held constant for this project in order to allow for the examination of the impact of sources of uncertainty within the analysis process itself.

The FY17 analysis was performed for the Public Protection DRL calculation and considered only Cs-137 and the Early Phase (Total Dose) time phase. The proposed scenarios for FY18 analyses consider different time phases and radionuclide source terms, as well as more complex atmospheric dispersion conditions.

2.1. Cs-137 for Early Phase (AD) and First Year Time Phases

The Early Phase (TD) time phase includes dose from all four exposure pathways – plume inhalation, plume submersion, resuspension inhalation, and groundshine. Because 80% of the total dose comes from plume inhalation for this case, the plume inhalation inputs are shown to be most important in the total dose.

Plume pathways are not included in the Early Phase (Avoidable Dose) and First Year time phases. The motivation for performing uncertainty analyses for these two time phases is to explore how the inputs to the two ground pathways will drive uncertainty in the total dose.

2.2. Am-241 for Early Phase (TD), Early Phase (AD), and First Year Time Phases

The FY17 analysis considered only Cs-137, which has a 30-year half-life and emits beta and gamma radiations. Am-241 was selected for use in additional analyses because it has a longer 432-year half-life and emits alpha and gamma radiations. Alpha radiation poses a larger internal exposure hazard than the beta and gamma radiations emitted by Cs-137. Using Am-241 will allow for exploration of how the most important inputs to overall uncertainty will change given different radiological characteristics.

2.3. Mixture of Cs-137 and Am-241 for Early Phase (TD), Early Phase (AD), and First Year Time Phases

Because the FY17 analysis included only one radionuclide, the uncertainty results for the DRLs showed that the contributions to uncertainty from atmospheric dispersion projections and measurement data were unimportant. This was because a single radionuclide (Cs-137) was the sole contributor to total dose. In order to see the effect of measurement data and atmospheric dispersion uncertainty on DRLs, an uncertainty analysis was performed using a 1:1 mixture of Cs-137 and Am-241. This ratio was selected to allow for more direct comparison to the analyses performed previously using single-radionuclide source terms. (In the future, a more realistic ratio should be considered based on likely Am-241 and Cs-137 source activities.)

2.4. Repeat 2.1, 2.2, and 2.3 using complex weather and terrain

The FY17 analysis considered a simple release scenario with well-resolved winds, uniform land cover, and flat terrain. In FY18, the analyses described in Sections 2.1, 2.2, and 2.3 will be

repeated using a more complex NARAC dataset to explore the impact of NARAC atmospheric dispersion uncertainty for a more complex terrain and wind flow environment.

2.5. Derived Response Levels for Scenarios

The DRLs for the scenarios described in Sections 2.1, 2.2, and 2.3 are provided in Table 2.5-1 and Table 2.5-2 for Deposition and Integrated Air, respectively. These values were calculated from a single Turbo FRMAC© simulation using all Federal Radiological Monitoring and Assessment Center (FRMAC) defaults, as specified in the FRMAC Assessment Manual, Vol. 1 [4]. The particle size distribution was assumed to be fixed at 1-micron Activity Median Aerodynamic Diameter. The DRLs in Table 2.5-1 and Table 2.5-2 are the results that are currently used to generate data products and will be referred to throughout the remainder of this report as "default". The Early Phase (TD) scenarios use a PAG of 1 rem, as do the Early Phase (AD) scenarios. The First Year scenarios use a PAG of 2 rem. There is no uncertainty associated with the PAGs.

Table 2.5-1. Deposition DRLs for scenarios.

Scenario		Deposition DRL ($\mu Ci/m^2$)	
		Cs-137	Am-241
Single RN	Early Phase (TD)	3.30E+02	4.64E-02
	Early Phase (AD)	1.70E+03	8.66
	First Year	42.0	4.15
Mixed 1:1	Early Phase (TD)	4.64E-02	4.64E-02
	Early Phase (AD)	8.62	8.62
	First Year	3.78	3.78

Table 2.5-2. Integrated Air DRLs for scenarios.

Scenario		Integrated Air DRL ($\mu Ci\text{-}s/m^3$)	
		Cs-137	Am-241
Single RN	Early Phase (TD)	1.10E+05	15.5
	Early Phase (AD)	5.67E+05	2.89E+03
	First Year	1.40E+04	1.38E+03
Mixed 1:1	Early Phase (TD)	15.5	15.5
	Early Phase (AD)	2.87E+03	2.87E+03
	First Year	1.26E+03	1.26E+03

2.6. Dose Pathway Contributions per Scenario

In order to calculate DRLs, Dose Parameters (DP) must also be calculated. A DP represents the integrated dose to a receptor from a particular dose pathway over the time phase. The four primary pathways considered in FRMAC Assessments for the Early Phase (TD) Time Phase are Plume Inhalation, Plume Submersion, Resuspension Inhalation, and Groundshine. The DPs for these pathways are summed to get a Total DP, which is then used to calculate DRLs.

Table 2.6-1 contains an overview of which of the four dose pathways drives total dose for each of the scenarios. When the plume is included, plume inhalation typically dominates total dose. When the plume is excluded, total dose is driven by groundshine for Cs-137, which is primarily an external hazard, and resuspension inhalation for Am-241, which is primarily an internal hazard. When both radionuclides are present in a 1:1 ratio, the dose from Am-241 is much greater than the dose from Cs-137 groundshine. This information is useful for understanding the results of the probabilistic analyses.

Table 2.6-1. Dose pathway contributions per scenario.

Source Term	Time Phase	Plume Inhalation	Plume Submersion	Resuspension Inhalation	Groundshine
Cs-137 only	Early Phase (TD)	80%	1%	0%	19%
	Early Phase (AD)	N/A	N/A	2%	98%
	First Year	N/A	N/A	0%	100%
Am-241 only	Early Phase (TD)	99%	0%	1%	0%
	Early Phase (AD)	N/A	N/A	100%	0%
	First Year	N/A	N/A	100%	0%
1:1 mixture of Cs-137:Am-241	Early Phase (TD)	99%	0%	1%	0%
	Early Phase (AD)	N/A	N/A	99%	1%
	First Year	N/A	N/A	91%	9%

3. UNCERTAINTY QUANTIFICATION METHODS

3.1. Introduction to Uncertainty Quantification & Methods

The goal of this project is to develop and execute methods for characterizing uncertainty in data products that are developed and distributed by CM. In order to accomplish this goal, the concepts of error and uncertainty in the context of this project must first be defined. For the purposes of this project, the inherent error in a given measurement, or variation of a measurement from the exact value being measured, can also be termed as uncertainty in the fixed value of the measurement. Thus, for the purposes of this project, the terms error and uncertainty are used interchangeably and will be referred to as uncertainty throughout this chapter.

The development of data products employs mathematical models to calculate results related to the release of nuclear material in a given environment. These models are based on data and known physical principals, but cannot provide exact descriptions of all potential release scenarios due to limitations in the amount of data available, limitations in the level of understanding of processes following a release, and inherent randomness in physical parameters and processes. This means that the models employed are approximations of reality and their results contain a certain level of uncertainty.

The scope of this project seeks to identify the uncertainty in data products resulting from the uncertainties in model input parameters. The project does not seek to quantify model uncertainty; the same models that are currently available in Turbo FRMAC© and are employed for the scenario of interest are used for every simulation. The current practice for the calculation of quantities such as DRLs for data products is to use a set of constant default input parameter values. These input parameters, though supported by standard-practice, literature, and data, are inherently approximations. In addition, parameters and inputs derived from data collection during an event are uncertain due to a variety of factors including those related to the measurement device and methods, field contamination, etc.

A Monte Carlo analysis was used to characterize uncertainty in data products for the purposes of this project. Monte Carlo type analyses are often employed to characterize uncertainty in simulation results [5], [6]. The process of executing a Monte Carlo analysis is fairly straightforward [6]. First, the uncertainty in model inputs is characterized using probability distributions. These distributions are then sampled many times. A single deterministic simulation is run for each sample, propagating uncertainty through the model (Section 3.2). The final collection of simulation results is then analyzed to characterize overall uncertainty and contribution of each variable to the overall uncertainty (Section 3.3). The following sections describe each of these steps and how they have been implemented for this project in detail.

3.2. Uncertainty Propagation

The first step in a Monte Carlo analysis is to define a probability distribution for each uncertain input. These distributions are selected based on published data and/or expert opinion and describe the uncertainty that might be expected for a given parameter. The basis for and selection of distributions for the uncertain inputs considered in this project is described in detail in Chapter 4. Following the selection of distributions, a sampling method must be selected and used to sample each of the input distributions. The Latin Hypercube Sampling (LHS) algorithm in the Dakota toolkit [7] was utilized to sample input distributions for both the FY17 and FY18

projects. More details regarding the selection of this sampling method and the use of Dakota are given in [1].

The sampled inputs must be propagated through the model of interest, in this case Turbo FRMAC©, to produce a simulation result for each sample. The same uncertainty propagation methods were used in the FY17 and FY18 projects. Figure 3-1 shows a typical Turbo FRMAC© run with constant/fixed inputs. Each Turbo FRMAC© realization uses a single value for each input that is used to calculate the final result.

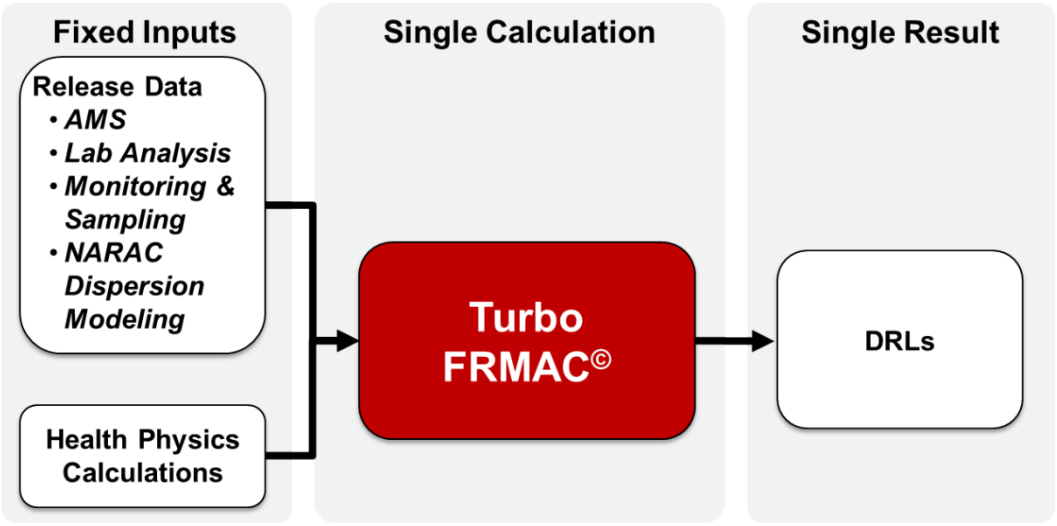

Figure 3-1. Typical Turbo FRMAC© simulation.

The application of Monte Carlo analysis techniques requires the process shown in Figure 3-1 to be executed many times using samples of input distributions defined for each of the inputs used to calculate the final result. This requires the development of a probabilistic framework that samples inputs, passes the inputs to the simulation code, and collects the results. This process is shown in Figure 3-2.

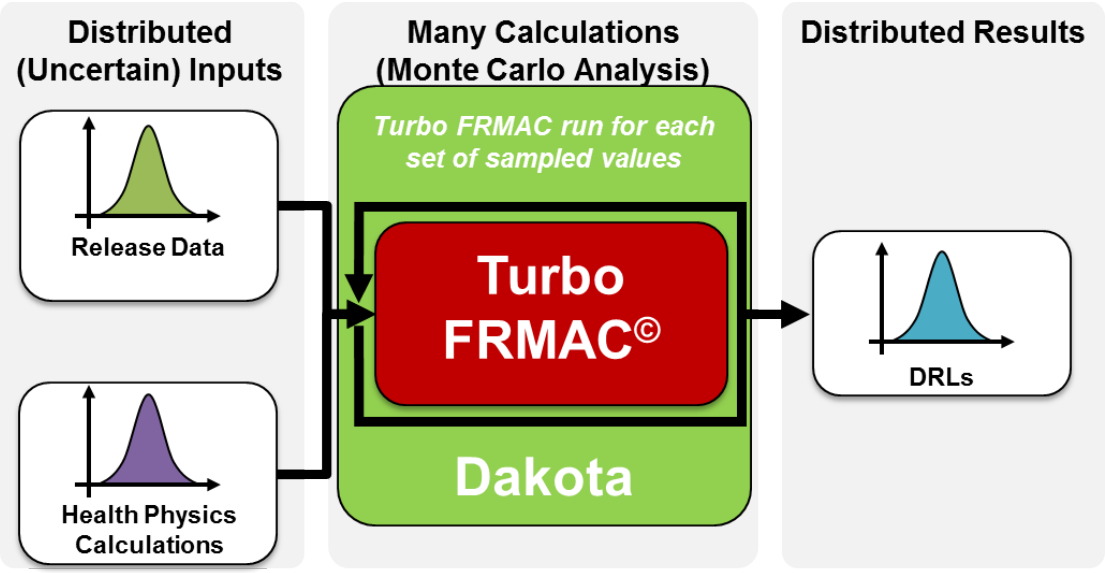

Figure 3-2. Turbo FRMAC© execution under probabilistic framework.

The Dakota Error Analysis Tool was added to Turbo FRMAC© in FY17 to enable batch runs of Public Protection DRL calculations, as described in [1]. However, it was only able to perform a calculation for a preset scenario – Cs-137 and Early Phase (TD) time phase. The capability of this tool was expanded in FY18 to allow a user to select any of the five default time phases included in Turbo FRMAC© Public Protection DRL calculations (Early Phase (TD), Early Phase (AD), First Year, Second Year, and Fifty Year). Additionally, the tool now performs the Public Protection DRL calculation for any mixture of radionuclides included in the database. The software does this by parsing the calculation input distribution data from a specifically-structured input file, rather than from direct input via the Turbo FRMAC© user interface. The graphical user interface for the tool is shown in Figure 3-3.

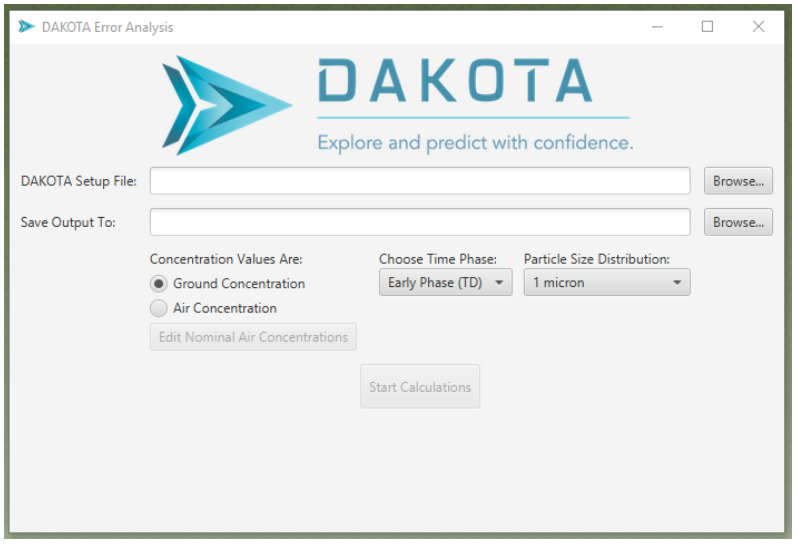

Figure 3-3. Turbo FRMAC© Dakota Error Analysis Tool graphical user interface.

The Dakota Error Analysis Tool is designed to automatically run the calculations, format the calculation results as structured data, and write that structured data to an output file with minimal user intervention. Without any attempt to optimize run time, 10,000 simulations takes about 2 hours to complete for a single-radionuclide source term and 6 hours to complete for a two-radionuclide source term. The uncertainty in the outputs and the sensitivity of this uncertainty to uncertainty in simulation inputs is characterized using the statistical methods described in Section 3.3.

3.3. Statistical Post-processing Methods

Following a probabilistic run of Turbo FRMAC© for a scenario of interest, the results must be analyzed to generate statistical information regarding result uncertainty and the sensitivity of this uncertainty to uncertainty in simulation inputs. A post-processing code was developed in the open-source statistical software "R" to accomplish this [8] for the FY17 project. This code calculates summary statistics that describe the distributions of results and characterize the uncertainty in each output of interest, as is described in Section 3.3.1. This code also applies a linear rank regression analysis to the inputs and outputs of interest to determine and quantify the sensitivity of the uncertainty in the result outputs to the uncertainty in the simulation inputs, as is presented in Section 3.3.2. The examples presented in these sections are used to explain the applied statistical methods. Results presented in these sections will be presented in Chapter 5 along with additional explanations and analysis.

3.3.1. Uncertainty Analysis Methods & Results

The collection of results from a given Turbo FRMAC© representation for a single output of interest represents an estimate of the true distribution of this output. Thus, the simulation results represent an estimate of the uncertainty in this output, for example the Deposition DRL, given the uncertainty in the inputs. Uncertainty analysis results can be quantified by calculating percentiles of the output of interest over all of the samples for a simulation.

The uncertainty analysis results are presented in tables that show these summary statistics along with the default value for the output that is calculated using a single simulation of Turbo FRMAC© with fixed, default values. This default value represents the normal operating defaults for Turbo FRMAC© for the scenario of interest before any uncertainty is applied to the inputs. An example of the display of uncertainty analysis results in this report is shown in Table 3.3-1 below. This table is a replicate of Table 5.2-1. Section 5.2 provides an interpretation of these results in the context of the study scenario. The ratios of the mean to default and 95th to 5th are also included in the tables as a metric that can be used to compare different sets of results.

Table 3.3-1. Example of Cs-137 Deposition DRL (μCi/m^2) uncertainty results.

Scenario	Default	Mean	5th	50th	95th	Mean/ Default	95th/ 5th
Early Phase (TD)	3.31E+02	7.10E+02	2.05E+02	6.87E+02	1.31E+03	2.15	6.42
Early Phase (AD)	1.70E+03	1.86E+03	1.20E+03	1.80E+03	2.75E+03	1.10	2.30
First Year	42.0	47.8	31.1	46.3	69.6	1.14	2.24

3.3.2. Sensitivity Analysis Methods & Results

The goal of sensitivity analysis is to characterize the relationship between the uncertainty in model inputs and the uncertainty in model outputs. Sensitivity analysis can be used to identify the amount of uncertainty in the outputs that can be attributed to each of the inputs for a probabilistic analysis. This allows the inputs that have the most significant impact on model results to be identified in a quantitative fashion. These inputs can then be targeted for future review if a reduction in output uncertainty is required. The application of a sensitivity analysis begins with the selection of a regression model to quantify the relationship between simulation inputs and outputs. A linear rank regression model was selected for both the FY17 and FY18 projects. More details regarding this regression model are given in [1].

The quantitative metrics that are output from the application of a linear rank regression model provide information on model fit as well as the impact of individual inputs and the strength of their relationship with the output of interest. An example of these regression outputs is presented in Table 3.3-2 below. The R^2 for the model, shown in the first row of the table, quantifies the portion of the variance in the model response, i.e., Deposition DRL, that is captured by the linear rank regression model using the inputs sampled for the simulation. Generally, the closer that this R^2 value is to 1, the better the fit of the regression model. The R^2 column in this table denotes the cumulative R^2 value as each input is added to the regression model. This value can be used to quantitatively assess how much of the variance in the model response can be attributed to each input individually. The standardized rank regression coefficient (SRRC) column represents the strength of the influence of each input and can be notionally interpreted as the slope of the line fitted to the ranks of each input and the output of interest. A positive SRRC value indicates that as an input increases, the output of interest also increases. Conversely, a negative SRRC value indicates that as an input decreases, the output of interest increases.

The rows of the tables used to present the sensitivity analysis results in this report are ordered in terms of variable importance to the outputs of interest with the most important variable appearing in the first row of each table. In this context, importance means that the variable has the strongest relationship with the output of interest and explains the greatest amount of output variance.

Table 3.3-2. Example of sensitivity analysis results for the Cs-137 Deposition DRL.

Cs-137 Deposition DRL, R^2 = 0.931		
Variable Name	**R^2**	**SRRC**
Deposition Velocity	0.654	0.809
Cs-137 Inhalation Dose Coefficient Multiplier	0.786	-0.360
Breathing Rate, Light Exercise, Adult Male	0.854	-0.261
Weathering Coefficient Multiplier	0.893	0.197
Deposition External Dose Coefficient Multiplier	0.922	-0.172
Ground Roughness Factor	0.927	-0.072
Resuspension Coefficient Multiplier	0.931	-0.061
Cs-137 Activity per Area	0.931	0.000
Plume External Dose Coefficient Multiplier	0.931	0.000
Breathing Rate, Activity Averaged, Adult Male	0.931	-0.009

Table 3.3-2 is a replicate of Table 5.2-2. Section 5.2 provides an interpretation of these results in the context of the study scenario.

Scatter plots are often used to corroborate the results of sensitivity analyses. These plots can be used to confirm that the relationships between inputs and outputs are correctly quantified by the selected regression model. They can also be used to identify areas of the input space that may have been under-sampled and could be targeted for additional analysis. Examples of scatter plots for the first four important variables given in Table 3.3-2 are shown in Figure 3-4 below.

The scatter plot in the upper left of Figure 3-4 shows that deposition velocity has a strong, positive relationship with the Cs-137 Deposition DRL. The inhalation dose coefficient multiplier in the upper right is shown to have a slightly less strong, negative relationship with the Cs-137 Deposition DRL. The remaining two inputs shown in the bottom of the figure have relatively slight relationships with the Cs-137 Deposition DRL. These scatter plots therefore confirm the quantitative results shown in Table 3.3-2. Scatter plots like these are used to support the results discussion in Chapter 5.

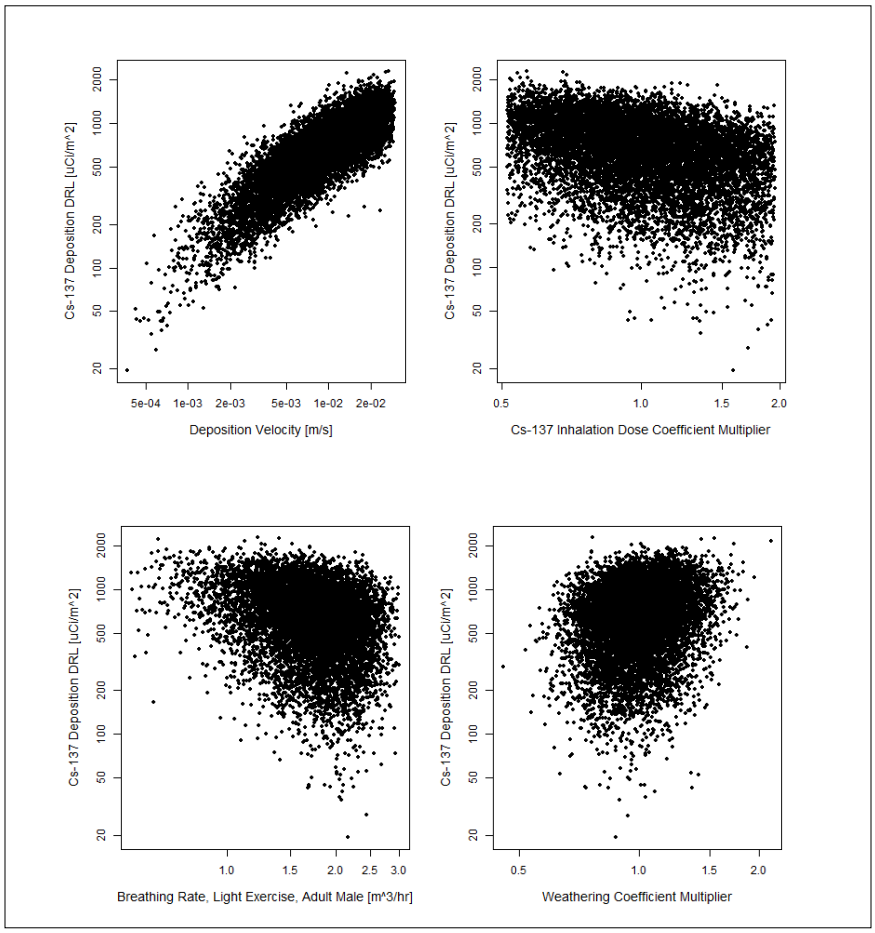

Figure 3-4. Example of scatter plots for the Cs-137 Deposition DRL for the first four inputs shown in Table 3.3-2.

3.3.3. Sampling Confidence Intervals

The finite number of samples used to characterize the uncertainty in data products for the purposes of this report must also be taken into consideration; the characterization of uncertainty could only be exact if an infinite number of samples were used. Thus, the sampling uncertainty, or uncertainty due to a finite sample size, must be quantified to determine whether results can be considered to be stable or whether additional samples are needed to provide a precise estimate of uncertainty. A nonparametric bootstrap approach was used to quantify sampling uncertainty about the mean for each of the outputs under consideration in this analysis [9]. The application of this method to the mean of each of the outputs is a 95% sampling confidence interval (CI) that can be interpreted as follows: 'there is a 95% confidence that the true mean falls in this interval.' The width of this CI can be used to determine whether more samples are needed to adequately capture the mean. More detail on the application of the bootstrap method for this project can be found in [1].

Sampling CIs were calculated for each output of interest following a probabilistic simulation completed for each activity source. CI results are discussed in Chapter 5, Probabilistic Analysis Results.

4. SOURCES OF UNCERTAINTY & INPUT DISTRIBUTIONS

The following sections describe the probability distributions defined for the sources of error and uncertainty identified in each portion of the CM analysis process. Calculation inputs that contribute to uncertainty in the health physics calculations of Public Protection DRLs are described and assigned probability distributions in Section 4.1. Sections 4.2 and 4.2.4 include probability distributions for deposition (also referred to as "activity per area") and integrated air activity, respectively. In a typical response, source term information is initially provided by atmospheric modeling (NARAC) and eventually informed by field and laboratory measurements. For purposes of this analysis, source terms and associated uncertainties from NARAC, in situ deposition measurements, AMS measurements, and laboratory analysis were treated as separate source term inputs.

4.1. Public Protection DRL Input Distributions

Section 4.1 of the FY17 uncertainty analysis report describes the probability distributions which were assigned to the Public Protection DRL inputs [1]. These distributions remained the same for the FY18 analyses, with the exception of a slight change to the Cs-137 Inhalation Dose Coefficient Multiplier. Because FY18 analyses include Am-241, distributions for Am-241 dose coefficients were also needed.

4.1.1. Am-241 Deposition External Dose Coefficient

Keith Eckerman, Ph.D. of Oak Ridge National Laboratory developed probability distributions for use by the Nuclear Regulatory Commission (NRC) State-of-the-Art Reactor Consequence Analysis (SOARCA) uncertainty analyses [10]. Eckerman recommends a multiplicative uncertainty for ground plane dose rate coefficients for all radionuclides and organs. This distribution is not radionuclide-dependent, so the same multiplier that was used in FY17 for the Cs-137 deposition external dose coefficient will be applied to Am-241, as shown in Figure 4-1.

4.1.2. Am-241 Plume External Dose Coefficient

Eckerman does not provide uncertainty information for plume external dose coefficients because the document was written in support of the NRC SOARCA uncertainty analyses, in which "the dominant route of exposure…is exposure to contaminated surfaces" [10]. For the FY17 analysis, Eckerman recommended using the uncertainty for ground plane dose rate coefficients for the plume submersion dose coefficients. The same multiplier that was used in FY17 for the Cs-137 plume external dose coefficient will be applied to Am-241 at Eckerman's recommendation, with the note that this is likely conservative relative to Cs-137 due to the lower photon energy from Am-241.[*] The distribution is shown in Figure 4-2.

[*] Personal communication, K. Eckerman, Oak Ridge National Laboratory, May 2018.

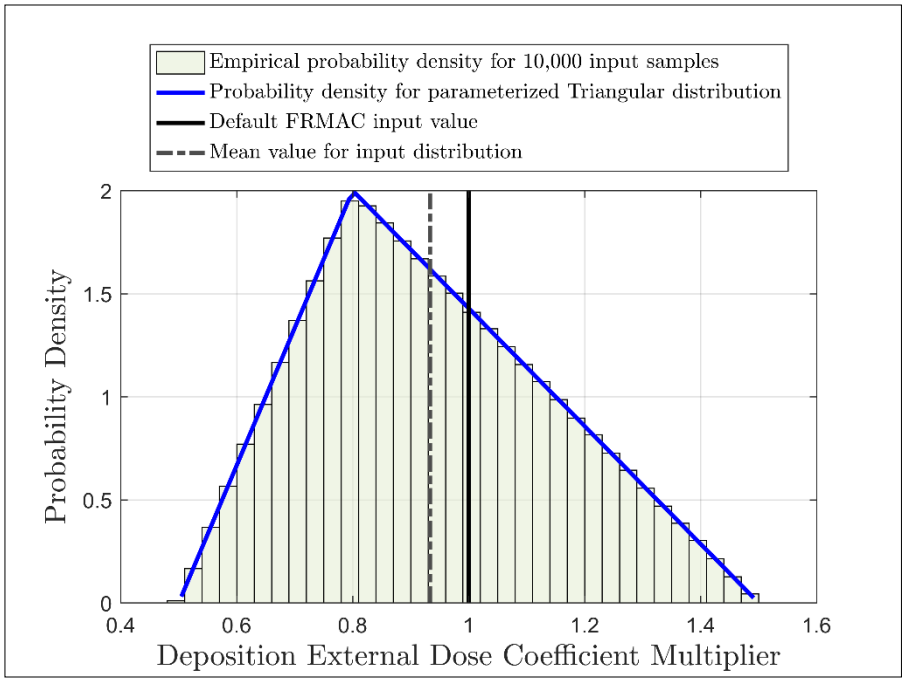

Figure 4-1. Empirical and parameterized probability densities for the deposition external dose coefficient multiplier.

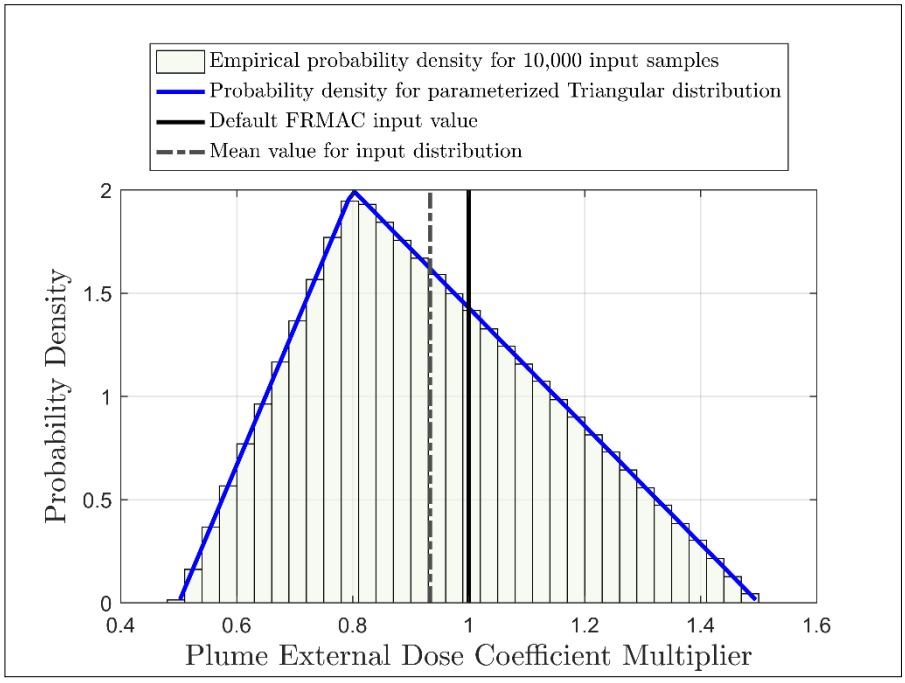

Figure 4-2. Empirical and parameterized probability densities for the plume external dose coefficient multiplier.

4.1.3. Am-241 Inhalation Dose Coefficient

Eckerman recommends lognormal distributions for radionuclide- and organ-specific inhalation dose coefficients [10]. For Am-241 Type M (ICRP Recommended lung clearance type), a geometric standard deviation (GSD) of 1.50 is given for lung, bone, breast, thyroid, liver, colon, and residual. A GSD of 1.78 is given for leukemia. This distribution is truncated lognormal using 90% CI as upper and lower values and was developed for use in the NRC SOARCA uncertainty analyses. An effective dose coefficient was not included in SOARCA because doses were calculated for the specific organs (cancer sites) previously listed. Eckerman recommended a GSD of 2 for the Am-241 effective dose coefficient.[†]

Turbo FRMAC© assigns dose coefficients to radionuclides by calling them from a dose coefficient library rather than by direct user input. Instead of replacing the dose coefficient in the software with a sampled value for every realization, a dose coefficient multiplier is used to apply dose coefficient uncertainty. The Am-241 inhalation dose coefficient uncertainty multiplier was assigned a lognormal distribution with a geometric mean (GM) of 1 and GSD of 2. The distribution for the Am-241 inhalation dose coefficient uncertainty multiplier is shown in Figure 4-3.

4.1.4. Cs-137 Inhalation Dose Coefficient

The FY17 analyses included a distribution for the Cs-137 inhalation dose coefficient. This distribution was not truncated at the 90% CI as it was in the NRC SOARCA uncertainty analyses. For the FY18 analyses, this distribution is truncated at the 90% CI and retains a lognormal shape with a geometric (GM) of 1 and GSD of 1.50, as shown in Figure 4-4. This difference is noted in order to account for slight differences in results for Scenario 1a (Cs-137 only, Early Phase (TD)) compared to the FY17 results.

[†] Personal communication, K. Eckerman, Oak Ridge National Laboratory, May 2018.

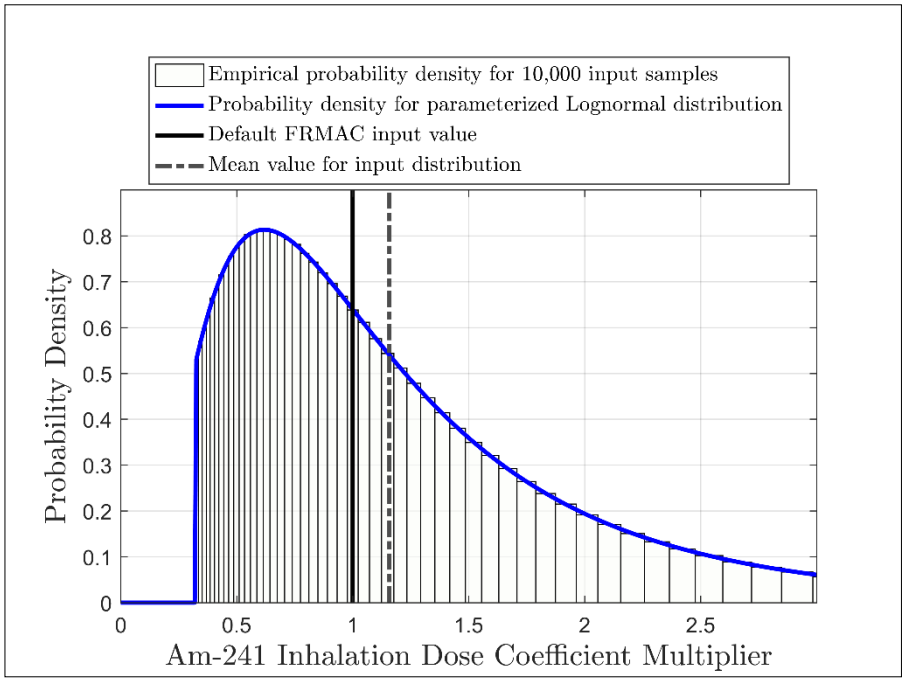

Figure 4-3. Empirical and parameterized probability densities for the Am-241 inhalation dose coefficient multiplier.

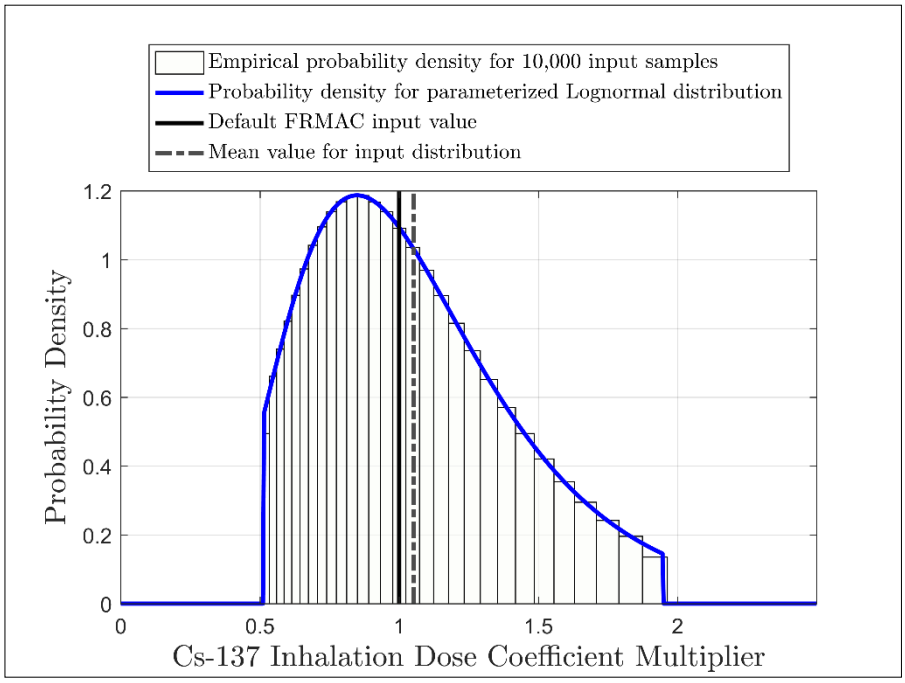

Figure 4-4. Empirical and parameterized probability densities for the Cs-137 inhalation dose coefficient multiplier.

4.2. Data Collection Sources of Uncertainty

The health physics dose calculations are based on measured or projected concentrations of radionuclides in the environment. Measured values can be provided through multiple sources, including analytical laboratory results or field measurements obtained either through AMS or ground-based monitoring teams. Projections are usually obtained from atmospheric dispersion modelling calculations performed using NARAC plume projections.

Sources of uncertainty in measurement values are discussed in this section. Sources of uncertainty from NARAC modelling projections are discussed in Section 4.2.4.

4.2.1. Laboratory Analysis

The analytical techniques considered for the Laboratory Analysis measurements include gamma spectroscopy for Cs-137 and both gamma and alpha spectroscopy for Am-241. It is assumed that gamma spectroscopy is used to analyze Am-241 for the Early Phase scenarios because it is faster than alpha spectroscopy and requires less sample preparation work. For the First Year scenarios, it is assumed that there is enough time to perform alpha spectroscopy analysis on the samples and that this type of analysis is performed even if DRL is large enough to use gamma spectroscopy.

4.2.1.1. Gamma Spectroscopy

The gamma spectroscopy uncertainty calculation has been adjusted slightly from what was done in FY17. As in FY17, the sample collected is considered to be a standard FRMAC ground deposition sample (10cm x 10cm x 2cm). It is assumed that the material is uniformly deposited on the ground with a resolution of a minimum of 1 m^2. In addition to this, the adjusted calculation now also takes into account sample mass. An assumed soil density of 1.7 g/cm^3 yields a sample mass of 340 g. A sample aliquot mass of 340.0 ± 0.5 g is assumed to account for uncertainty in the measurement of sample mass. This sample information is used to calculate the sample activity concentration for contamination at the Deposition DRL for each scenario, shown in Table 4.2-1.

Table 4.2-1. Sample activity concentrations for Cs-137 and Am-241.

Scenario		Cs-137		Am-241	
		Deposition DRL (µCi/m²)	Sample Activity Conc. (Bq/g)	Deposition DRL (µCi/m²)	Sample Activity Conc. (Bq/g)
Single RN	Early Phase (TD)	3.30E+02	3.59E+02	4.64E-02	5.05E-02
	Early Phase (AD)	1.70E+03	1.85E+03	8.66	9.42
	First Year	42.0	45.7	4.15	4.52
Mixed 1:1	Early Phase (TD)	4.64E-02	5.05E-02	4.64E-02	5.05E-02
	Early Phase (AD)	8.62	9.38	8.62	9.38
	First Year	3.78	4.11	3.78	4.11

A standard Poisson-based uncertainty model is applied to gamma spectroscopy. This assumes that the uncertainty in any measurement of radioactivity is proportional to the square root of the number of counts observed. When any adjustment or correction is made to the number of counts observed, their errors are combined in quadrature following the law of propagation of uncertainty [11]. The expected measured counts per minute is calculated as shown in Equation (1):

$$C_i = \epsilon_i(E) * A_i * \nu * \gamma_i(E) \quad (1)$$

where:

C_i: Observed net counts per minute of the detector system for nuclide, i (cpm)

$\epsilon_i(E)$: Detection efficiency at the energy in keV of the primary gamma ray of nuclide, i (counts per gamma)

A_i: Sample activity concentration of the nuclide, i (Bq/g)

ν: Sample aliquot mass (g)

$\gamma_i(E)$: Radiative yield of the primary gamma ray of nuclide, i (gammas per disintegration)

The detection efficiency and yield of the primary line are functions of the gamma ray energy and radionuclide of interest, respectively. For the purpose of this analysis, a gamma spectrometer at Sandia National Laboratories (SNL) was used to estimate detection efficiency and background response. This is a Canberra GX3018, an Extended-range Closed-end coaxial High Purity Germanium (HPGe) detector. The detector is placed in a low background Gamma Products® Graded Shield commonly found in radiochemical counting facilities. The counting geometry was assumed to be a jar of soil in which the entire deposition sample fits. The source distribution is assumed to be homogeneous after soil preparation and packaging. Typical laboratory measurements of counting efficiency in this geometry yield total propagated uncertainties in the neighborhood of 3-4% considering source certificate error and efficiency measurement counting uncertainty.

For detection of the 661.7 keV gamma ray from Ba-137m (daughter of Cs-137), efficiency is assumed to be 0.00964 ± 0.000386 counts per gamma. A 4% uncertainty is assumed for the efficiency calibration. The 661.7 keV primary peak yield is 0.851 ± 0.005 gammas per decay.

For detection of the 59.5 keV gamma ray from Am-241, efficiency is assumed to be 0.02423 ± 0.00078 counts per gamma. A 3.21% uncertainty is assumed for the efficiency calibration. The 59.5 keV primary peak yield is 0.35 ± 0.005 gammas per decay.

The number of observed counts is calculated using Equation (2)

$$N_i = C_i * T \quad (2)$$

where:

N_i: Gross observed number of counts in the measurement of nuclide, i (counts)

C_i: Observed net counts per minute of the detector system for nuclide, i (cpm)

T: Count time of the measurement (min)

By default FRMAC assumes the ratio of the analytical action level (AAL) to the required measurement critical level (Lc) is 10 and that this will yield satisfactory statistics. The DRL is converted to the AAL for ground deposition samples by multiplying by the sample area and dividing by the sample mass. The required Lc is then used by the laboratory to choose an appropriate analysis method and count time. In this analysis, the count times were set such that the measurement Lc was below the required Lc. The count times assumed are 600 s and 1000 s for Cs-137 and Am-241, respectively.

Every gamma spectroscopy system will respond to background differently as it is a function of the detector size (efficiency), the location of the count, and the amount of shielding around the detector. In addition to the counting system dependencies, the background is highly dependent on sample characteristics, such as: matrix, geometry, and the presence and concentration of radionuclides that contribute to the continuum. As such, it is impossible to generate an *a-priori* estimation of the background for all situations. What is presented is an idealized scenario, using an empty shield background for the same detector used in this analysis, the background was 0.533 ± 0.231 cpm for Cs-137 and 1.871 ± 0.335 cpm for Am-241. The background count rate uncertainties were calculated following the law of propagation of uncertainty using Equation (3):

$$\sigma_{B_i} = \frac{\sqrt{B_i * T}}{T} \tag{3}$$

where:

σ_{B_i}: 1-sigma counting uncertainty of the background count rate measurement

B_i: Observed counts per minute of the background spectrum in the region of interest (ROI) for nuclide, i (cpm)

T: Count time of the measurement (min)

In gamma spectroscopy, the background and signal are “paired observations” meaning the continuum is a function of the sample itself. It is important to note that any radionuclides detected in the spectrum with photons that have energies greater than the energy of interest will contribute to the continuum for that energy. For the single radionuclide source terms, only the environmental empty shield background is considered in estimating the background. The ROI for the primary peaks of Cs-137 and Am-241 are used to tally up the counts per minute of the empty shield background. This is then scaled up for the sample count time to yield a background uncertainty. The background uncertainty should always be considered in the uncertainty budget unless it is shown to be negligible. In the case of this analysis, the uncertainty in the background is significant.

For the mixed source term scenarios, the continuum of the Cs-137 photopeak increases the continuum of the Am-241 peak as it is lower energy. For an accurate analysis of measurement uncertainty, this must be accounted for. A simple experiment was performed on the GX3018 HPGe detector used in this analysis to estimate this crosstalk. A pure Cs-137 button source was counted behind scattering material to simulate a real sample. An analysis of the Am-241 ROI showed that roughly 3.8% of the Cs-137 peak area shows up as additional continuum that must be added to the empty shield continuum for Am-241. This yields a coupled background count rate for Am-241 of 7.223 ± 0.658 cpm for a 1000-s mixed source term count.

Equation (4) shows how the counting uncertainty is calculated, taking into account background count uncertainty:

$$\sigma_i = \sqrt{N_i + B_i * T} \tag{4}$$

where:

σ_i: 1-sigma counting uncertainty of the measurement

N_i: Net observed number of counts in the measurement of nuclide, i

B_i: Observed counts per minute of the background spectrum in the ROI for nuclide, i (cpm)

T: Count time (min)

Using Equations (1) through (4), the sample net counts for the Cs-137 and Am-241 Deposition DRLs are calculated as shown in Table 4.2-2.

Table 4.2-2. Sample net counts and uncertainties for laboratory gamma spectroscopy of Cs-137 and Am-241.

Scenario		Cs-137			Am-241		
		Sample Activity Conc. (Bq/g)	Counts	Counting Uncertainty	Sample Activity Conc. (Bq/g)	Counts	Counting Uncertainty
Single RN	Early Phase (TD)	3.59E+02	6.01E+05	7.75E+02	5.05E-02	1.46E+02	13.3
	Early Phase (AD)	1.85E+03	3.10E+06	1.76E+03	9.42	2.72E+04	1.65E+02
	First Year	45.7	7.65E+04	2.77E+02	Alpha spec is used		
Mixed 1:1	Early Phase (TD)	5.05E-02	1.41E+02	12.2	5.05E-02	1.46E+02	16.3
	Early Phase (AD)	9.38	2.62E+04	1.62E+02	9.38	2.70E+04	2.09E+02
	First Year	4.11	6.88E+03	83.0	Alpha spec is used		

In the calculation of radioactivity, the net count rate is corrected for efficiency and radiative yield. Furthermore, there is uncertainty in the actual sampling size. All of these uncertainties must be considered in the uncertainty calculation for measured sample activity, which is shown in Equation (5):

$$\sigma_{A_i} = A_i * \sqrt{\left(\frac{\sigma_i}{N_i}\right)^2 + \left(\frac{\sigma_{\gamma_i}}{\gamma_i}\right)^2 + \left(\frac{\sigma_{\epsilon_i}}{\epsilon_i}\right)^2 + \left(\frac{\sigma_v}{v}\right)^2} \quad (5)$$

where:

σ_{A_i}: Sample activity concentration uncertainty of nuclide, i (Bq/g)

A: Sample activity concentration of nuclide, i (Bq/g)

σ_{γ_i}: Radiative yield uncertainty of the primary gamma ray of nuclide, i (gammas per disintegration)

σ_{ϵ_i}: Detection efficiency uncertainty at the energy in keV of the primary gamma ray of nuclide, i (counts per gamma)

σ_v: Sample aliquot mass uncertainty (g)

Using Equation (5) to propagate these uncertainties, the sample activity concentration uncertainties are calculated as shown in Table 4.2-3.

Table 4.2-3. Sample activity concentrations and uncertainties for laboratory gamma spectroscopy of Cs-137 and Am-241.

Scenario		Cs-137		Am-241	
		Sample Activity Conc. (Bq/g)	Sample Activity Conc. Uncertainty (Bq/g)	Sample Activity Conc. (Bq/g)	Sample Activity Conc. Uncertainty (Bq/g)
Single RN	Early Phase (TD)	3.59E+02	14.5	5.05E-02	4.94E-03
	Early Phase (AD)	1.85E+03	74.9	9.42	3.36E-01
	First Year	45.7	1.86	Alpha spec is used	
Mixed 1:1	Early Phase (TD)	5.05E-02	4.84E-03	5.05E-02	5.93E-03
	Early Phase (AD)	9.38	3.84E-01	9.38	3.38E-01
	First Year	4.11	1.74E-01	Alpha spec is used	

4.2.1.2. Alpha Spectroscopy

The same sample information as assumed in Section 4.2.1.1 is used to calculate the sample activity concentration for the Deposition DRL for each scenario, shown in Table 4.2-1.

In addition to accounting for efficiency, radiative yield, and sample size, alpha spectroscopy requires chemical preparation. The radiochemical tracer yield and associated uncertainty must be included in the calculation of expected counts per minute, shown in Equation (6):

$$C_i = \epsilon_i(E) * A_i * \nu * \gamma_i(E) * \tau \quad (6)$$

where:

C_i: Observed counts per minute of the detector system for nuclide, i (cpm)

$\epsilon_i(E)$: Detection efficiency of nuclide, i (counts per alpha)

A_i: Sample activity concentration of the nuclide, i (Bq/g)

ν: Sample aliquot mass (g)

$\gamma_i(E)$: Integrated alpha yield of nuclide, i (alphas per disintegration)

τ: Radiochemical tracer yield (unitless)

An integrated alpha yield of 0.994 ± 0.0005 alphas per decay is assumed for Am-241. Detection efficiency is assumed to be 0.258 ± 0.005 counts per alpha. This is a typical efficiency based on using the second shelf of a 1-inch Passivated Implanted Planar Silicon (PIPS) detector in the SNL Radiation Protection Sample Diagnostics (RSPD) laboratory.

A sample aliquot mass of 1 ± 0.005 g is assumed. This is the typical mass used in a soil analysis at RPSD, but this value can vary quite a bit among laboratories. For a 1-g soil analysis, the typical recovery yield achieved at RPSD is 0.75 ± 0.044. The uncertainty in this tracer yield assumes 3% certificate error, 0.5% balance error, and 5% tracer counting error.

Equation (2) is used to calculate the number of observed counts. A count time of 60,000 s is assumed. Typical background at RPSD is 5.00E-05 cpm. Equation (6) is used to calculate net counts, and Equation (3) and Equation (4) are used to calculate background count rate uncertainty and net count uncertainty, respectively. Table 4.2-4 contains the net counts and uncertainties for alpha spectroscopy of Am-241.

Table 4.2-4. Sample net counts and uncertainties for laboratory alpha spectroscopy of Am-241.

Scenario	Time Phase	Sample Activity Conc. (Bq/g)	Counts	Counting Uncertainty
Single RN	First Year	4.52	5.21E+04	2.28E+02
Mixed 1:1	First Year	4.11	4.75E+04	2.18E+02

Equation (7) shows how sample activity concentration uncertainty is calculated for alpha spectroscopy:

$$\sigma_{A_i} = A_i * \sqrt{\left(\frac{\sigma_i}{N_i}\right)^2 + \left(\frac{\sigma_{\gamma_i}}{\gamma_i}\right)^2 + \left(\frac{\sigma_{\epsilon_i}}{\epsilon_i}\right)^2 + \left(\frac{\sigma_v}{v}\right)^2 + \left(\frac{\sigma_\tau}{\tau}\right)^2} \quad (7)$$

where:

σ_{A_i}: Sample activity concentration uncertainty of nuclide, i (Bq/g)

A: Sample activity concentration of nuclide, i (Bq/g)

σ_{γ_i}: Integrated alpha yield uncertainty of nuclide, i (alphas per disintegration)

σ_{ϵ_i}: Detection efficiency uncertainty of nuclide, i (counts per alpha)

σ_v: Sample aliquot mass uncertainty (g)

σ_τ: Radiochemical tracer yield uncertainty (uncertainty)

Using Equation (7) to propagate these uncertainties, the sample activity concentration uncertainties are calculated as shown in Table 4.2-5.

Table 4.2-5. Sample activity concentrations and uncertainties for laboratory alpha spectroscopy of Am-241.

Scenario	Time Phase	Sample Activity Conc. (Bq/g)	Sample Activity Conc. Uncertainty (Bq/g)
Single RN	First Year	4.52	2.80E-01
Mixed 1:1	First Year	4.11	2.55E-01

4.2.1.3. Laboratory Analysis Uncertainties for Scenarios

The radiochemical analysis of a ground deposition sample is modeled with a normal distribution. The mean is the expected radioactivity in a 100-cm^2 ground deposition taken at the probed location. Sample mass and area are used to convert the sample activity concentrations into deposition values in $\mu Ci/m^2$. For the Deposition DRLs listed in Table 3.3-1, the overall uncertainty propagation yields the standard deviations (SD) listed in Table 4.2-6. The distributions for the activity values calculated with uncertainties for laboratory analysis are shown in Figure 4-5 for the single radionuclide scenarios and Figure 4-6 for the scenarios with a 1:1 mixture of Cs-137 and Am-241. The distributions were truncated with a minimum value of 0 to ensure that physical values are sampled for use in the Turbo FRMAC© calculations.

Table 4.2-6. Normal distribution parameters for laboratory analysis of Cs-137 and Am-241.

Scenario		Cs-137		Am-241	
		Mean ($\mu Ci/m^2$)	Standard Deviation ($\mu Ci/m^2$)	Mean ($\mu Ci/m^2$)	Standard Deviation ($\mu Ci/m^2$)
Single RN	Early Phase (TD)	3.30E+02	13.4	4.64E-02	4.54E-03
	Early Phase (AD)	1.70E+03	68.8	8.66	3.09E-01
	First Year	42.0	1.71	4.15	2.57E-01
Mixed 1:1	Early Phase (TD)	4.64E-02	4.45E-03	4.64E-02	5.45E-03
	Early Phase (AD)	8.62	3.53E-01	8.62	3.10E-01
	First Year	3.78	1.60E-01	3.78	2.34E-01

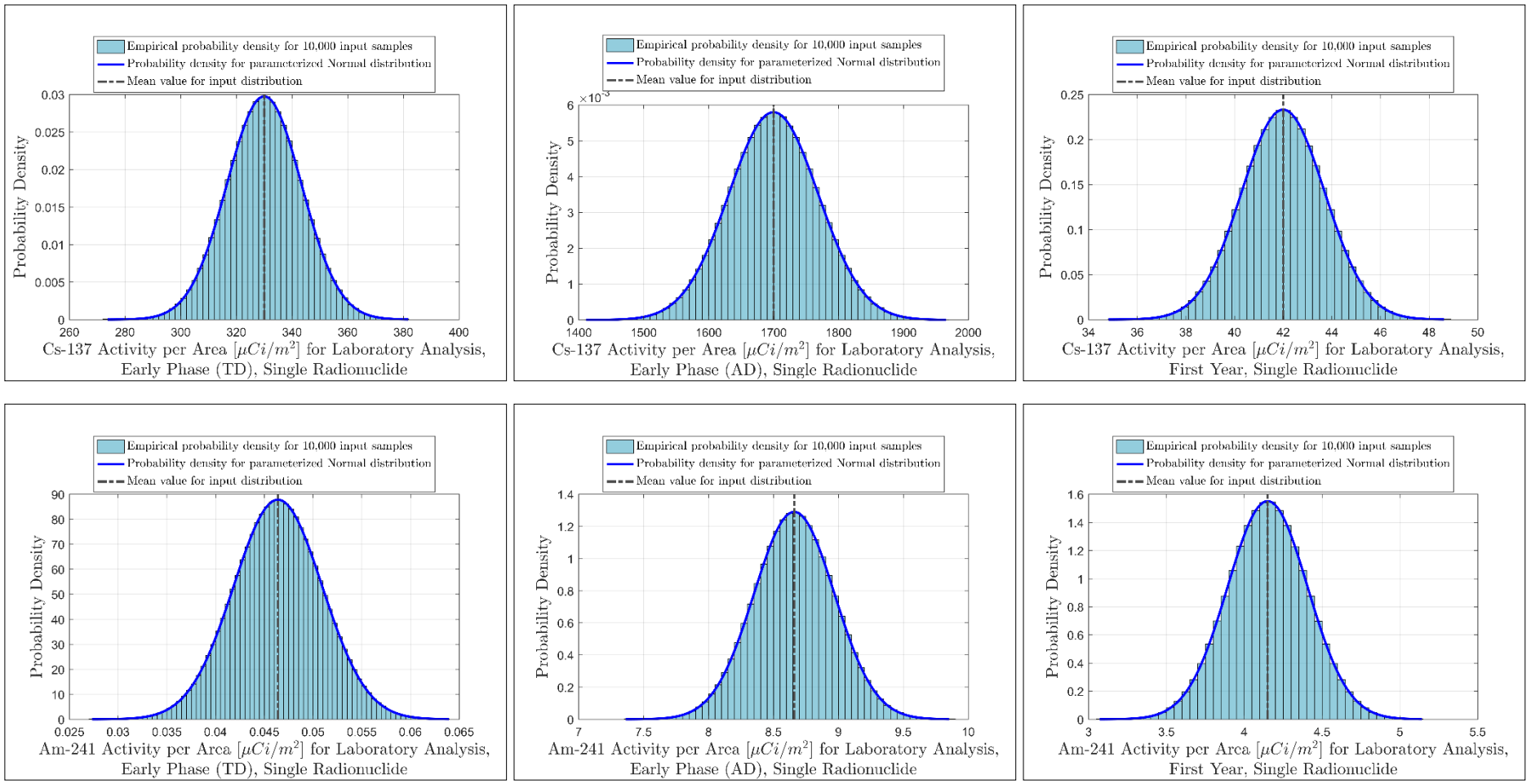

Figure 4-5. Empirical and parameterized probability densities for activity per area for laboratory analysis of single radionuclide source terms of Cs-137 and Am-241 for three time phases.

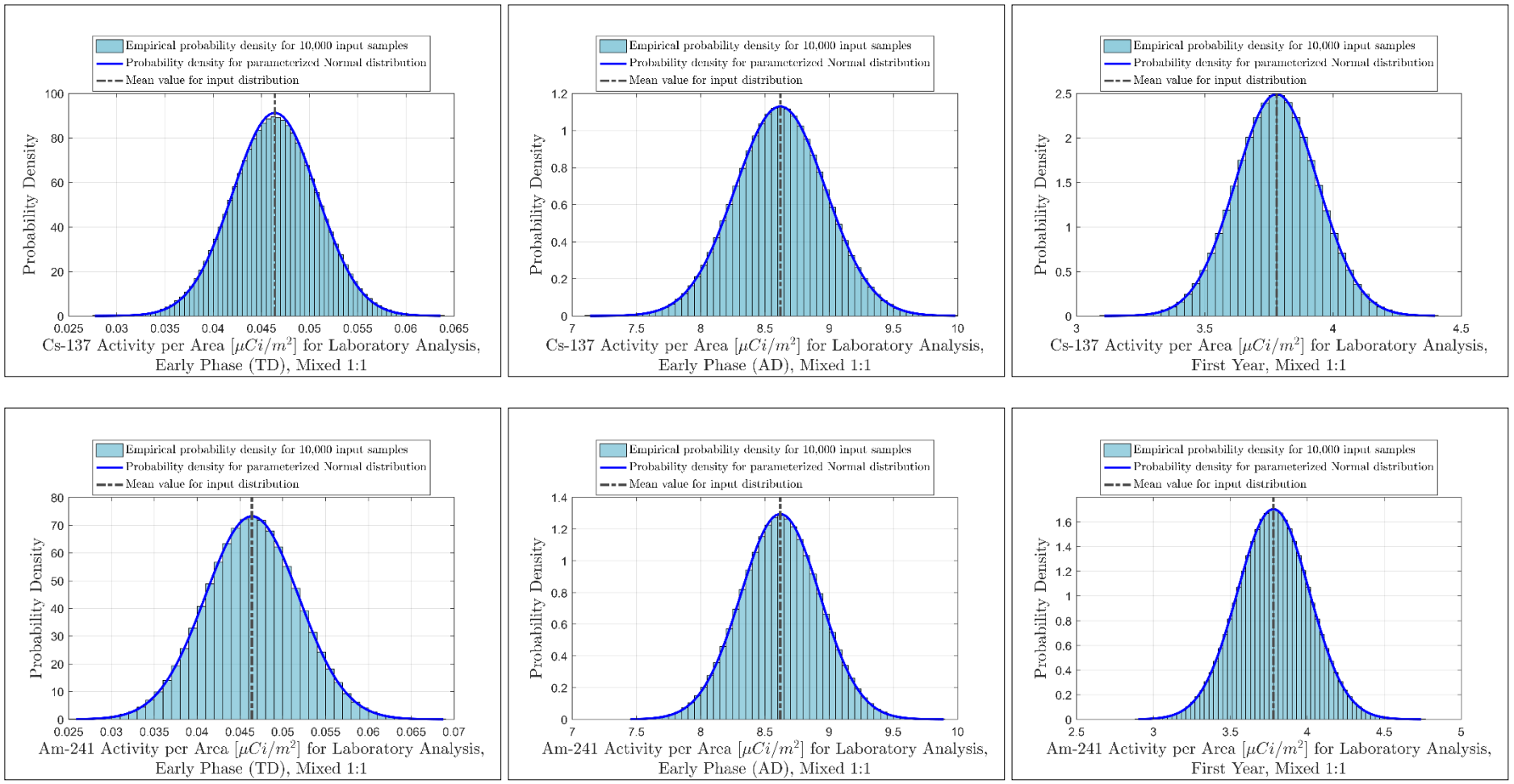

Figure 4-6. Empirical and parameterized probability densities for activity per area for laboratory analysis of a 1:1 mixture of Cs-137 and Am-241 for three time phases.

4.2.2. In Situ Deposition Measurements

The same process as was used for determining the efficiency for in situ measurements of Cs-137 contamination in FY17 [1] was carried out to get a distribution for the deposition efficiency for Am-241. Through this process, the mean efficiency for 59.54 keV gamma rays is 10.66 cps per gamma s^{-1} cm^{-2}. The distribution of efficiencies has an SD, calculated as the square root of the variance, of 0.17 cps per gamma s^{-1} cm^{-2}. Figure 4-7 shows this distribution.

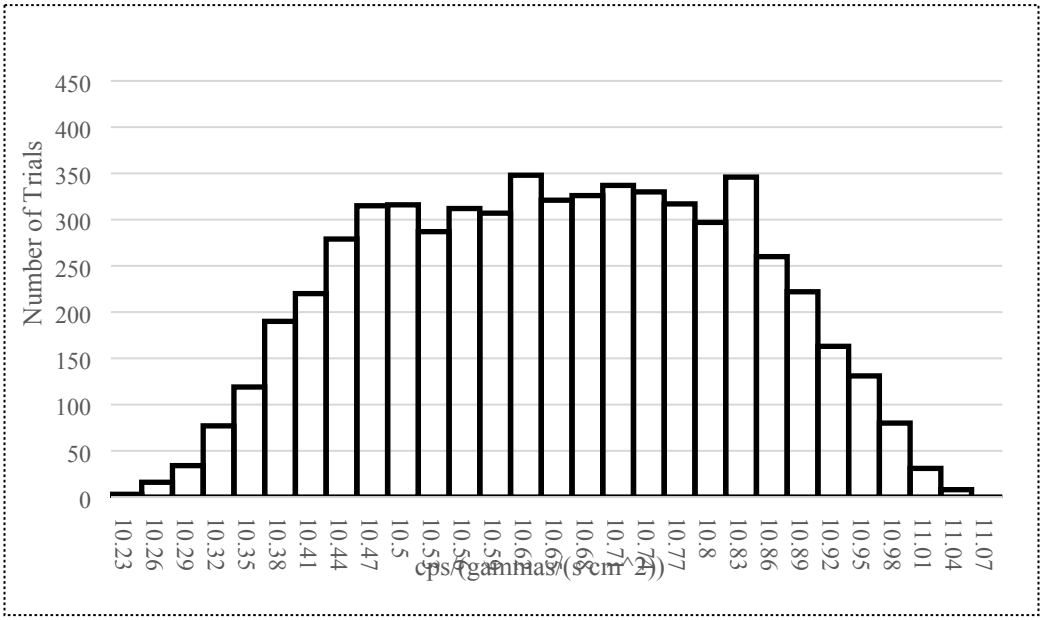

Figure 4-7. Distribution of the efficiency for a uniform surface deposition of 59.54 keV gamma rays for a DetectiveEX-100.

A 59.54 keV gamma ray is emitted 35.9% of the time in Am-241 decays. The count rate in the detector is calculated by multiplying the decay rates for the corresponding DRLs by the efficiency of 10.66 cps per gamma s^{-1} cm^{-2}. A spectrum with 300 seconds live time is assumed to calculate the gross, G, and background, B, peak counts. The uncertainty of the counts in the peak is expected to follow normal counting statistics. For this analysis, the uncertainty from the counts from the background in the spectrum are large in comparison to the supposed signal. For the purposes of this calculation, a background count rate of 6 cps is assumed. This results in a background of 1800 counts and a background count uncertainty of 42.4 counts. The combined uncertainty on the signal, σ_N, is then calculated as shown in Equation (8):

$$\sigma_N = \sqrt{\sigma_G + \sigma_B} \tag{8}$$

where:

σ_N: Net count uncertainty

σ_G: Gross count uncertainty

σ_B: Background count uncertainty

Table 4.2-7. Uncertainties in peak and background Am-241 in situ counts.

Deposition DRL (μCi/m²)	Count Rate in Detector (cps)	Gross Peak Area (counts)	Gross Uncertainty (counts)	Background (counts)	Background Uncertainty (counts)	Combined Uncertainty (counts)
4.64E-02	6.57E-01	1.97E+02	14.0	1.80E+03	42.4	44.7
3.78	53.5	1.61E+04	1.27E+02	1.80E+03	42.4	1.34E+02
4.15	58.8	1.76E+04	1.33E+02	1.80E+03	42.4	1.39E+02
8.62	1.22E+02	3.66E+04	1.91E+02	1.80E+03	42.4	1.96E+02
8.66	1.23E+02	3.68E+04	1.92E+02	1.80E+03	42.4	1.96E+02

With the counts in the peak, live time, and efficiency, the deposited activity can be re-calculated using Equation (9):

$$A = \frac{N \quad 1}{t\, y(E) \varepsilon_{dep}(E)} \tag{9}$$

where:

A: Deposition concentration of the radioactivity (Bq/m^2)

N: Net counts in the peak at energy E of a gamma ray spectrum

t: Live time of the spectrum (s)

$y(E)$: Gamma rays per decay at energy E

$\varepsilon_{dep}(E)$: Efficiency for ground deposited gamma rays of energy E (cps gamma^{-1} m^2)

The uncertainty on the deposited activity is calculated by combining the uncertainties for the counts and the efficiency as shown in Equation (10):

$$\sigma_A = \sqrt{\sigma_N^2 \times \left(\frac{1}{ty(E)\varepsilon_{dep}(E)}\right)^2 + \sigma_{eff\,dep}^{\;2} \times \left(\frac{N}{ty(E)\varepsilon_{dep}^{\;2}(E)}\right)^2} \tag{10}$$

where:

σ_A: Deposited activity uncertainty

$\sigma_{eff\,dep}(E)$: Efficiency uncertainty

For the Am-241 Deposition DRLs listed in Table 3.3-1, this propagation yields the SDs listed in Table 4.2-8. In situ uncertainties are also calculated for the Cs-137 Deposition DRLs listed in Table 3.3-1 according to the methodology described in the FY17 analysis [1]. These SDs are also listed in Table 4.2-8. The normal distributions for the activity values calculated with uncertainties for in situ deposition measurements are shown in Figure 4-8 for the single radionuclide scenarios and Figure 4-9 for the scenarios with a 1:1 mixture of Cs-137 and Am-241. The distributions were truncated with a minimum value of 0 to ensure that physical values are sampled for use in the Turbo FRMAC© calculations.

Table 4.2-8. Normal distribution parameters for in situ measurements of Cs-137 and Am-241.

Scenario		Cs-137		Am-241	
		Mean ($\mu Ci/m^2$)	Standard Deviation ($\mu Ci/m^2$)	Mean ($\mu Ci/m^2$)	Standard Deviation ($\mu Ci/m^2$)
Single RN	Early Phase (TD)	3.30E+02	3.73	4.64E-02	1.05E-02
	Early Phase (AD)	1.70E+03	19.2	8.66	1.46E-01
	First Year	42.0	4.79E-01	4.15	7.39E-02
Mixed 1:1	Early Phase (TD)	4.64E-02	2.35E-03	4.64E-02	1.05E-02
	Early Phase (AD)	8.62	1.01E-01	8.62	1.45E-01
	First Year	3.78	4.65E-02	3.78	6.80E-02

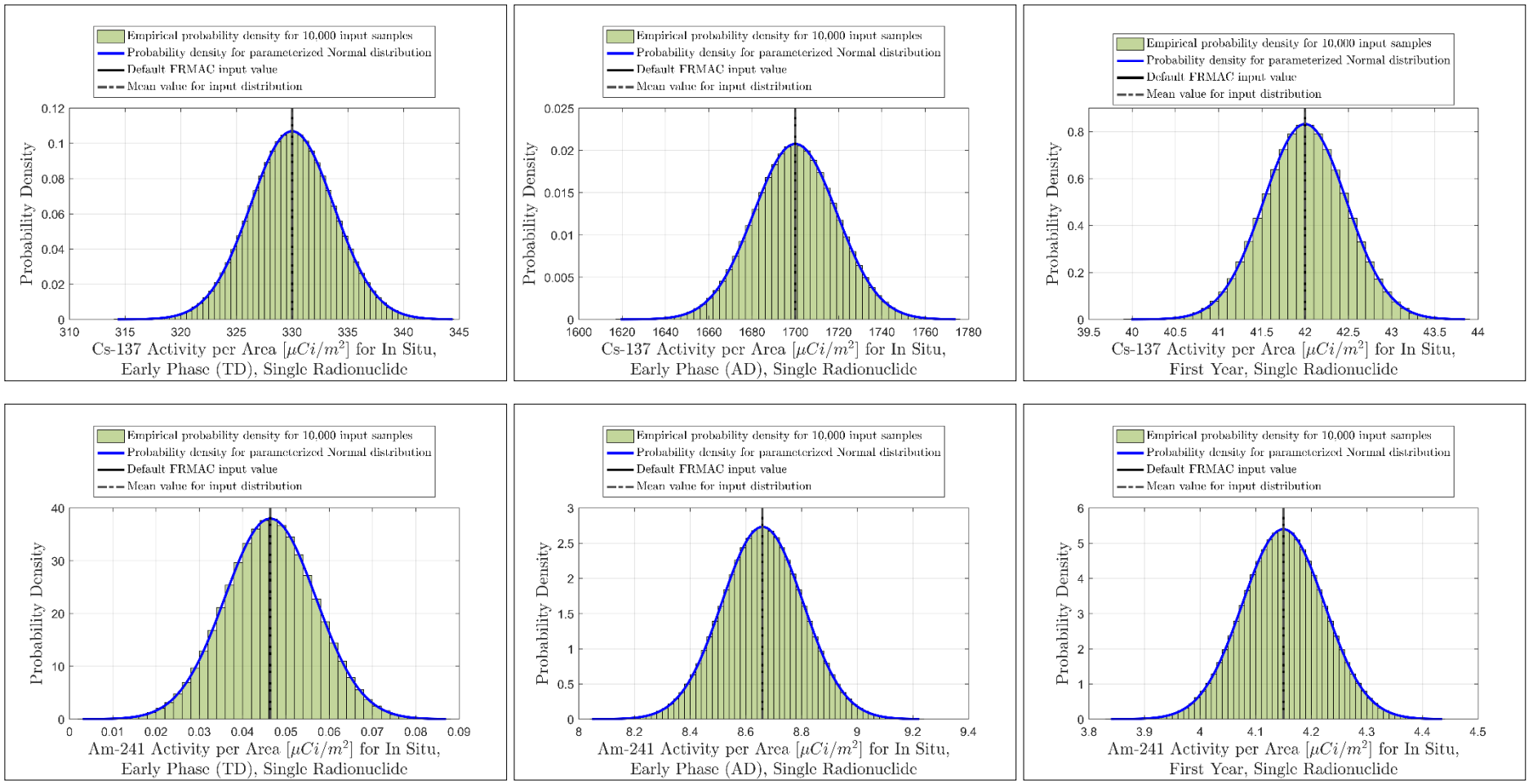

Figure 4-8. Empirical and parameterized probability densities for activity per area for in situ deposition measurements of single radionuclide source terms of Cs-137 and Am-241 for three time phases.

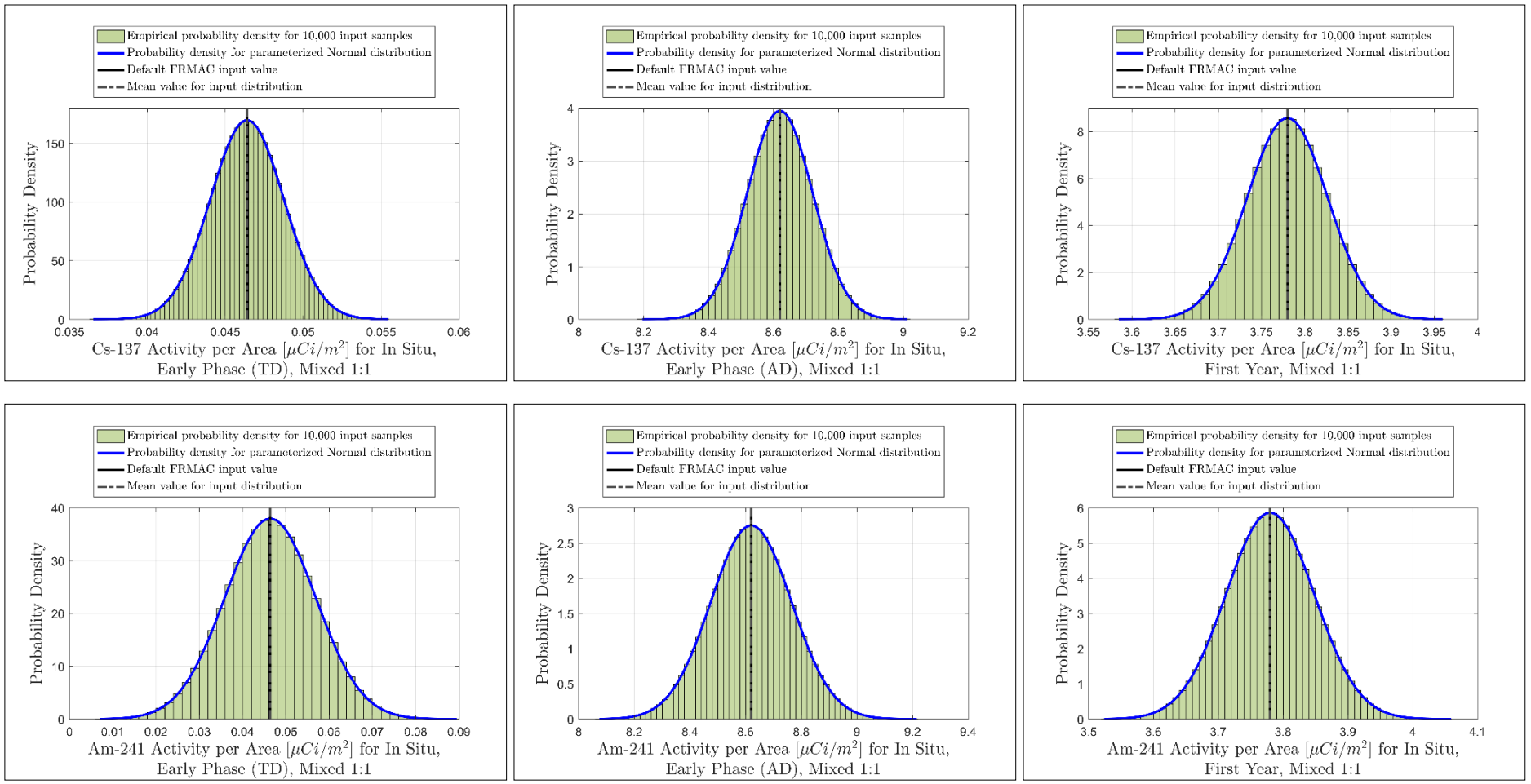

Figure 4-9. Empirical and parameterized probability densities for activity per area for in situ deposition measurements of a 1:1 mixture of Cs-137 and Am-241 for three time phases.

4.2.3. AMS Measurements

For extraction of a low-level Am-241 signal from the data collected with an aerial platform, a 3-window extraction process is likely to be used. In this process, the spectrum is broken down into three components: Am-241 signal region (36-72 keV) and two background regions (21-36 and 72-87 keV). A ratio, R, of the counts in the signal region ($N_{a,0}$) to the counts in the background region ($N_{b,0}$,$N_{c,0}$) is determined by data collected over an uncontaminated area, as shown in Equation (11):

$$R = \frac{N_{a,0}}{N_{b,0} + N_{c,0}} \tag{11}$$

The ratio is used to calculate the expected counts in the signal region, in the absence of contamination. The excess counts in the signal region are taken to be from the contamination, N_{Am}, as shown in Equation (12):

$$N_{Am} = N_a - R \times (N_b + N_c) \tag{12}$$

The extracted counts must be corrected for the measurement altitude, and a scale factor to convert the result to an activity concentration on the ground. This correction is shown in Equation (13):

$$A = K \times \left(N_a - R \times (N_b + N_c)\right) \times e^{\mu\left(z - z_0\right)} \tag{13}$$

where:

A: Deposited activity

K: Conversion factor for the count rate at altitude z_0

μ: Effective attenuation coefficient = 6.74E-03 (m^{-1})

z: Altitude above ground level (AGL)

z_0: Nominal altitude

The uncertainty for the activity concentration that has been derived from this process should include the contributions from all of the components. If the uncertainties are propagated in the normal manner, the variance, σ_A^2, is given by Equation (14):

$$\sigma_A^2 = \sigma_K^2\left(N_a - R \times (N_b + N_c)\right)^2 \times e^{2\mu\left(z - z_0\right)} + \sigma_\mu^2 K^2\left(N_a - R \times (N_b + N_c)\right)^2 e^{2\mu\left(z - z_0\right)}\left(z - z_0\right)^2 + \sigma_z^2 K^2\left(N_a - \right. \tag{14}$$

with a ratio variance, σ_R^2, given by Equation (15):

$$\sigma_R^2 = \frac{\sigma_{a,0}^{\ 2}}{\left(N_{b,0} + N_{c,0}\right)^2} + \frac{N_{a,0}^{\ 2} \times \left(\sigma_{b,0}^{\ 2} + \sigma_{c,0}^{\ 2}\right)}{\left(N_{b,0} + N_{c,0}\right)^4}. \quad (15)$$

The correction of only the count rate and its uncertainty will be considered first. To accomplish this, the conversion factor is set to 1 and it is assumed that the mission is flown at the nominal altitude (i.e., $z = z_0$). With these simplifications, the uncertainty on the corrected count rate reduces to Equation (16):

$$\sigma_A^2 = \sigma_z^2\left(N_a - R \times \left(N_b + N_c\right)\right)^2\mu^2 + \left(\sigma_a^2 + R^2 \times \left(\sigma_b^2 + \sigma_c^2\right) + \left(N_b + N_c\right)^2 \times \sigma_R^2\right) \quad (16)$$

The counts in the two background regions will be the same over the uncontaminated area and the contaminated area if only Am-241 is present. The uncertainty then reduces further to Equation (17):

$$\sigma_A^2 = \sigma_z^2 N_{Am}^{\ 2}\mu^2 + \left(\left(N_{Am} + N_{a,0}\right) + R^2 \times \left(N_{b,0} + N_{c,0}\right) + \left(N_{b,0} + N_{c,0}\right)^2 \times \sigma_R^2\right) \quad (17)$$

Table 4.2-9 provides counts for the ROIs and the calculated ratios and ratio uncertainties for fixed-wing and helicopter at different nominal altitudes and using different altitude measurement methods. From the analysis performed in FY17, the uncertainty in the measurement altitude depends on the mechanism used for measuring the altitude: ±3 m for GPS; ±0.7 m for radar altimeter (RA).

Table 4.2-9. ROI inputs for fixed-wing and helicopter aerial systems.

Platform	Nominal Altitude	ROI a0 (36-72 keV)	ROI b0 (21-36 keV)	ROI c0 (72-87 keV)	Ratio	Ratio Uncertainty
Fixed-wing	50 m AGL	841.4	140	503.2	1.31	0.069
	150 m AGL	617.3	103.8	289.4	1.57	0.101
Helicopter	50 m AGL	3365.7	559.9	2012.8	1.31	0.034
	150 m AGL	3341	557.5	1827.3	1.40	0.038

Table 4.2-10 shows the results from the uncertainty propagation using Equation (17) for the fixed-wing platform at 150 m.

Table 4.2-10. Uncertainty in estimated count rate in the aerial detectors flying over an area that is uniformly contaminated at the Am-241 DRLs.

Deposition DRL (μCi/m²)	cps per DRL in μCi/m²	Uncertainty of Corrected Counts	Percent Uncertainty
4.64E-02	1.79	56.3	3148
3.78	1.46E+02	57.7	40
4.15	1.60E+02	57.8	36
8.62	3.33E+02	59.6	18
8.66	3.34E+02	59.6	18

The uncertainties in this table must then be propagated to a ground contamination value that includes calibration uncertainty. This process is described in the FY17 report [1]. The calibration line activity is assumed to be close to the activity of the First Year DRL, or 3.78 μCi/m². Using the in situ uncertainty calculation described in Section 4.2.2, the calculated uncertainty of the calibration activity is equal to 6.80E-02 μCi/m². The full propagation yields the ground contamination uncertainties listed in Table 4.2-11.

AMS uncertainties were also calculated for the Cs-137 Deposition DRLs listed in Table 3.3-1 according to the methodology described in the FY17 analysis [1], with a slight change in accounting for background. In FY17, Cs-137 background was assumed to be negligible compared to the DRL for the analyzed scenario. In FY18, a background count rate of 0.5 cps for 300 s is assumed. The SDs calculated for the Cs-137 Deposition DRLs are listed in Table 4.2-11.

The distributions for the activity values calculated with uncertainties for AMS measurements are shown in Figure 4-10 for the single radionuclide scenarios and Figure 4-11 for the scenarios with a 1:1 mixture of Cs-137 and Am-241. The distributions were truncated with a minimum value of 0 to ensure that physical values are sampled for use in the Turbo FRMAC© calculations. This truncation is visually noticeable in the distributions for the small Early Phase (TD) DRLs (4.64E-02 µCi/m^2).

Table 4.2-11. Normal distribution parameters for AMS measurements of Cs-137 and Am-241.

Scenario		Cs-137		Am-241	
		Mean (µCi/m^2)	Standard Deviation (µCi/m^2)	Mean (µCi/m^2)	Standard Deviation (µCi/m^2)
Single RN	Early Phase (TD)	3.30E+02	9.31	4.64E-02	1.46
	Early Phase (AD)	1.70E+03	47.9	8.66	1.71
	First Year	42.0	1.27	4.15	1.54
Mixed 1:1	Early Phase (TD)	4.64E-02	4.81E-01	4.64E-02	1.46
	Early Phase (AD)	8.62	5.34E-01	8.62	1.71
	First Year	3.78	4.90E-01	3.78	1.53

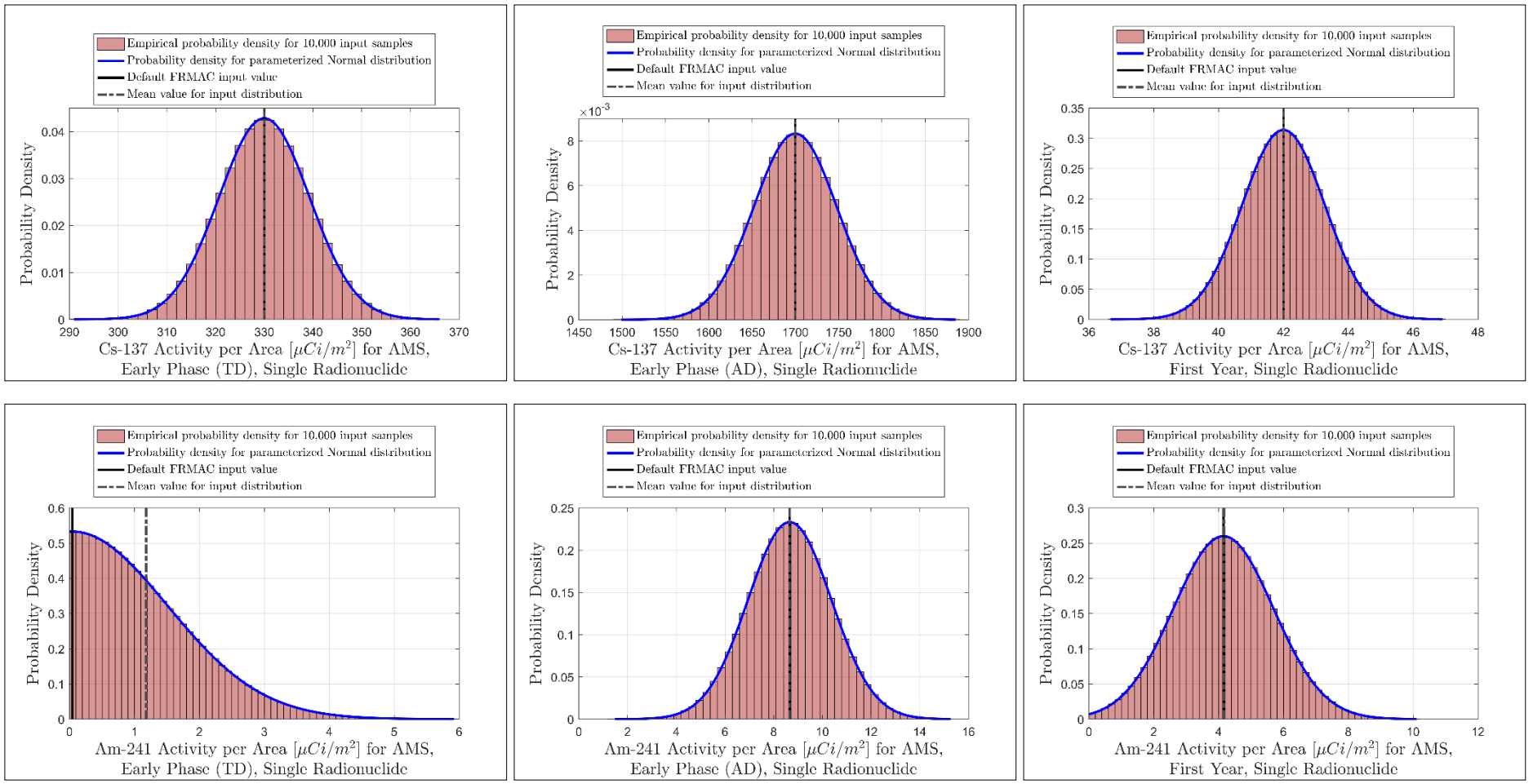

Figure 4-10. Empirical and parameterized probability densities for activity per area for AMS measurements of single radionuclide source terms of Cs-137 and Am-241 for three time phases.

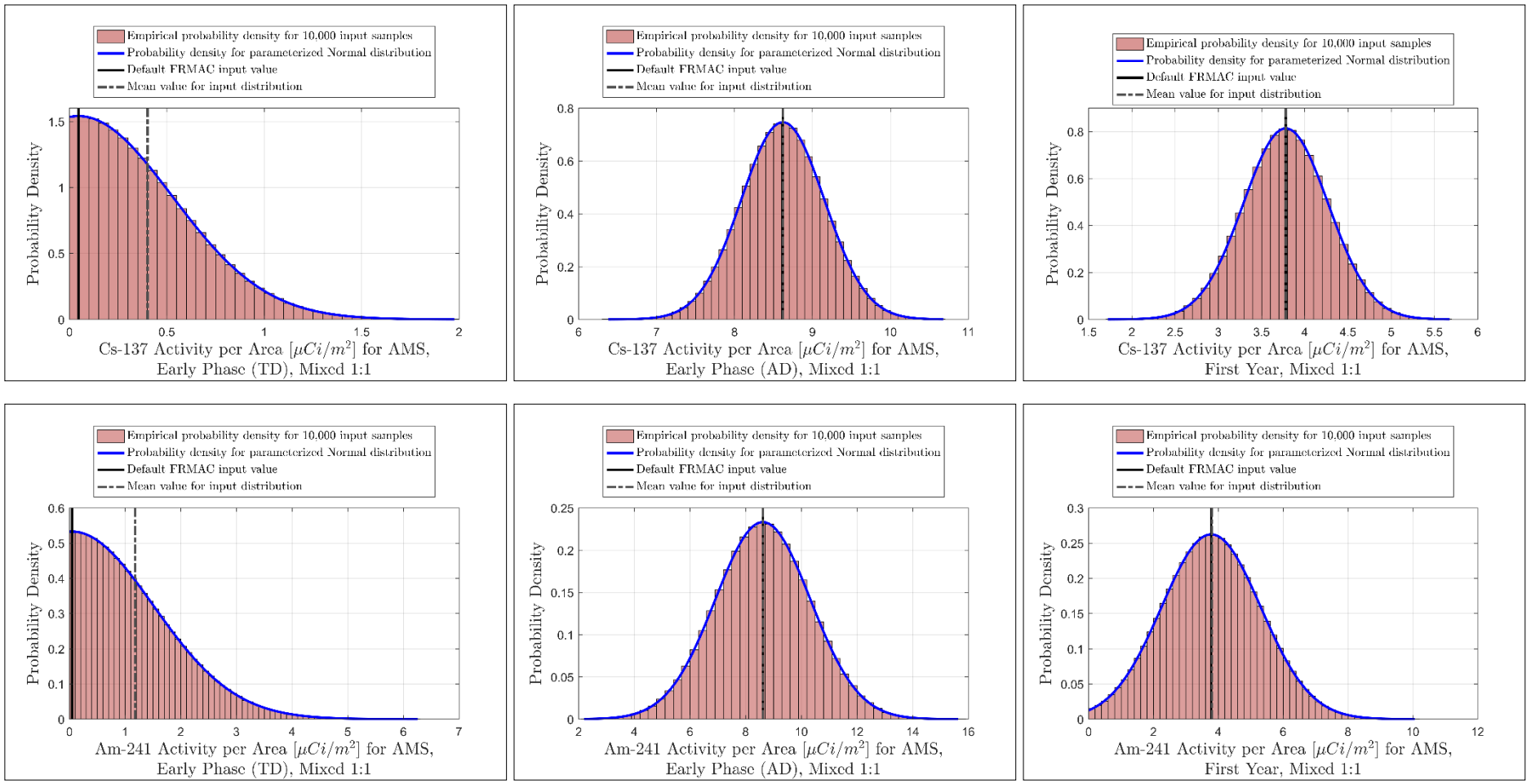

Figure 4-11. Empirical and parameterized probability densities for activity per area for AMS measurements of a 1:1 mixture of Cs-137 and Am-241 for three time phases.

4.2.4. Relative Error Summary

Table 4.2-12 includes a summary of the relative errors associated with each measurement type for each scenario of interest. The relative errors are presented as percentage that equals the ratio of the absolute error (standard deviation) to the measurement (mean). For the single-radionuclide scenarios, the errors associated with measurement of Cs-137 are very similar among the measurement types. For Am-241, the AMS measurement error becomes relatively large for the smaller DRLs. For the 1:1 mixed source scenarios, the presence of Am-241 drives down the DRL for Cs-137, causing its associated measurement error to increase compared to Cs-137 alone.

Table 4.2-12. Relative errors for Laboratory Analysis, In Situ, and AMS measurement of DRLs.

Scenario		Cs-137			Am-241		
		Laboratory Analysis	In Situ	AMS	Laboratory Analysis	In Situ	AMS
Single RN	Early Phase (TD)	4%	1%	3%	10%	23%	3148%
	Early Phase (AD)	4%	1%	3%	4%	2%	20%
	First Year	4%	1%	3%	6%	2%	37%
Mixed 1:1	Early Phase (TD)	10%	5%	1037%	12%	23%	3148%
	Early Phase (AD)	4%	1%	6%	4%	2%	20%
	First Year	4%	1%	13%	6%	2%	40%

4.3. NARAC Atmospheric Dispersion for a Complex Release

This section documents the method used to quantify NARAC deposition plume uncertainty in relation to the project demonstration case study scenario. In Section 4.3.1, NARAC predicted air concentration uncertainty metrics developed using experimental data for a complex terrain and wind flow environment are discussed. NARAC air concentration uncertainty quantification for this scenario is documented in Section 4.3.2. Final quantified NARAC plume uncertainty for implementation in the uncertainty analysis is summarized in Section 4.3.3.

4.3.1. Benchmark Data

Concentration measurement data used to quantify NARAC model error for a 'complex scenario' were collected during the Diablo Canyon Tracer Experiment (hereafter referred to as 'DOPPTEX'). The DOPPTEX field campaign [12], [13] consisted of eight independent release tests of sulfur hexafluoride (SF_6) gas over the period of August 31 to September 17, 1986. SF_6 is an ideal gas for tracer experiments since it is inert, does not undergo dry or wet deposition, and has relatively low background levels except in localized regions where high and medium voltage switchgear stations are present. For each experiment, tracer gas was released for eight hours near

the surface from the Diablo Canyon Nuclear Power Plant (DCNPP), which is located along the central California coast near the city of San Luis Obispo (Figure 4-12). Complex terrain surrounds the DCNPP with numerous canyons and ridges with peak heights of around 500 m above sea level. In addition to complex terrain, the occurrence of moderate strength sea breeze induced coastal circulations makes atmospheric dispersion modeling particularly challenging within the region.

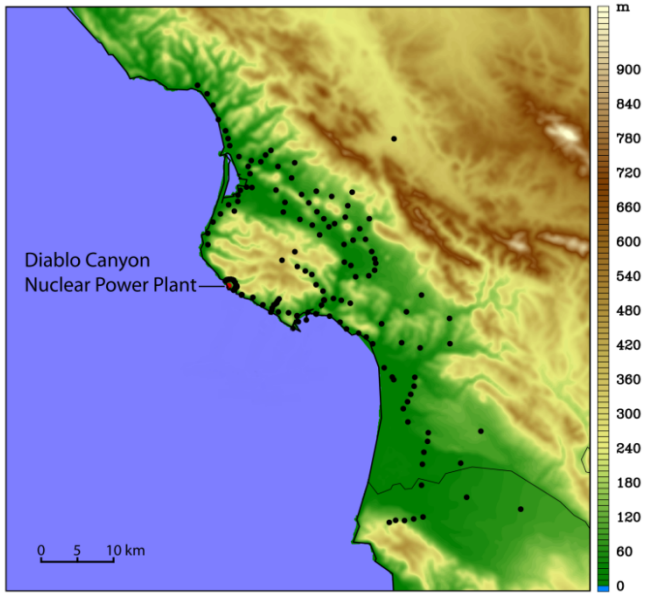

Figure 4-12. Map of DOPPTEX sensor locations and topography.

A total of 150 surface sensors were used to build an air concentration sampling network during DOPPTEX. Most of the sensors were located within a 35 km radius of the DCNPP. Sensor locations (denoted by black dots) and terrain elevation of the study area are shown in Figure 4-12. Placement of the air concentration sensors was selected to optimally record the path and spatial extent of tracer gas plumes as they interact with terrain features (e.g., canyons). The sensors provided hourly average air concentrations from the start of daily experimental releases (8am PDT) until 3 hours after the tracer release ended (7pm PDT). Air concentration measurements from tracer release #3, which occurred on September 4, 1986, are used for this model error analysis. This specific test case is utilized for the FY18 complex dispersion scenario since previous research revealed it to be among the most challenging periods to model due to complicated local wind flow patterns [14].

Due to the complex terrain and highly complicated local winds, high-resolution meteorological fields for DOPPTEX case study period #3 were generated using the Weather Research and Forecast (WRF) atmospheric model [15] since available reanalysis data were too coarse for accurate atmospheric transport modeling. A total of 5 WRF model domains were used to nest down to a horizontal grid spacing of 300 m within the innermost domain. The WRF four-dimensional data assimilation option was used to nudge the outer domains towards gridded reanalysis fields. Surface METAR and DCNPP multi-level tower weather observations were assimilated within the inner WRF domains to improve modeling accuracy.

4.3.2. Quantifying NARAC Concentration Uncertainty

Hourly air concentration fields for DOPTTEX tracer release #3 were predicted using the WRF simulated wind fields previously described and the NARAC Lagrangian dispersion model, LODI [16], [17]. Model generated concentration data were compared with hourly DOPPTEX measurements based on corresponding averaging period and geographic location. A total of 481 model to measurement comparisons were available based on the atmospheric plume evolution and sensor locations.

A metric useful for quantifying dispersion model accuracy is the ratio, *r,* of observed concentration values to predicted values at the same time and location. Metrics such as r are useful for comparing observed and predicted air and depositions concentration values that can range over several orders of magnitude. The equation for *r* is given by Equation (18):

$$r = \frac{observed\ value}{model\ predicted} \tag{18}$$

Based on the above equation, predicted concentration values within a factor of 2 of observations means ½ < r < 2. For example, if an arbitrary concentration measurement is 1 ng/m^2, then both predicted values of 0.5 and 2 ng/m^2 are within a factor of 2 of the observed value.

A summary of the *r* values distribution for the NARAC DOPTTEX experiment simulation is shown in Table 4.3-1. Roughly 19% of NARAC predicted air concentration values are within a factor of 2 of the observed value while around 46% are within a factor of 5. Just over 59% of NARAC predicted values are within a factor of 10 of DOPPTEX measured concentrations.

Table 4.3-1. Distribution of NARAC observed to predicted concentration ratios for the Diablo Canyon tracer gas experiment.

Experiment	% *r* in factor 2	% *r* in factor 5	% *r* in factor 10
Diablo Canyon	19	46	59

The key points listed below regarding the NARAC model error distribution need to be acknowledged in the context of the full CM product uncertainty modeling. The FY18 complex scenario NARAC model error distribution:

- represents error for the current state of NARAC modeling capabilities (both meteorological and dispersion modeling)
- provides a reasonable upper range of model uncertainty for complex terrain and wind fields
- represents error for a simulation made in the past (often called a hindcast) versus a pure forecast where the weather uncertainty can be much larger particularly for extended forecast horizons

- assumes the atmospheric release source amount, timing, and physical characteristics are known, and
- provides a model error distribution in terms of air concentration and requires an additional level of uncertainty modeling for deposition processes (as was demonstrated in FY17) to quantify CM surface contamination uncertainty.

4.3.3. Implementation of NARAC Uncertainty

Although the ratio of the observed value to the model prediction, given in Equation (18), can be used to characterize the uncertainty in a prediction at a fixed point in the plume, the direct use of this ratio for all measurements taken through time to generate a probability distribution for the integrated air concentration is not straightforward given the more complicated nature of the scenario of interest.

A spatial mapping of the log of the measured air concentration (left) and simulated air concentration (right) values for each measurement time are compared in Figure 4-13 through Figure 4-23 below. These air concentration values are averaged over the hour of measurement. The color scale used to denote the log of the air concentration is the same for both of the air concentration sources for ease of comparison. In addition, the space between stations is linearly interpolated using a nearest neighbor approach to better represent the distribution of air concentration values across the measurement field. This interpolation is used for visualization purposes only and does not impact the comparison calculations.

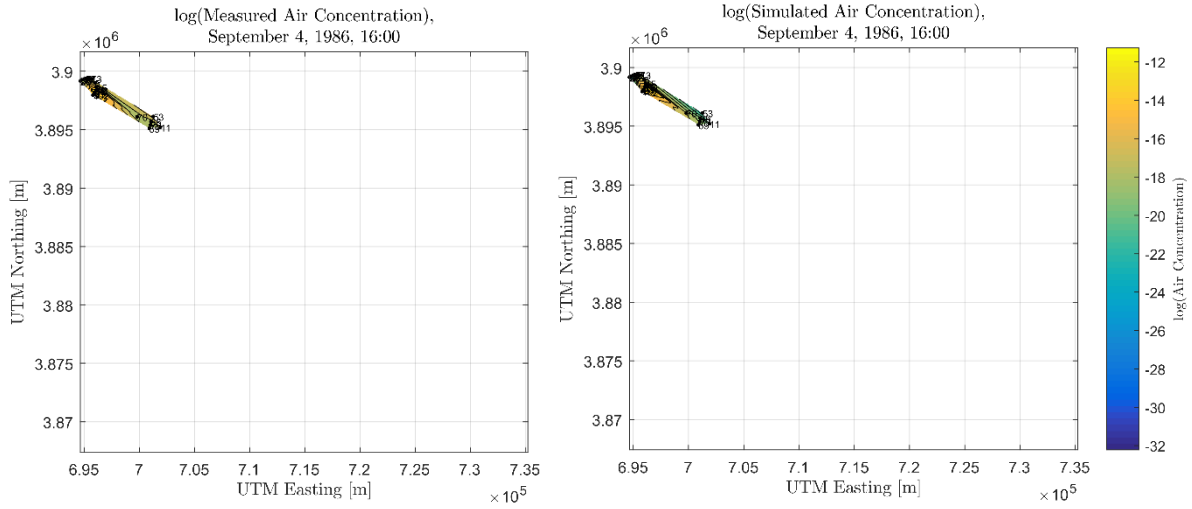

Figure 4-13. Comparison spatial distribution of log of measured air concentration (left) and log of simulated air concentration (right) for September 4, 1986, 16:00.

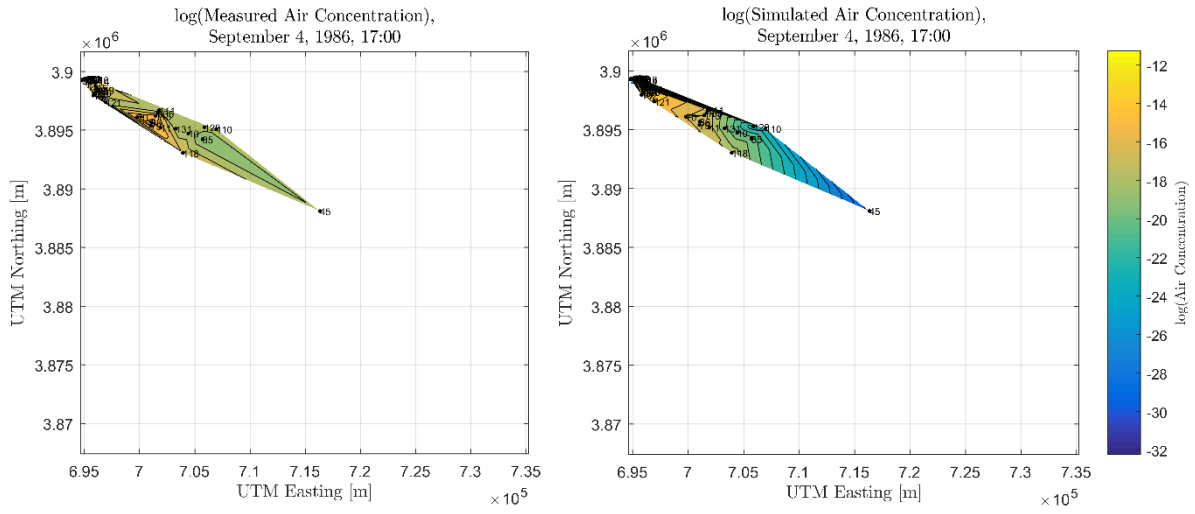

Figure 4-14. Comparison spatial distribution of log of measured air concentration (left) and log of simulated air concentration (right) for September 4, 1986, 17:00.

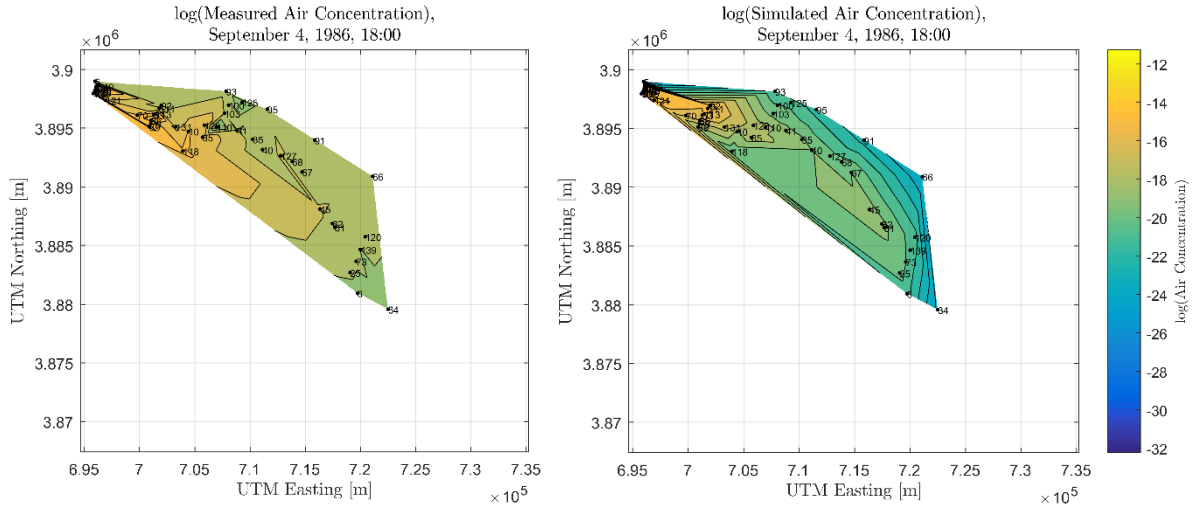

Figure 4-15. Comparison spatial distribution of log of measured air concentration (left) and log of simulated air concentration (right) for September 4, 1986, 18:00.

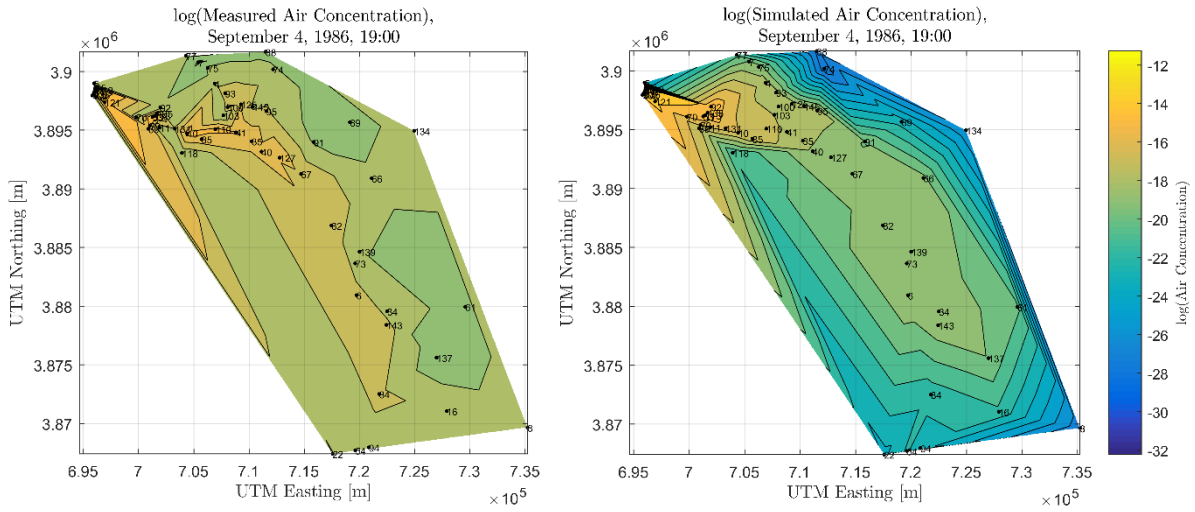

Figure 4-16. Comparison spatial distribution of log of measured air concentration (left) and log of simulated air concentration (right) for September 4, 1986, 19:00.

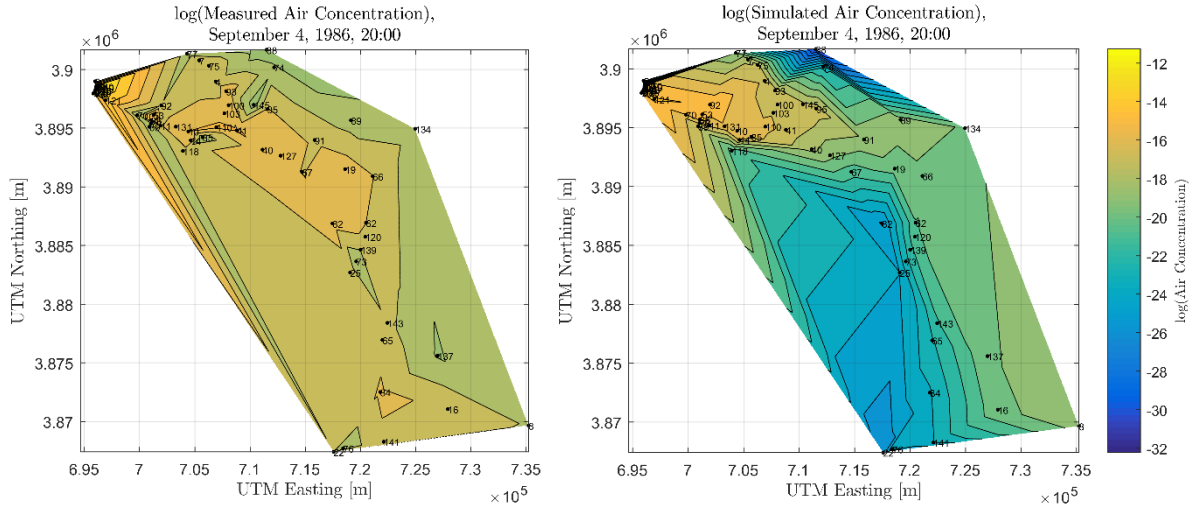

Figure 4-17. Comparison spatial distribution of log of measured air concentration (left) and log of simulated air concentration (right) for September 4, 1986, 20:00.

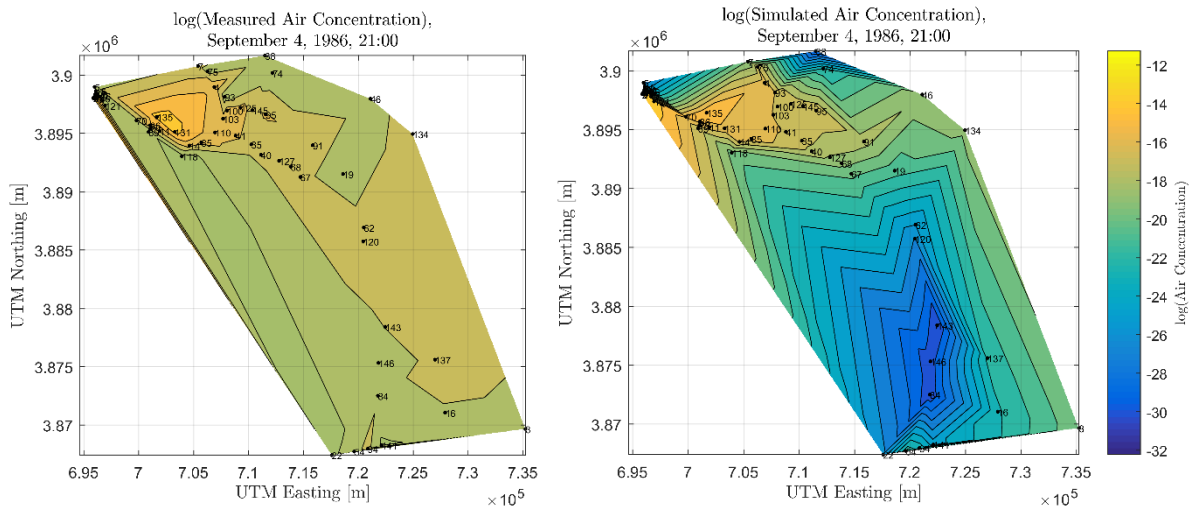

Figure 4-18. Comparison spatial distribution of log of measured air concentration (left) and log of simulated air concentration (right) for September 4, 1986, 21:00.

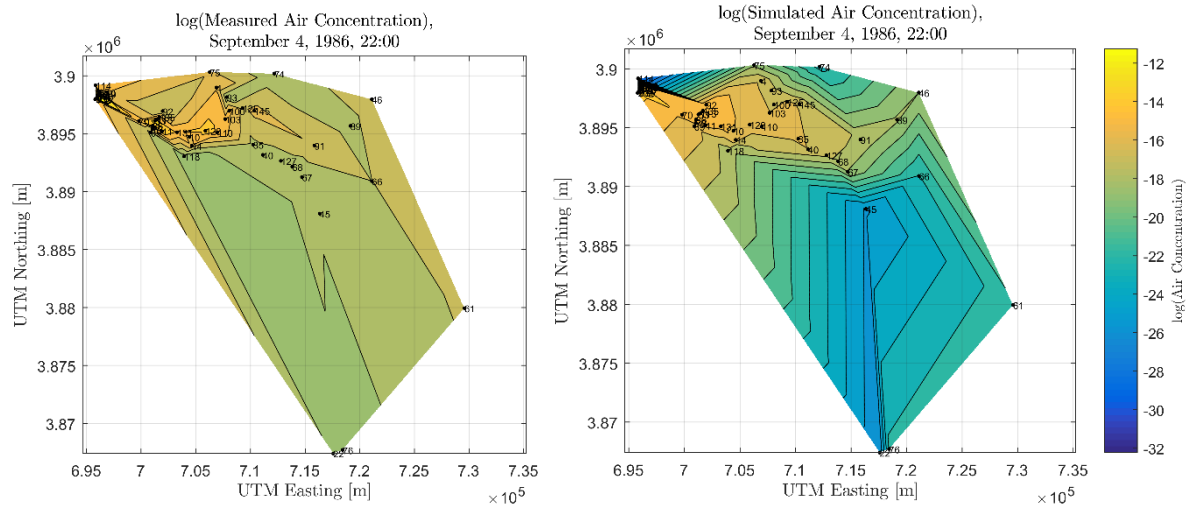

Figure 4-19. Comparison spatial distribution of log of measured air concentration (left) and log of simulated air concentration (right) for September 4, 1986, 22:00.

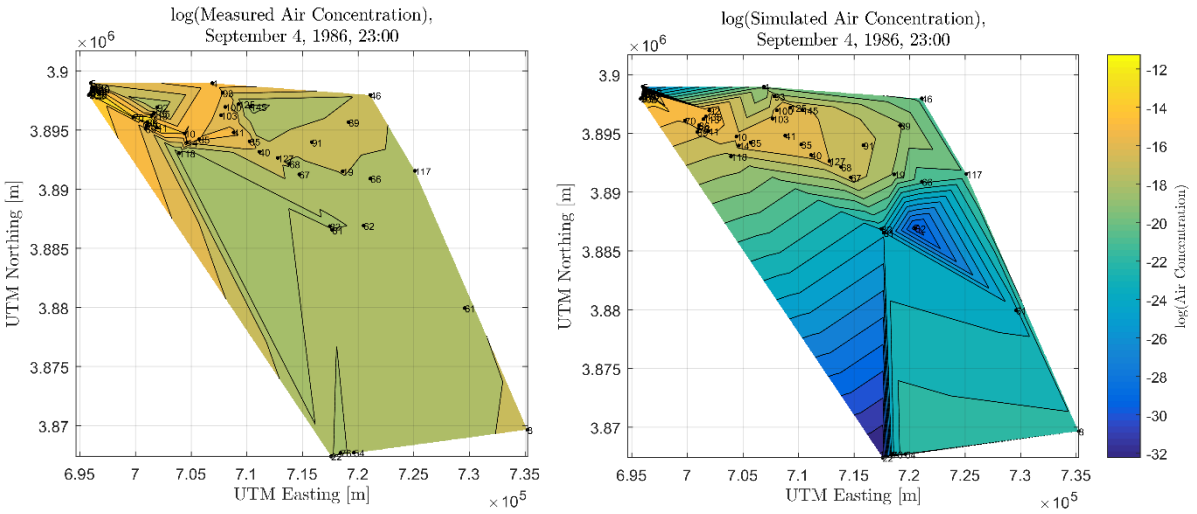

Figure 4-20. Comparison spatial distribution of log of measured air concentration (left) and log of simulated air concentration (right) for September 4, 1986, 23:00.

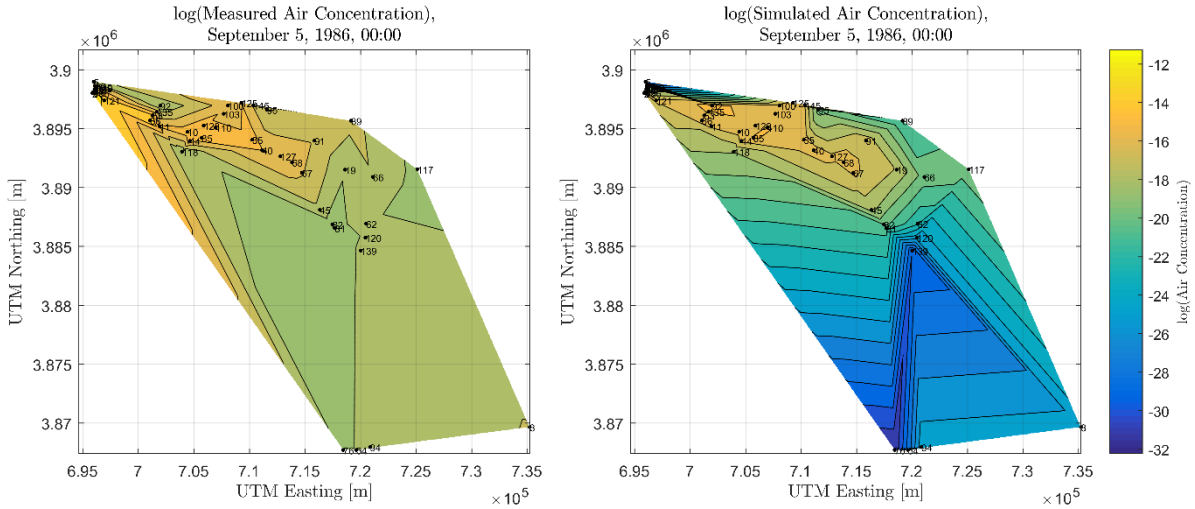

Figure 4-21. Comparison spatial distribution of log of measured air concentration (left) and log of simulated air concentration (right) for September 5, 1986, 00:00.

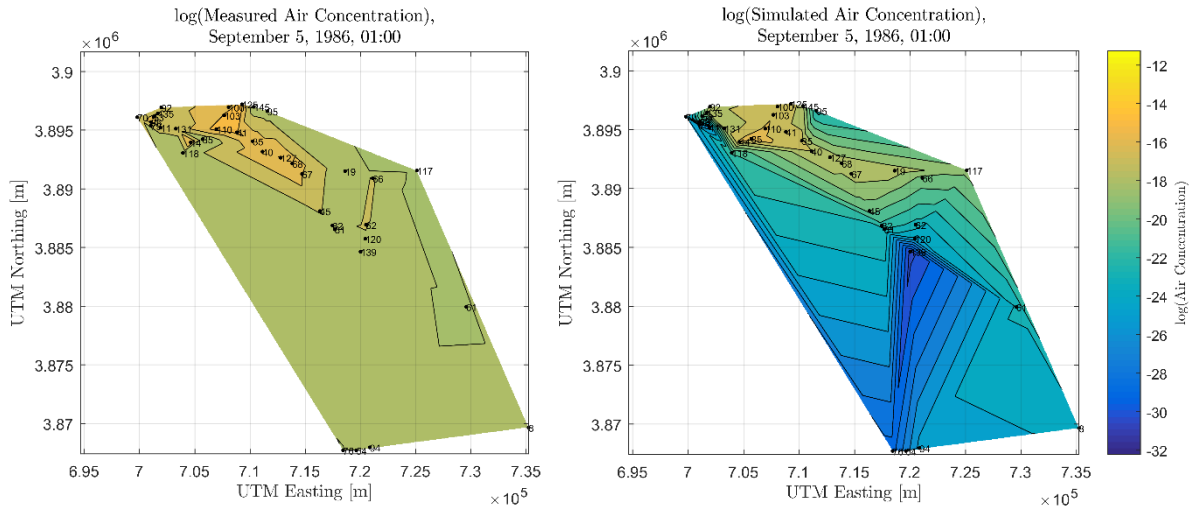

Figure 4-22. Comparison spatial distribution of log of measured air concentration (left) and log of simulated air concentration (right) for September 5, 1986, 01:00.

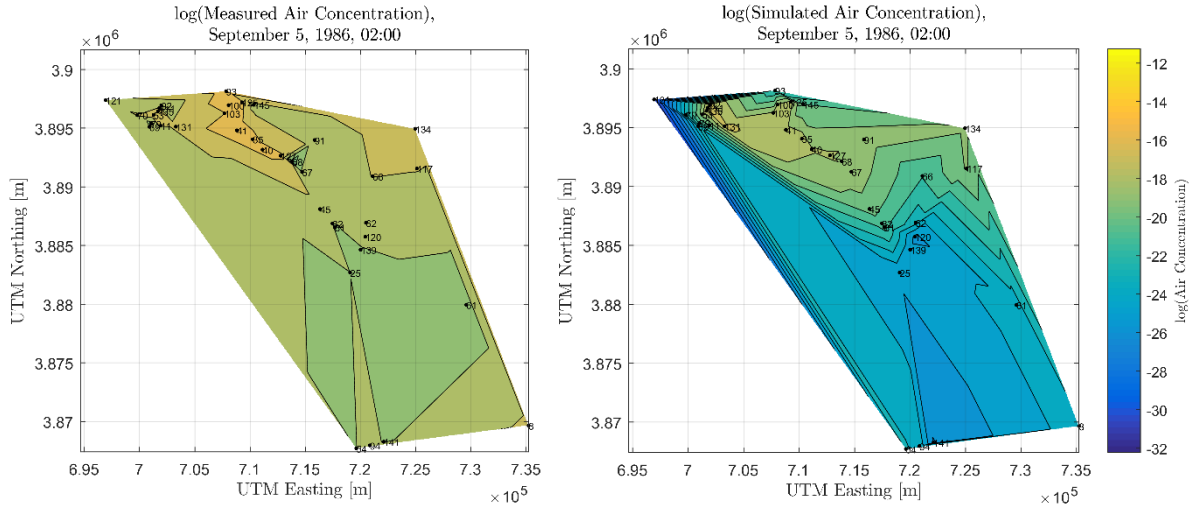

Figure 4-23. Comparison spatial distribution of log of measured air concentration (left) and log of simulated air concentration (right) for September 5, 1986, 02:00.

Turbo FRMAC© Public Protection DRL calculations require integrated air concentrations for each radionuclide in the source term, rather than individual point estimates like the data provided by DOPTTEX. The integrated air concentration can be estimated for each measurement station for both the measurements and corresponding simulations using the values at each station as a function of time through a trapezoidal approximation. This method was used to estimate the integrated air concentration for all stations for both the measured air concentration and the simulated air concentration data. Stations for which only a single measurement was available were excluded from the collection of integrated air concentration values. This resulted in a set of 80 stations with estimated measurement and simulation integrated air concentrations.

For each station, the ratio of measurement and simulated integrated air concentration values was calculated as described in Equation (18). A plot of the log of this ratio is shown in Figure 4-24.

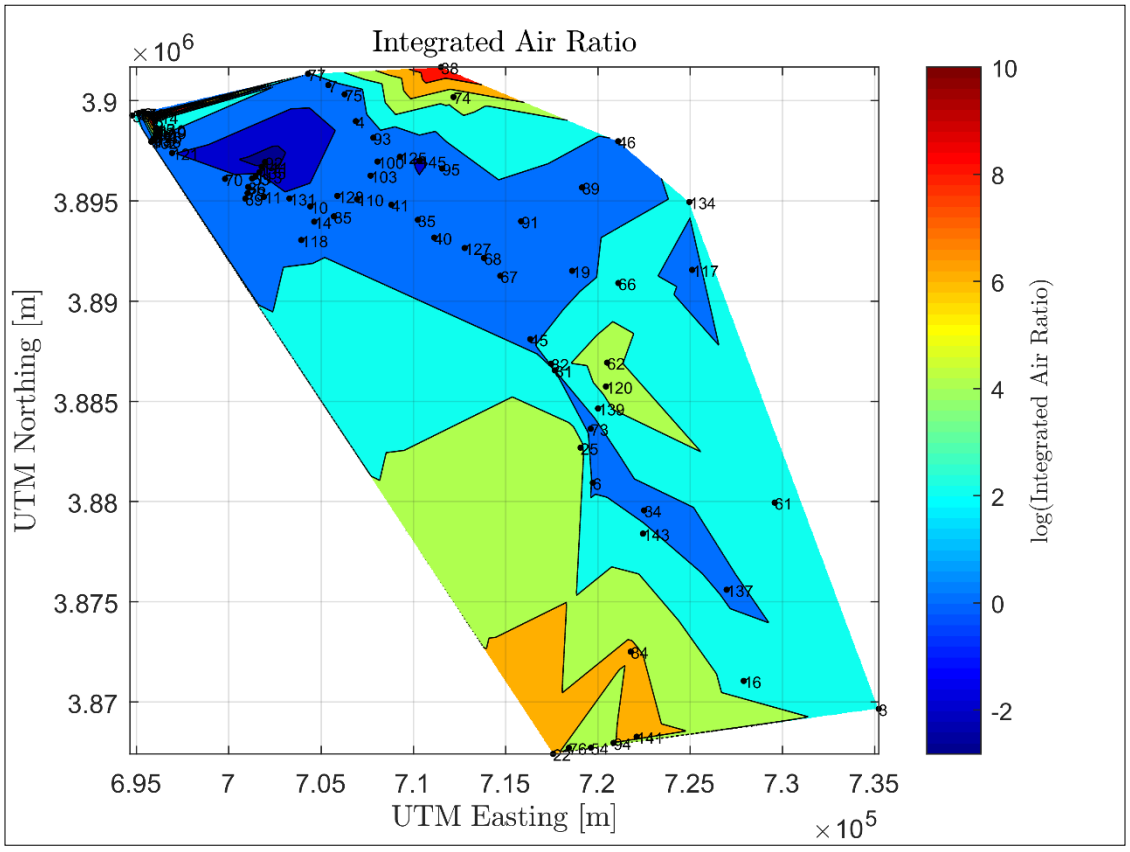

Figure 4-24. Spatial distribution of the integrated air concentration ratio calculated for sites with more than one measurement.

The spatial distribution of the integrated air concentration ratio shown in Figure 4-24 is a better representation of the distribution comparing the observed and predicted values for probabilistic simulations using NARAC inputs as the activity source. However, the distribution shown in Figure 4-24 remains convoluted by spatial differences at each measurement location that may hinder the selection of a distribution for this comparison. Outliers further from the center of the plume would not necessarily be used for simulations in a realistic CM response scenario.

The use of an outlier removal technique to identify and remove outliers in NARAC field data was demonstrated and implemented as described in [18]. This technique uses Peirce's Criterion, presented and refined in [19], [20], and [21], to determine if outliers should be removed from the data. Peirce's Criterion was used to remove outliers from the spatial distribution shown in Figure 4-24. This outlier removal was completed using the 'Peirce' package in R [22] and resulted in the removal of 10 outliers. The spatial distribution of the log of the integrated air concentration ratio with these outliers removed is shown in Figure 4-25.

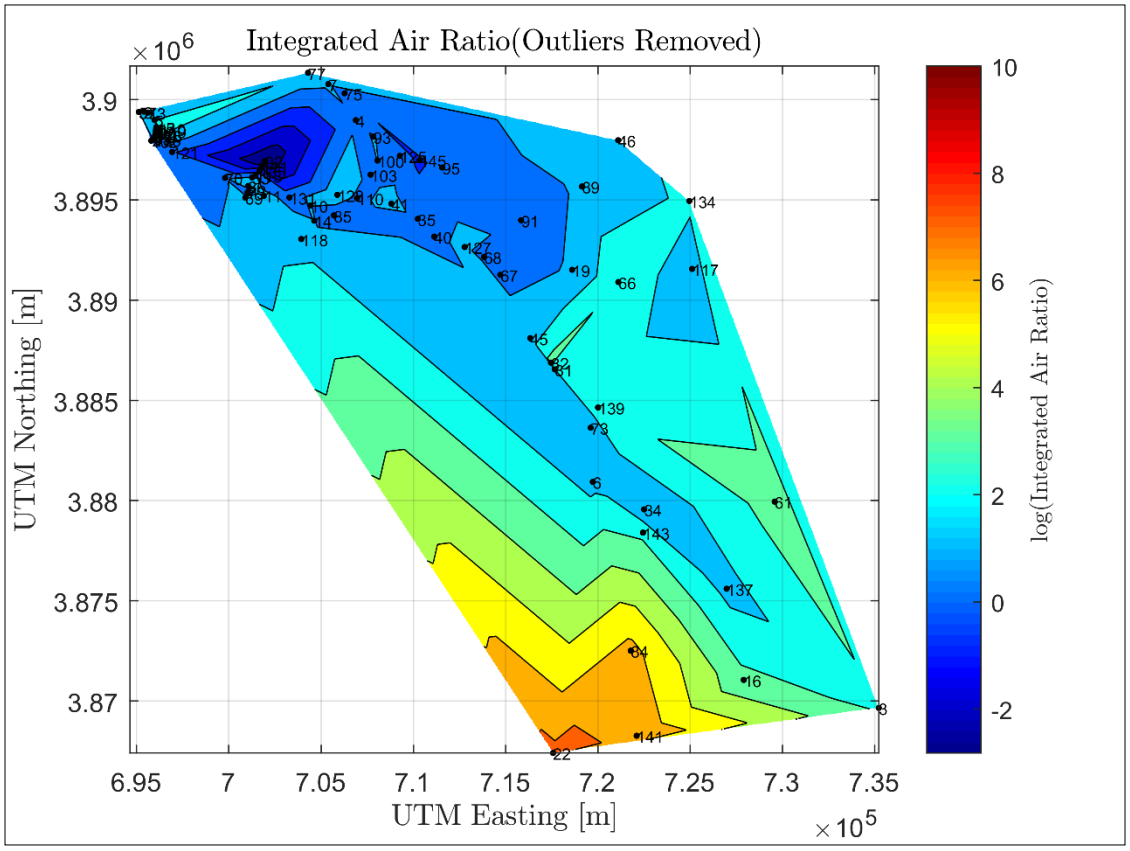

Figure 4-25. Spatial distribution of the integrated air concentration ratio calculated for sites with more than one measurement with outliers removed using Peirce's Criterion.

A lognormal distribution was fit to the final integrated air concentration data. This fitted distribution is compared to the empirical distribution in Figure 4-26. Each data point is shown with its station number for reference and is color coded using the color scale of the log of the integrated air concentration shown in Figure 4-25 above.

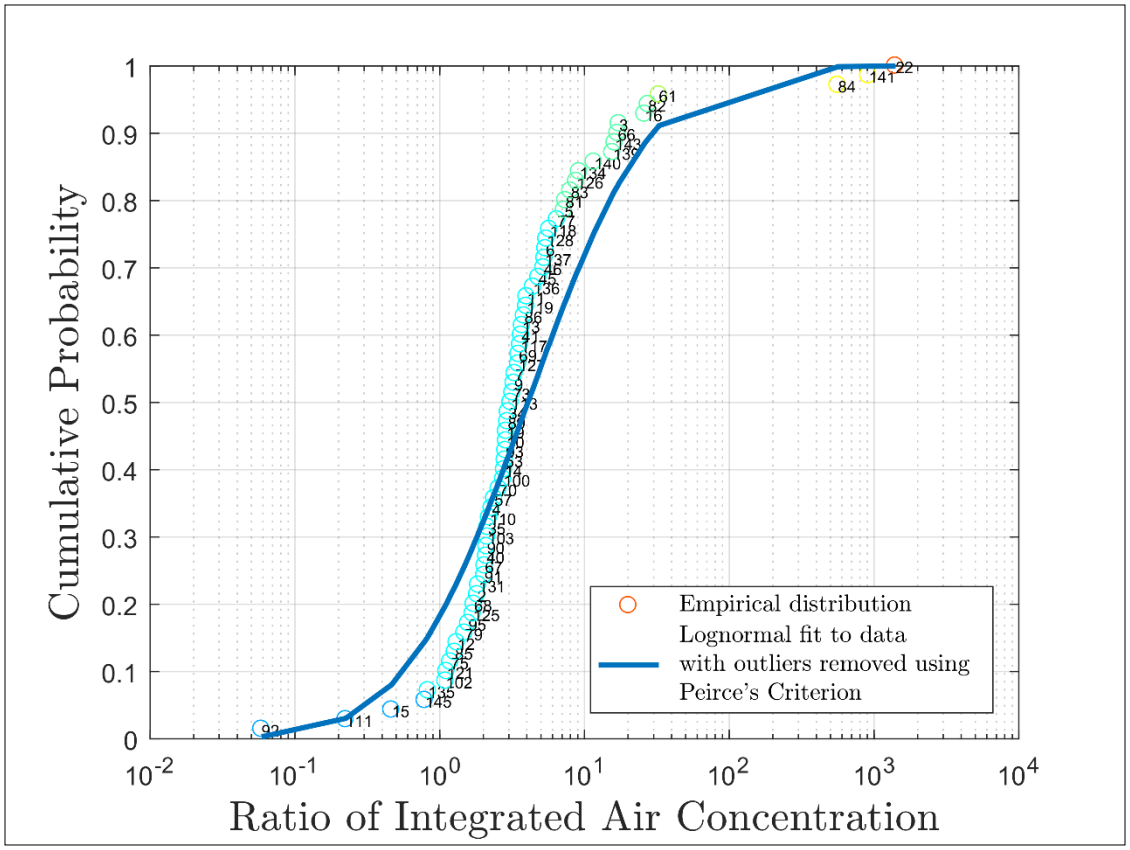

Figure 4-26. Cumulative probability of the empirical distribution of the ratio of integrated air concentrations for measured and simulated data (points) compared to a fitted lognormal distribution (line).

The lognormal distribution shown above is not necessarily the best representation of the distribution of integrated air concentration ratios as this fit performs poorly at the distribution tails. Although the outliers were removed using Peirce's Criterion, the behavior of the empirical distribution remains convoluted by the spatial differences across measurement stations. In addition, this data is further convoluted by the uncertainty in each of the measurements. The refinement of this distribution remains an area of active research. The final fitted lognormal distribution has a log mean of 1.40 and a log SD of 1.55. This yields a GM of 4.06 and a GSD of 4.69. The distribution is shown in Figure 4-27 and was applied as a multiplier to a nominal air concentration value selected for each scenario of interest, as shown in Table 2.5-2. The multiplier in Figure 4-27 is shown for Cs-137, but the same multiplier was sampled for each radionuclide because it is radionuclide-independent.

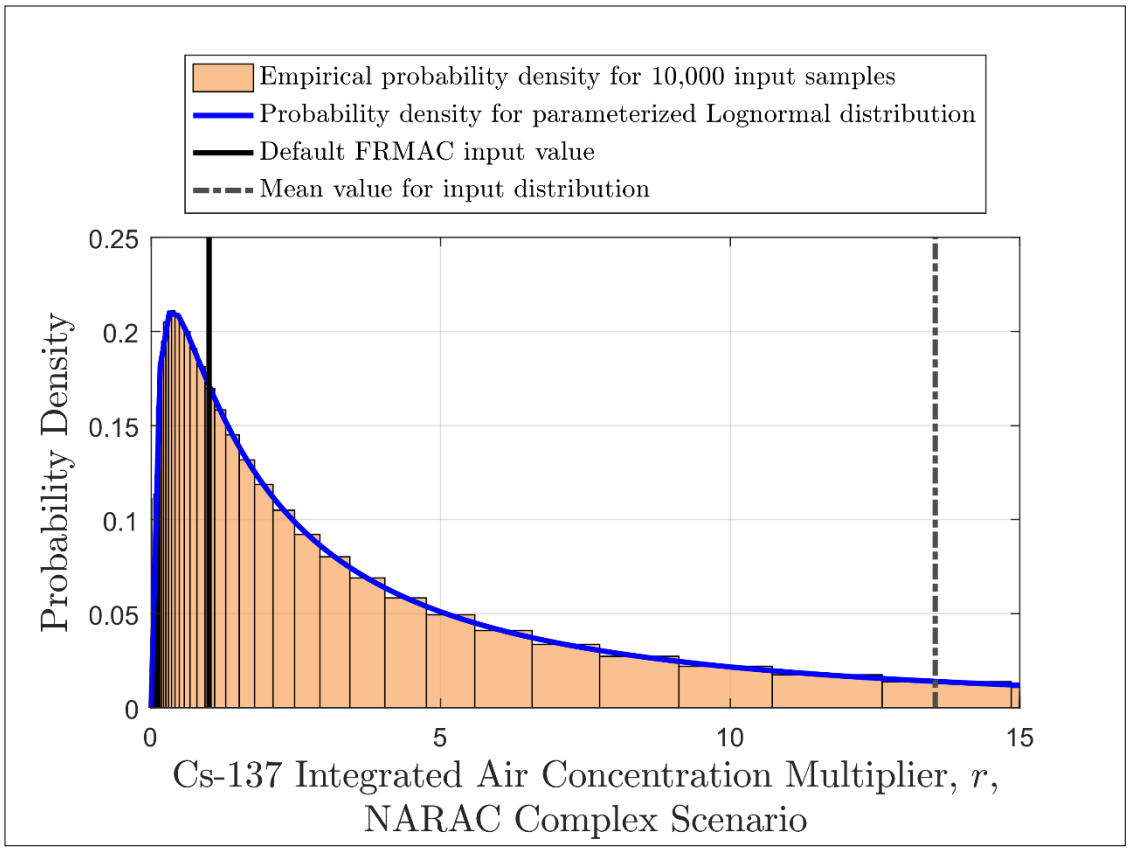

Figure 4-27. Empirical and parameterized probability densities for the NARAC Complex air concentration multiplier.

4.4. Summary of Assigned Input Distributions

Table 4.4-1 summarizes the probability distributions assigned to the inputs to the Public Protection DRL calculation. The uncertainties associated with the dose coefficient inputs are applied via multipliers because dose coefficients are not directly entered into Turbo FRMAC© by the user. Turbo FRMAC© pulls these dose coefficients from a database based on the user-supplied radionuclide source term.

Table 4.4-1. Summary of input distributions for the FY18 uncertainty analyses.

Input	Default Value	Distribution Type	Mean	SD	Mode	Lower Bound	Upper Bound	Units
Air Concentration Uncertainty Multiplier – NARAC Simplified*	1	Lognormal+	0.59	3.99				---
Air Concentration Uncertainty Multiplier – NARAC Complex*	1	Lognormal+	4.06	4.69				---
Activity per Area‡	DRL	Normal	DRL	See note		0		$\mu Ci/m^2$
Deposition Velocity	3.00E-3	Triangular			3.00E-3	3.00E-4	3.00E-2	m/s
Breathing Rate – Light Exercise, Adult Male	1.50	Normal	1.75	0.42		0.54	3.00	m^3/hr
Breathing Rate – Activity-Averaged, Adult Male	0.92	Triangular			0.92	0.54	1.50	m^3/hr
Ground Roughness Factor	0.82	Normal	0.82	0.082		0	1	--
Resuspension Coefficient Multiplier§	1	Lognormal+	1	4.2				--
Weathering Coefficient Multiplier§	1	Lognormal+	1	1.2				--
Deposition External Dose Coefficient Multiplier	1	Triangular			0.8	0.5	1.5	--
Cs-137 Inhalation Dose Coefficient Multiplier**	1	Lognormal+	1	1.5		1.67	7.02	--
Am-241 Inhalation Dose Coefficient Multiplier++	1	Lognormal+	1	2		1.38	22.8	--
Plume External Dose Coefficient Multiplier	1	Triangular			0.8	0.5	1.5	--

* This uncertainty multiplier is multiplied by a user-defined air concentration value to sample air concentration with uncertainty.

+ The means and standard deviations (SD) listed for lognormal distributions on this table are the geometric mean and geometric standard deviation, respectively. The lognormal distribution is defined by parameters μ, the mean of the natural logarithm of the data, and σ, the standard deviation of the natural logarithm of the data. Then, the geometric mean (GM) is given by $GM = e^{\mu}$ and the geometric standard deviation (GSD) is given by $GSD = e^{\sigma}$. This treatment is also applied to the lower and upper bounds where applicable.

‡ The uncertainty associated with activity per area is dependent on the quantity being measured and the measurement type. For details, see Section 4.2.

§These multipliers are to be applied only to the coefficients outside the exponentials in the Resuspension and Weathering Factors

** This multiplier is specifically for Cs-137, Lung Clearance Type F, Effective (Whole Body). Ba-137m is present at equilibrium with Cs-137 at the start of the time phase. The uncertainty in the Ba-137m inhalation dose coefficient is neglected because its ingrowth from Cs-137 over the dose commitment period dominates the delivered dose. The Cs-137 inhalation dose coefficient accounts for dose and uncertainty from the ingrowth of Ba-137m. (per communication with Keith Eckerman on May 10, 2017)

++ This multiplier is specifically for Am-241, Lung Clearance Type M, Effective (Whole Body)

5. PROBABILISTIC ANALYSIS RESULTS

In order to characterize the uncertainty in data products due to varying sources of radioactivity concentration data, a probabilistic analysis was completed for each activity source. The runs for Laboratory Analysis, In Situ Deposition, and AMS used a source term based on activity per area. The runs for NARAC used either a "simplified" or "complex" distribution for integrated air activity instead of activity per area.

The results presented in this chapter were calculated using the methods described in Section 3.3. Section 3.3 provides an example showing the meaning of each of the metrics given in various tables and provides the statistical background required for interpreting the results. The FY18 analyses yielded 45 sets of results – nine scenarios were run for each of the five sources of radioactivity concentration data. 10,000 realizations were used to obtain each set of results. This number of simulations was found to sufficiently minimize the sampling uncertainty in the results. In an effort to keep this report more concise, only the results of interest are presented and are organized topically in this chapter. The results discussion focuses on the radionuclide-specific Deposition DRLs in particular, as this is the most commonly used quantity for CM data products. The NARAC Simplified results are not presented for brevity throughout as they were not as uncertain as the more realistic NARAC Complex results. The full set of results can be requested through the primary author of this report.

The goal of this project is to develop the methods that could be used to execute a probabilistic analysis for the values used to generate CM data products; this project does not seek to provide specific and final information regarding the uncertainty in data products as a whole. Therefore, the results presented in this report should be considered examples derived from a proof of concept of simulation methods and should not be explicitly applied or used to draw conclusions about the full range of potential uncertainties in data products.

5.1. Input Sampling Results

Table 5.1-1 shows the mean and 5^{th}, 50^{th}, and 95^{th} percentiles for the health physics inputs resulting from 10,000 simulations. These results are included to assist in the explanation of the uncertainty and sensitivity analysis results. There are two additional metrics provided in the table. The first, the ratio of the mean to the default value, assists in assessing the relationship between the sampled values of each input to the default value that would normally be used in a DRL calculation. The second, the ratio of the 95^{th} percentile to the 5^{th} percentile, characterizes the relative spread in the distribution for each of the inputs. Using the $95^{th}/5^{th}$ as a measure of the spread of the uncertainty of these distributions, the resuspension coefficient multiplier is relatively the most uncertain, followed by deposition velocity.

Table 5.1-1. Distributions of health physics inputs resulting from 10,000 simulations.

Input	Default	Mean	5th	50th	95th	Mean/ Default	95th/ 5th
Breathing Rate, Light Exercise, Adult Male [m^3/hr]	1.5	1.75	1.07	1.75	2.44	1.17	2.28
Ground Roughness Factor	0.82	8.17E-01	6.85E-01	8.19E-01	9.45E-01	1.00	1.38
Cs-137 Inhalation Dose Coefficient Multiplier	1	1.05	5.88E-01	1.00	1.70	1.05	2.90
Am-241 Inhalation Dose Coefficient Multiplier	1	1.16	4.03E-01	1.00	2.48	1.16	6.15
Resuspension Coefficient Multiplier	1	2.83	9.37E-02	1.00	10.7	2.83	114
Weathering Coefficient Multiplier	1	1.02	7.41E-01	1.00	1.35	1.02	1.82
Deposition Velocity [m/s]	0.003	1.11E-02	2.30E-03	9.98E-03	2.37E-02	3.70	10.3
Breathing Rate, Activity Averaged, Adult Male [m^3/hr]	0.92	9.87E-01	6.75E-01	9.72E-01	1.33	1.07	1.97
Deposition External Dose Coefficient Multiplier	1	9.33E-01	6.23E-01	9.08E-01	1.31	0.93	2.11
Plume External Dose Coefficient Multiplier	1	9.33E-01	6.23E-01	9.08E-01	1.31	0.93	2.11

5.2. Cs-137 vs. Am-241

The FY17 analysis considered a source term of Cs-137 only for the Early Phase (TD) time phase, which includes dose from the plume. In FY18, additional time phases were considered to determine how the absence of the plume impacts the results. Table 5.2-1 shows the results for the Cs-137 Deposition DRL for a source term of only Cs-137 based on In Situ measurement. The cumulative distribution functions (CDFs) for each scenario are shown in Figure 5-1. Using the $95^{th}/5^{th}$ as a measure of the spread of the result distributions, it is seen that the uncertainty decreases for the Early Phase (AD) and First Year scenarios in which the plume is excluded.

Table 5.2-1. Cs-137 Deposition DRL (μCi/m²) uncertainty results for In Situ single radionuclide simulations.

Scenario	Default	Mean	5th	50th	95th	Mean/ Default	95th/ 5th
Early Phase (TD)	3.31E+02	7.10E+02	2.05E+02	6.87E+02	1.31E+03	2.15	6.42
Early Phase (AD)	1.70E+03	1.86E+03	1.20E+03	1.80E+03	2.75E+03	1.10	2.30
First Year	42.0	47.8	31.1	46.3	69.6	1.14	2.24

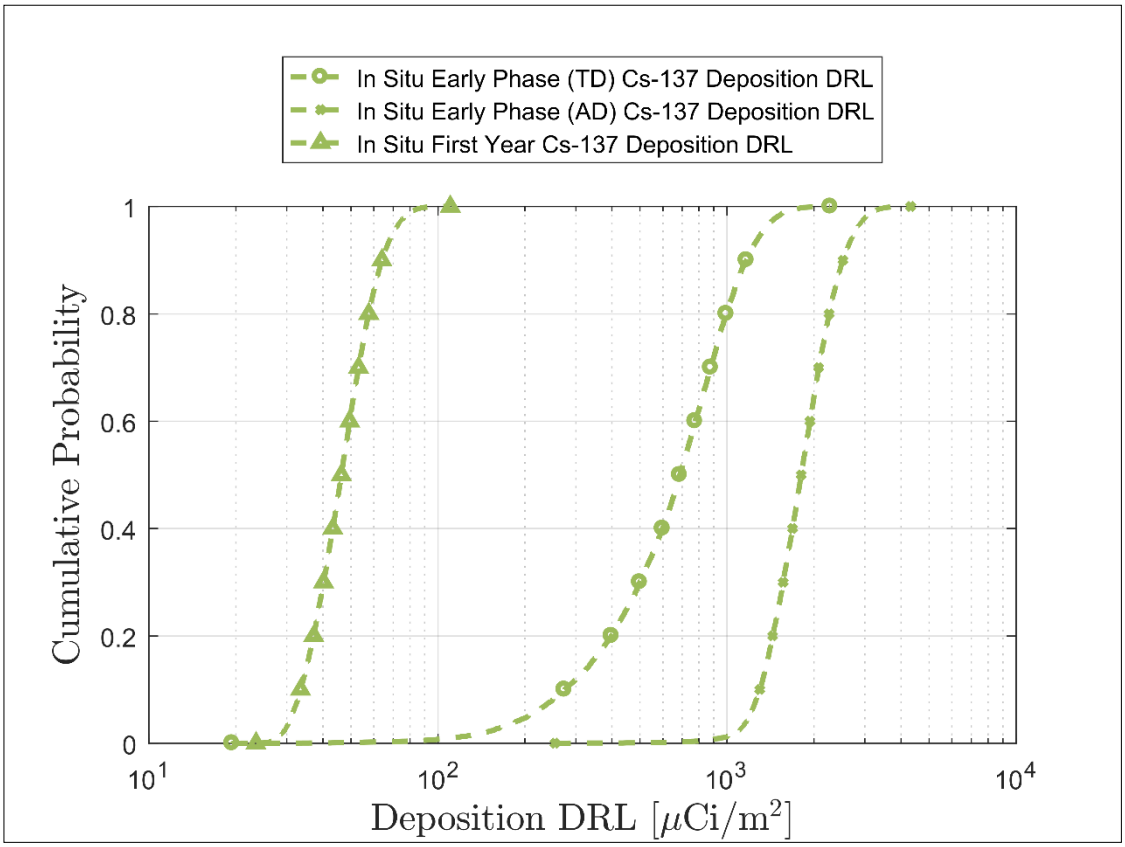

Figure 5-1. Cumulative probability for the Cs-137 Deposition DRL for In Situ single radionuclide simulations.

The sensitivity analysis results can be used to help explain why the uncertainty is reduced when the plume is excluded. Table 5.2-2 shows that the most important input to the Cs-137 Deposition DRL uncertainty when the plume is included is deposition velocity. Deposition velocity is used to convert the activity per area used to define the source term to integrated air concentration for use in plume dose calculations. Deposition velocity is one of the most uncertain inputs considered in these analyses, as shown in Table 5.1-1. This input becomes unimportant when the plume is excluded, as shown by its low ranking in Table 5.2-3 and Table 5.2-4. Groundshine drives dose from Cs-137 when the plume is excluded. Thus, the inputs for calculating groundshine (deposition external dose coefficient and ground roughness) become important for

the Early Phase (AD) and First Year time phases. These inputs are less uncertain compared to deposition velocity. Additionally, some of their contribution to uncertainty is eliminated by being present in both the denominator and the numerator of the Cs-137 Deposition DRL.

Table 5.2-2. Sensitivity analysis results for the Early Phase (TD) Cs-137 Deposition DRL for In Situ single radionuclide simulations.

Cs-137 Deposition DRL, R^2 = 0.931		
Variable Name	**R^2**	**SRRC**
Deposition Velocity	0.654	0.809
Cs-137 Inhalation Dose Coefficient Multiplier	0.786	-0.360
Breathing Rate, Light Exercise, Adult Male	0.854	-0.261
Weathering Coefficient Multiplier	0.893	0.197
Deposition External Dose Coefficient Multiplier	0.922	-0.172
Ground Roughness Factor	0.927	-0.072
Resuspension Coefficient Multiplier	0.931	-0.061
Cs-137 Activity per Area	0.931	0.000
Plume External Dose Coefficient Multiplier	0.931	0.000
Breathing Rate, Activity Averaged, Adult Male	0.931	-0.009

Table 5.2-3. Sensitivity analysis results for the Early Phase (AD) Cs-137 Deposition DRL for In Situ single radionuclide simulations.

Cs-137 Deposition DRL, R^2 = 0.901		
Variable Name	**R^2**	**SRRC**
Deposition External Dose Coefficient Multiplier	0.716	-0.847
Ground Roughness Factor	0.827	-0.333
Resuspension Coefficient Multiplier	0.895	-0.260
Cs-137 Inhalation Dose Coefficient Multiplier	0.899	-0.061
Breathing Rate, Activity Averaged, Adult Male	0.900	-0.039
Breathing Rate, Light Exercise, Adult Male	0.901	0.000
Cs-137 Activity per Area	0.901	0.000
Deposition Velocity	0.901	0.000
Plume External Dose Coefficient Multiplier	0.901	0.000
Weathering Coefficient Multiplier	0.901	0.033

Table 5.2-4. Sensitivity analysis results for the First Year Cs-137 Deposition DRL for In Situ single radionuclide simulations.

Cs-137 Deposition DRL, R^2 = 0.980		
Variable Name	**R^2**	**SRRC**
Deposition External Dose Coefficient Multiplier	0.845	-0.920
Ground Roughness Factor	0.980	-0.367
Cs-137 Inhalation Dose Coefficient Multiplier	0.980	-0.005
Resuspension Coefficient Multiplier	0.980	-0.017
Weathering Coefficient Multiplier	0.980	0.005
Breathing Rate, Activity Averaged, Adult Male	0.980	-0.003
Breathing Rate, Light Exercise, Adult Male	0.980	0.000
Cs-137 Activity per Area	0.980	0.000
Deposition Velocity	0.980	0.000
Plume External Dose Coefficient Multiplier	0.980	0.000

Am-241 was included in the FY18 analyses in order to determine how uncertainty results change when a radionuclide with different radiological properties than Cs-137 is included. Table 5.2-5 shows the results for the Am-241 Deposition DRL for a source term of only Am-241 based on In Situ measurement. The CDFs for each scenario are shown in Figure 5-2. Unlike with Cs-137, the overall uncertainty in the Am-241 Deposition DRL increases when the plume is excluded.

Table 5.2-5. Am-241 Deposition DRL (μCi/m²) uncertainty results for In Situ single radionuclide simulations.

Scenario	Default	Mean	5th	50th	95th	Mean/ Default	95th/ 5th
Early Phase (TD)	4.64E-02	1.74E-01	2.17E-02	1.23E-01	4.98E-01	3.76	22.9
Early Phase (AD)	8.66	28.1	6.38E-01	8.35	1.10E+02	3.24	173
First Year	4.15	12.4	3.07E-01	4.01	50.5	2.98	164

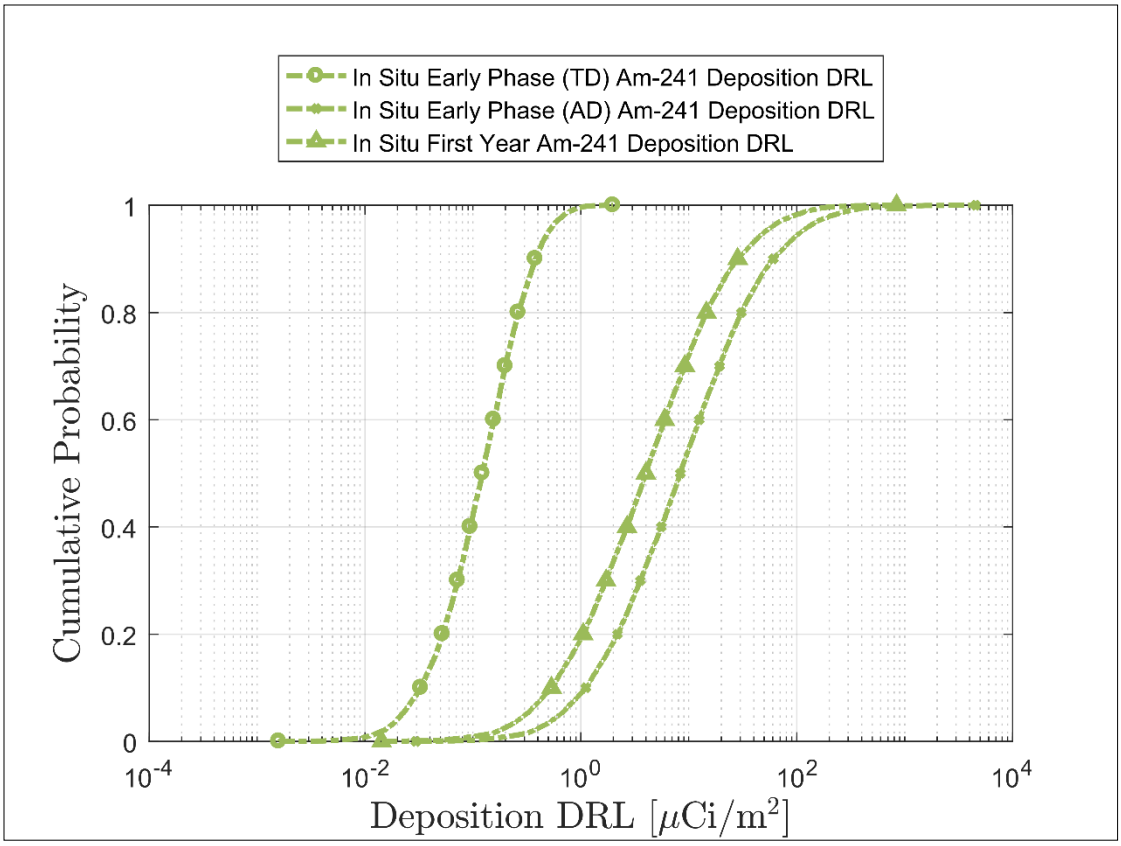

Figure 5-2. Cumulative probability for the Am-241 Deposition DRL for In Situ single radionuclide simulations.

The sensitivity analysis results presented in Table 5.2-6 show that deposition velocity is the most important input to the Am-241 Deposition DRL when the plume is included, like for the Cs-137 Deposition DRL. Deposition velocity is used in calculating the dose from plume inhalation. Because more of the total dose comes from plume inhalation for Am-241 than Cs-137 (see Table 2.6-1), the Am-241 Deposition DRL is more uncertain than the Cs-137 Deposition DRL.

Table 5.2-7 and Table 5.2-8 show the sensitivity analysis results for Early Phase (AD) and First Year, respectively, in which the plume is excluded. For both time phases, the resuspension coefficient multiplier is the most important input. This is because resuspension inhalation drives total dose for the Am-241-only scenarios that exclude the plume. The resuspension coefficient multiplier is the most uncertain health physics input considered in these analyses, as shown in Table 5.1-1. This causes the Early Phase (AD) and First Year Am-241 Deposition DRLs to be more uncertain than the Early Phase (TD) DRL. When compared to the Cs-137 Deposition DRL, the Am-241 Deposition DRL is more uncertain not only because resuspension inhalation drives total dose, but because the resuspension inhalation dose inputs are not used in the numerator of the Deposition DRL calculation, unlike the groundshine inputs which drive dose in the Cs-137 case.

In summary, the type of DRL being considered and the dose pathway that is the most significant contributor to total dose can impact overall uncertainty in the result in different ways.

Table 5.2-6. Sensitivity analysis results for the Early Phase (TD) Am-241 Deposition DRL for In Situ single radionuclide simulations.

Am-241 Deposition DRL, R^2 = 0.942		
Variable Name	**R^2**	**SRRC**
Deposition Velocity	0.516	0.718
Am-241 Inhalation Dose Coefficient Multiplier	0.849	-0.575
Breathing Rate, Light Exercise, Adult Male	0.905	-0.237
Weathering Coefficient Multiplier	0.938	0.181
Resuspension Coefficient Multiplier	0.942	-0.060
Breathing Rate, Activity Averaged, Adult Male	0.942	-0.009
Deposition External Dose Coefficient Multiplier	0.942	0.004
Ground Roughness Factor	0.942	0.000
Am-241 Activity per Area	0.942	0.000
Plume External Dose Coefficient Multiplier	0.942	0.000

Table 5.2-7. Sensitivity analysis results for the Early Phase (AD) Am-241 Deposition DRL for In Situ single radionuclide simulations.

Am-241 Deposition DRL, R^2 = 0.980		
Variable Name	**R^2**	**SRRC**
Resuspension Coefficient Multiplier	0.833	-0.911
Am-241 Inhalation Dose Coefficient Multiplier	0.951	-0.343
Breathing Rate, Activity Averaged, Adult Male	0.967	-0.125
Breathing Rate, Light Exercise, Adult Male	0.980	0.000
Ground Roughness Factor	0.980	0.000
Am-241 Activity per Area	0.980	0.000
Deposition Velocity	0.980	0.000
Deposition External Dose Coefficient Multiplier	0.980	0.000
Plume External Dose Coefficient Multiplier	0.980	0.000
Weathering Coefficient Multiplier	0.980	0.112

Table 5.2-8. Sensitivity analysis results for the First Year Am-241 Deposition DRL for In Situ single radionuclide simulations.

Am-241 Deposition DRL, R^2 = 0.980		
Variable Name	**R^2**	**SRRC**
Resuspension Coefficient Multiplier	0.833	-0.911
Am-241 Inhalation Dose Coefficient Multiplier	0.951	-0.343
Breathing Rate, Activity Averaged, Adult Male	0.967	-0.125
Breathing Rate, Light Exercise, Adult Male	0.980	0.000
Ground Roughness Factor	0.980	0.000
Am-241 Activity per Area	0.980	0.000
Deposition Velocity	0.980	0.000
Plume External Dose Coefficient Multiplier	0.980	0.000
Weathering Coefficient Multiplier	0.980	0.112
Deposition External Dose Coefficient Multiplier	0.980	-0.002

5.3. Single vs. Multiple Radionuclide Source Terms

The FY17 analysis demonstrated that the uncertainty associated with the source term activity, whether activity per area or integrated air concentration, does not contribute to DRL uncertainty in the case that the source term consists of a single radionuclide. In single-radionuclide DRL calculations, the source term activity is used both in the denominator of the DRL to calculate total dose and in the numerator of the DRL to calculate the measurable quantity to which field measurements or NARAC-projected concentrations should be compared. Thus, the activity assigned to the radionuclide is effectively unimportant in calculating DRLs and therefore does not contribute uncertainty to the DRL. In other words, in the case of a single-radionuclide source term, it is always known what activity per area or integrated air concentration will cause an exposed individual to receive a dose equal to the PAG for the time phase of interest.

In the FY18 analyses, when the source term was assumed to be only Cs-137 or only Am-241, the respective Cs-137 and Am-241 Deposition DRL distributions are nearly exactly the same whether the source term is considered to be based on In Situ, AMS, or Laboratory Analysis measurements or a NARAC air concentration. This is shown in Table 5.3-1 and Figure 5-3 for the First Year Cs-137 Deposition DRL and in Table 5.3-2 and Figure 5-4 for the First Year Am-241 Deposition DRL. Note that all four lines are plotted in the figures, but that they overlap. A slight difference can be seen in the tables between the results based on ground measurements (In Situ, AMS, and Laboratory Analysis) versus air concentration (NARAC Complex). The sensitivity analysis results further demonstrate the lack of importance of source term activity for single-radionuclide DRL calculations. Table 5.2-4 shows that Cs-137 activity per area contributes no uncertainty to the Cs-137 Deposition DRL through its low ranking and zero SRRC. Table 5.2-8 shows the same result for Am-241 activity per area in the Am-241 alone case. The same behavior is seen in the sensitivity results for the other time phases as well.

Table 5.3-1. First Year Cs-137 Deposition DRL (μCi/m^2) uncertainty results for single radionuclide simulations based on different sources of radioactivity concentration data.

Data Source	Default	Mean	5th	50th	95th	Mean/ Default	95th/ 5th
In Situ	42.0	47.799	31.119	46.322	69.578	1.14	2.24
AMS	42.0	47.799	31.119	46.322	69.578	1.14	2.24
Laboratory Analysis	42.0	47.799	31.119	46.322	69.578	1.14	2.24
NARAC Complex	42.0	47.793	31.126	46.323	69.816	1.14	2.24

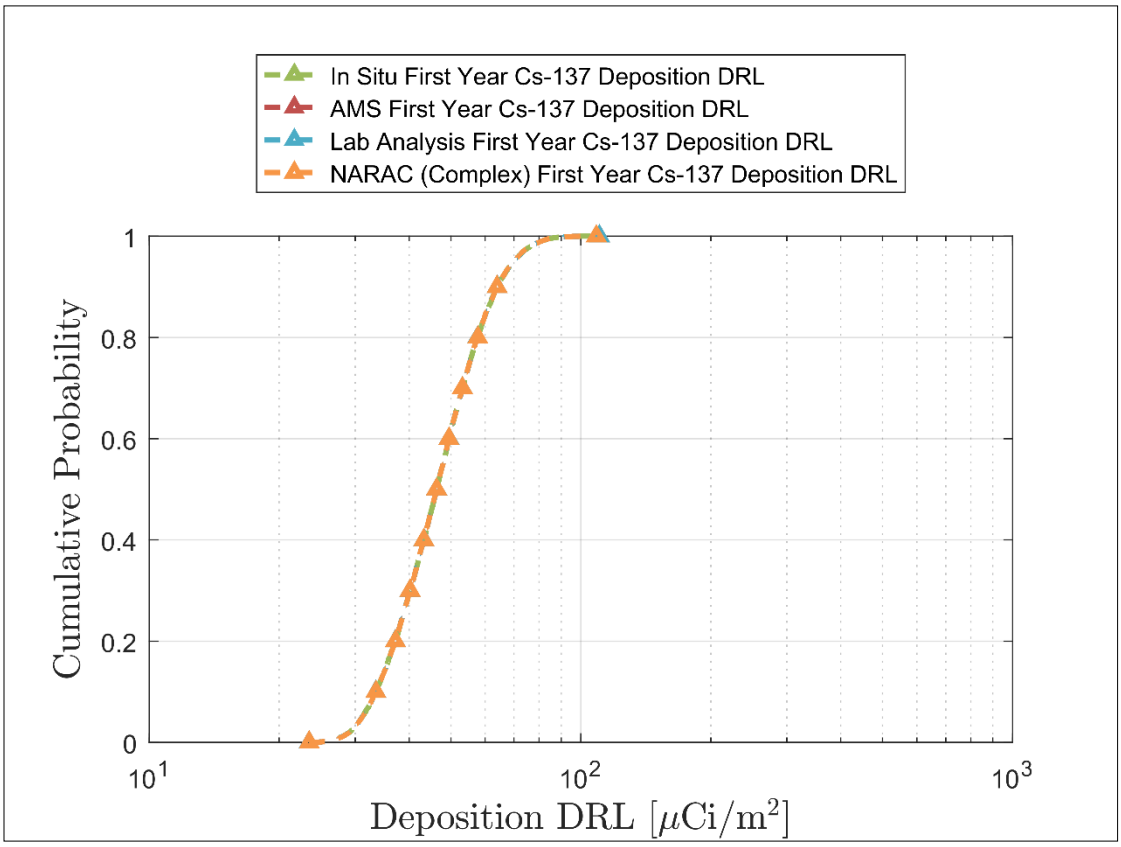

Figure 5-3. Cumulative probabilities for the First Year Cs-137 Deposition DRL for single radionuclide simulations based on different sources of radioactivity concentration data.

Table 5.3-2. First Year Am-241 Deposition DRL (μCi/m²) uncertainty results for single radionuclide simulations based on different sources of radioactivity concentration data.

Data Source	Default	Mean	5th	50th	95th	Mean/ Default	95th/ 5th
In Situ	4.15	12.369	0.307	4.007	50.461	2.98	164
AMS	4.15	12.369	0.307	4.007	50.461	2.98	164
Laboratory Analysis	4.15	12.369	0.307	4.007	50.461	2.98	164
NARAC Complex	4.15	12.310	0.305	3.965	49.143	2.96	161

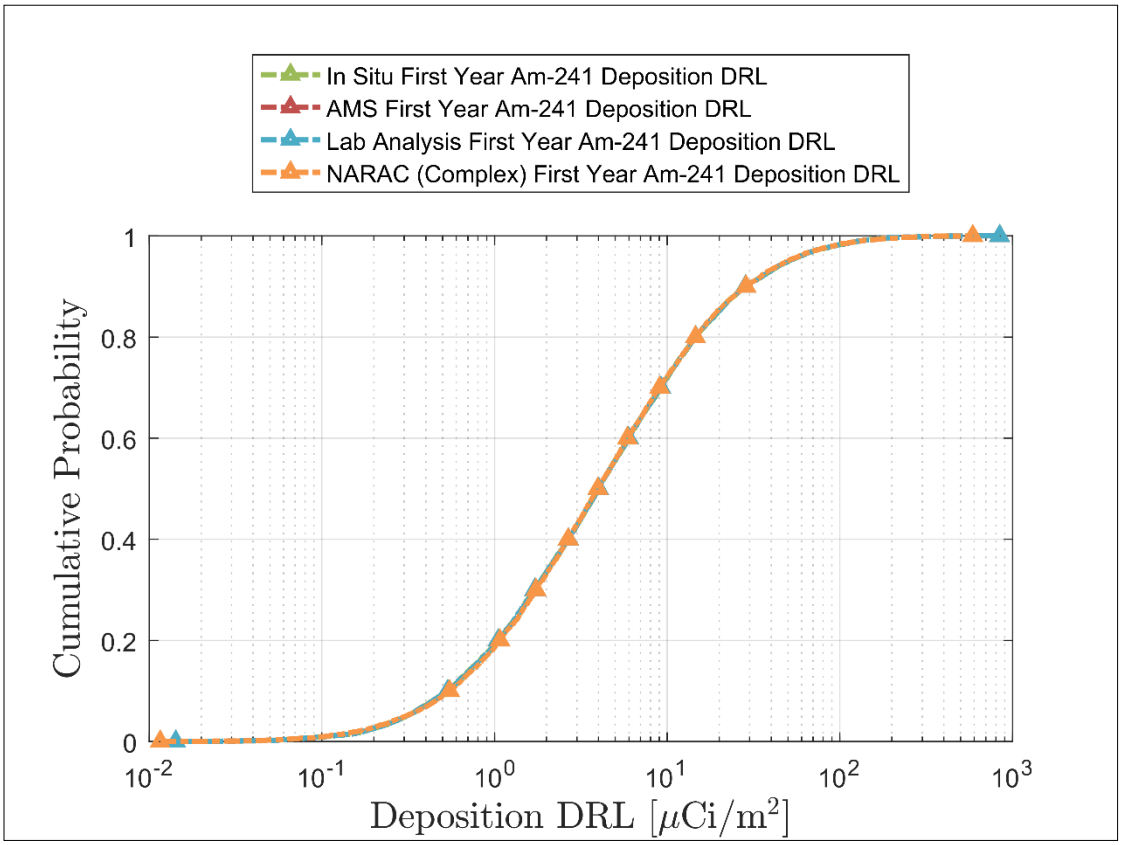

Figure 5-4. Cumulative probabilities for the First Year Am-241 Deposition DRL for single radionuclide simulations based on different sources of radioactivity concentration data.

In an effort to explore this phenomenon further, the FY18 analyses considered scenarios with a multiple-radionuclide source term of Cs-137 and Am-241 in a 1:1 ratio. The resulting Cs-137 and Am-241 Deposition DRL distributions are shown in Table 5.3-3 and Figure 5-5 for Cs-137 and Table 5.3-4 and Figure 5-6 for Am-241. Unlike the single-radionuclide scenarios, there is a difference in the distributions for the Deposition DRLs based on different sources of radioactivity concentration data when two radionuclides are present in the source term.

Table 5.3-3. First Year Cs-137 Deposition DRL (μCi/m²) uncertainty results for 1:1 Cs-137:Am-241 simulations based on different sources of radioactivity concentration data.

Data Source	Default	Mean	5th	50th	95th	Mean/ Default	95th/ 5th
In Situ	3.78	6.713	0.305	3.698	23.491	1.78	77.0
AMS	3.78	7.397	0.284	3.945	26.208	1.96	92.3
Laboratory Analysis	3.78	6.722	0.302	3.690	23.540	1.78	78.1
NARAC Complex	3.78	10.328	0.048	3.656	40.223	2.73	831

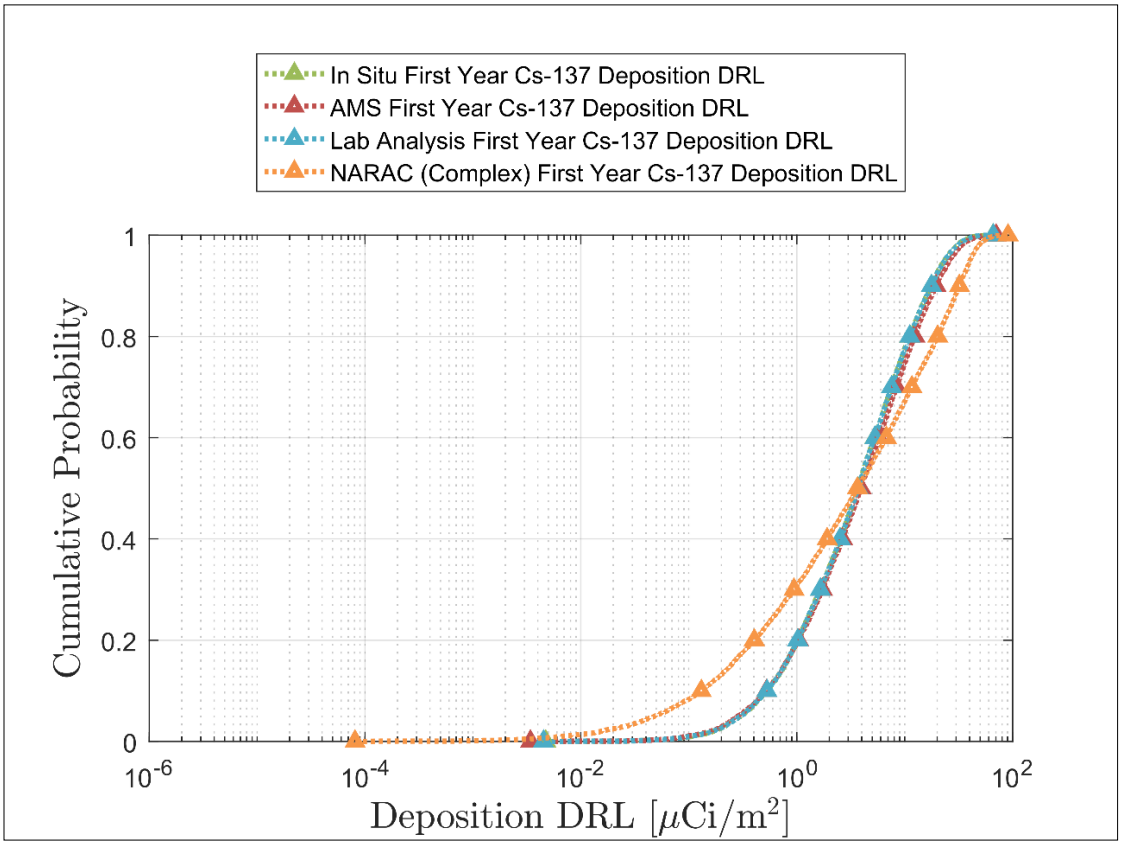

Figure 5-5. Cumulative probabilities for the First Year Cs-137 Deposition DRL for 1:1 Cs-137:Am-241 simulations based on different sources of radioactivity concentration data.

Table 5.3-4. First Year Am-241 Deposition DRL (μCi/m²) uncertainty results for 1:1 Cs-137:Am-241 simulations based on different sources of radioactivity concentration data.

Data Source	Default	Mean	5th	50th	95th	Mean/ Default	95th/ 5th
In Situ	3.78	6.712	0.304	3.686	23.497	1.78	77.4
AMS	3.78	6.529	0.299	3.562	22.600	1.73	75.6
Laboratory Analysis	3.78	6.710	0.304	3.684	23.201	1.78	76.4
NARAC Complex	3.78	6.507	0.236	2.668	24.742	1.72	105

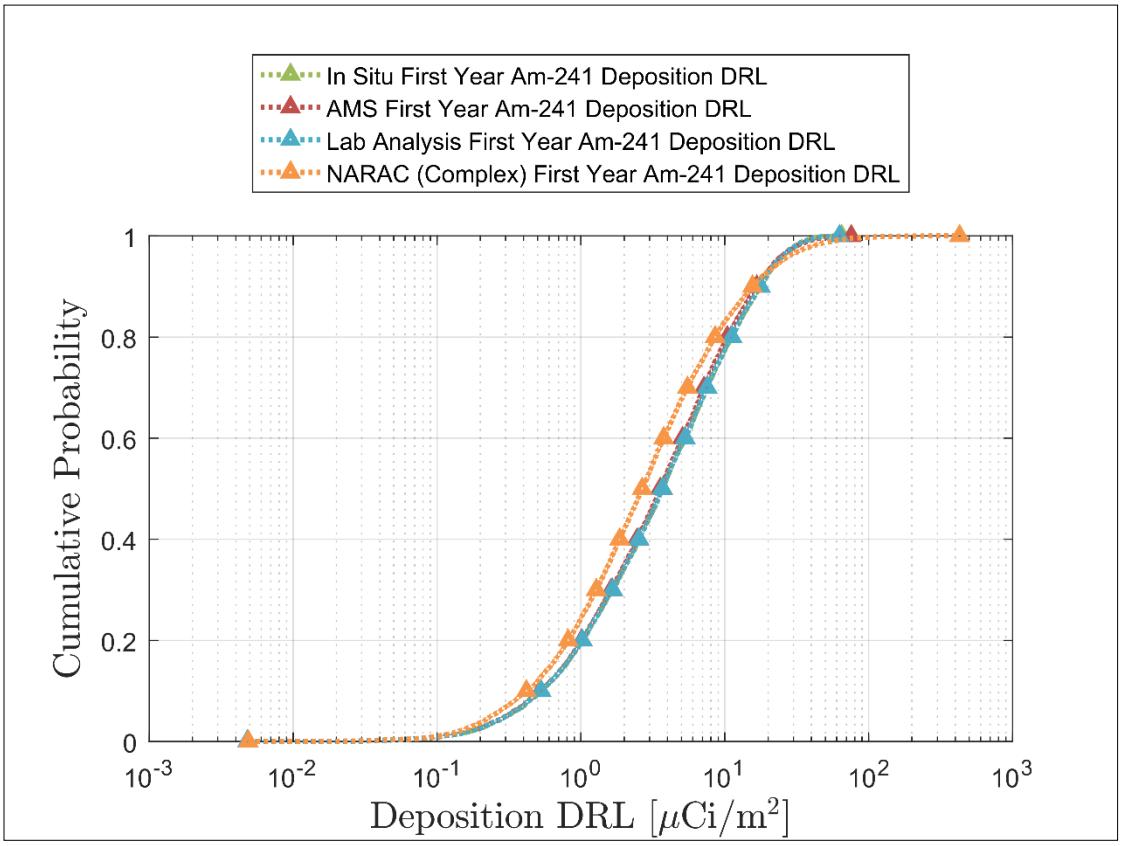

Figure 5-6. Cumulative probabilities for the First Year Am-241 Deposition DRL for 1:1 Cs-137:Am-241 simulations based on different sources of radioactivity concentration data.

The sensitivity analysis results show that source term activity now contributes uncertainty to the DRL. Table 5.3-5 includes the sensitivity analysis results for the Cs-137 Deposition DRL based on In Situ measurement and Table 5.3-6 includes the results for the DRL based on NARAC Complex air concentration. For the In Situ-based results, the resuspension coefficient multiplier

is the most important input. Even though this is a Cs-137 DRL, the total dose for the mixture is primarily driven by Am-241 resuspension inhalation dose. Therefore, the Am-241 resuspension

inhalation dose inputs are the most important. Cs-137 and Am-241 activity per area are low-ranked in comparison to these inputs, but some correlation between the activities and the DRL output uncertainty is seen through the SRRC. For the NARAC Complex-based results, a similar ranking is seen, except that the air concentration multiplier associated with the Cs-137 and Am-241 activities are the most important. This is because the air concentration multiplier probability distribution is incredibly uncertain, as shown in Figure 4-27, compared to the probability distributions associated with In Situ measurement of Cs-137 and Am-241 at the DRL.

Table 5.3-5. Sensitivity analysis results for the First Year Cs-137 Deposition DRL for 1:1 Cs-137:Am-241 In Situ simulations.

Cs-137 Deposition DRL, R^2 = 0.979		
Variable Name	**R^2**	**SRRC**
Resuspension Coefficient Multiplier	0.833	-0.912
Am-241 Inhalation Dose Coefficient Multiplier	0.949	-0.343
Breathing Rate, Activity Averaged, Adult Male	0.965	-0.126
Weathering Coefficient Multiplier	0.978	0.113
Deposition External Dose Coefficient Multiplier	0.978	-0.022
Ground Roughness Factor	0.978	-0.013
Cs-137 Activity per Area	0.979	0.010
Breathing Rate, Light Exercise, Adult Male	0.979	0.002
Am-241 Activity per Area	0.979	-0.009
Deposition Velocity	0.979	-0.002
Cs-137 Inhalation Dose Coefficient Multiplier	0.979	0.000
Plume External Dose Coefficient Multiplier	0.979	0.000

Table 5.3-6. Sensitivity analysis results for the First Year Cs-137 Deposition DRL for 1:1 Cs-137:Am-241 NARAC Complex simulations.

Cs-137 Deposition DRL, R^2 = 0.930		
Variable Name	**R^2**	**SRRC**
Am-241 Air Concentration Multiplier	0.313	-0.559
Cs-137 Air Concentration Multiplier	0.622	0.558
Resuspension Coefficient Multiplier	0.881	-0.508
Am-241 Inhalation Dose Coefficient Multiplier	0.919	-0.196
Breathing Rate, Activity Averaged, Adult Male	0.924	-0.072
Weathering Coefficient Multiplier	0.928	0.064
Deposition External Dose Coefficient Multiplier	0.929	-0.033
Breathing Rate, Light Exercise, Adult Male	0.930	0.000
Cs-137 Inhalation Dose Coefficient Multiplier	0.930	0.000
Deposition Velocity	0.930	0.000
Plume External Dose Coefficient Multiplier	0.930	0.000
Ground Roughness Factor	0.930	-0.017

For the same First Year scenario, Table 5.3-7 includes the sensitivity analysis results for the Am-241 Deposition DRL based on In Situ measurement and Table 5.3-8 includes the results for the DRL based on NARAC Complex air concentration. The ranking for the In Situ-based results is similar to those for the Cs-137 Deposition DRL, with Cs-137 and Am-241 activity per area again showing a low ranking but some correlation through the SRRC. For the NARAC Complex-based results, the air concentration multipliers are highly ranked, though not as highly ranked as they were for the Cs-137 Deposition DRL. This is likely because the total dose is driven by Am-241 so some uncertainty is eliminated in the Am-241 Deposition DRL versus the Cs-137 Deposition DRL (though not completely eliminated, as is the case for single-radionuclide source terms). Because the air concentration multipliers are more highly ranked for the Cs-137 Deposition DRL than the Am-241 Deposition DRL, there is more uncertainty in the Cs-137 Deposition DRL for the NARAC Complex-based results.

In summary, when multiple radionuclides are included in a source term, the associated measurement or modeled uncertainty can be very important to the resulting uncertainty in the DRL.

Table 5.3-7. Sensitivity analysis results for the First Year Am-241 Deposition DRL for 1:1 Cs-137:Am-241 In Situ simulations.

Am-241 Deposition DRL, R^2 = 0.979		
Variable Name	**R^2**	**SRRC**
Resuspension Coefficient Multiplier	0.833	-0.912
Am-241 Inhalation Dose Coefficient Multiplier	0.950	-0.343
Breathing Rate, Activity Averaged, Adult Male	0.965	-0.126
Weathering Coefficient Multiplier	0.978	0.112
Deposition External Dose Coefficient Multiplier	0.978	-0.022
Breathing Rate, Light Exercise, Adult Male	0.979	0.003
Ground Roughness Factor	0.979	-0.013
Am-241 Activity per Area	0.979	0.004
Deposition Velocity	0.979	-0.003
Cs-137 Activity per Area	0.979	0.000
Cs-137 Inhalation Dose Coefficient Multiplier	0.979	0.000
Plume External Dose Coefficient Multiplier	0.979	0.000

Table 5.3-8. Sensitivity analysis results for the First Year Am-241 Deposition DRL for 1:1 Cs-137:Am-241 NARAC Complex simulations.

Am-241 Deposition DRL, R^2 = 0.842		
Variable Name	**R^2**	**SRRC**
Resuspension Coefficient Multiplier	0.626	-0.789
Am-241 Inhalation Dose Coefficient Multiplier	0.715	-0.299
Am-241 Air Concentration Multiplier	0.768	0.229
Cs-137 Air Concentration Multiplier	0.821	-0.229
Breathing Rate, Activity Averaged, Adult Male	0.832	-0.105
Weathering Coefficient Multiplier	0.841	0.095
Deposition External Dose Coefficient Multiplier	0.842	-0.035
Ground Roughness Factor	0.842	-0.009
Breathing Rate, Light Exercise, Adult Male	0.842	0.000
Cs-137 Inhalation Dose Coefficient Multiplier	0.842	0.000
Plume External Dose Coefficient Multiplier	0.842	0.000
Deposition Velocity	0.842	-0.007

5.4. Default vs. Mean

An interesting comparison in the context of using uncertainty analyses to inform protective action decisions is the comparison of the "default" or once-through result that CM currently uses on its data products versus the mean of the 10,000 simulations from the uncertainty analysis. In the FY17 analysis, it was noted that the mean of the NARAC-based Cs-137 Deposition DRL distribution was twice the default, implying that the default was conservative (i.e., the default allows half the activity on the ground to meet the DRL compared to the mean).

For all 45 sets of results generated in the FY18 analyses, the mean Deposition DRLs were greater than default, despite the mean Total DP sometimes being greater than the default Total DP. Comparing the single-radionuclide In Situ Cs-137 and Am-241 Total DP uncertainty results (Table 5.4-1 and Table 5.4-2) and NARAC Complex Cs-137 and Am-241 Total DP uncertainty results (Table 5.4-3 and Table 5.4-4), the NARAC Complex results always project a greater total dose on average than the default, whereas the In Situ results only do for Early Phase (AD) and First Year, which do not include the plume. However, the DRL distributions come out the same for both sets of results for a single radionuclide source term, as discussed in Section 5.3. Thus, even in the case of a NARAC-based mixture where the projected Total DP is much greater on average than the default, that uncertainty does not contribute to the DRL in the single-radionuclide case.

Table 5.4-1. Cs-137 Total DP (mrem) uncertainty results for single radionuclide In Situ simulations.

Scenario	Default	Mean	5th	50th	95th	Mean/ Default	95th/ 5th
Early Phase (TD)	9.97E+02	6.51E+02	2.49E+02	4.87E+02	1.57E+03	0.65	6.32
Early Phase (AD)	9.99E+02	9.93E+02	5.67E+02	9.44E+02	1.59E+03	0.99	2.80
First Year	2.00E+03	1.90E+03	1.10E+03	1.81E+03	3.00E+03	0.95	2.73

Table 5.4-2. Am-241 Total DP (mrem) uncertainty results for single radionuclide In Situ simulations.

Scenario	Default	Mean	5th	50th	95th	Mean/ Default	95th/ 5th
Early Phase (TD)	1.00E+03	6.48E+02	87.5	3.70E+02	2.06E+03	0.65	23.6
Early Phase (AD)	1.00E+03	3.41E+03	83.9	1.03E+03	1.35E+04	3.42	161
First Year	2.00E+03	6.80E+03	1.75E+02	2.06E+03	2.69E+04	3.41	154

Table 5.4-3. Cs-137 Total DP (mrem) uncertainty results for single radionuclide NARAC Complex simulations.

Scenario	Default	Mean	5th	50th	95th	Mean/ Default	95th/ 5th
Early Phase (TD)	9.97E+02	2.30E+04	4.57E+02	6.55E+03	8.86E+04	23.1	194
Early Phase (AD)	9.99E+02	4.98E+04	6.02E+02	1.15E+04	1.97E+05	49.8	327
First Year	2.00E+03	9.54E+04	1.16E+03	2.20E+04	3.72E+05	47.7	320

Table 5.4-4. Am-241 Total DP (mrem) uncertainty results for single radionuclide NARAC Complex simulations.

Scenario	Default	Mean	5th	50th	95th	Mean/ Default	95th/ 5th
Early Phase (TD)	1.00E+03	1.91E+04	3.05E+02	4.92E+03	7.28E+04	19.1	239
Early Phase (AD)	1.00E+03	1.63E+05	2.76E+02	1.25E+04	5.95E+05	163	2154
First Year	2.00E+03	3.24E+05	5.72E+02	2.50E+04	1.18E+06	162	2064

As noted in Section 5.2, deposition velocity is the most important input to the Deposition DRL when the plume is included (Early Phase (TD)), and it is positively correlated with the DRL, as shown in the right scatter plot in Figure 5-7. Deposition velocity is also the most important input to the Cs-137 Total DP, but is negatively correlated. This is shown in the left scatter plot in Figure 5-7. As deposition velocity increases, more material is deposited on the ground and less is available in the air to cause plume inhalation dose. The scatter plots show that deposition velocity is skewed to be much greater than the default of 0.003 m/s. This is what causes the Deposition DRL to be about two times greater on average than the default, as shown in Table 5.2-1.

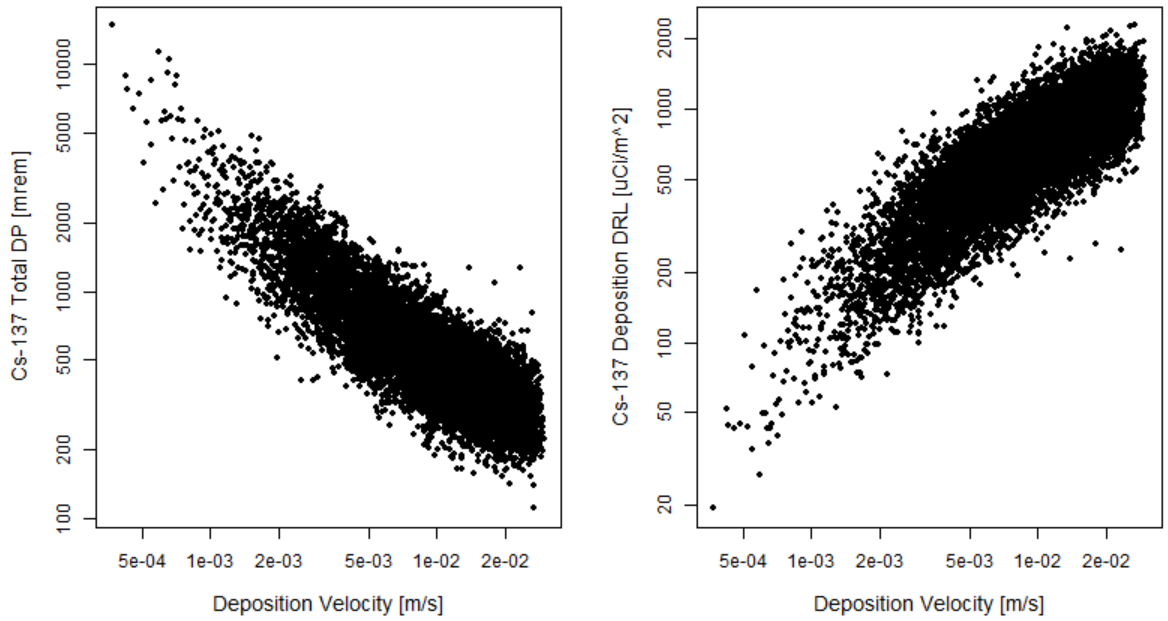

Figure 5-7. Scatter plots for the Cs-137 Total DP (left) and Cs-137 Deposition DRL (right) as a function of deposition velocity for the single-radionuclide Early Phase (TD) In Situ scenario.

For the Early Phase (AD) time phase where the plume is excluded, groundshine inputs are the most important to both the Cs-137 Deposition DRL (Table 5.2-3) and the Cs-137 Total DP. The most important input, the deposition external dose coefficient multiplier, has a similar relationship to the Total DP and DRL as deposition velocity did for the Early Phase (TD) time phase, though less strong. This is shown on the left for the Total DP and the right for the Deposition DRL in Figure 5-8. However unlike deposition velocity, the deposition external dose coefficient multiplier is much more evenly sampled. This causes the Total DP and Deposition DRL to be not much different than the default on average, as shown in Table 5.2-2.

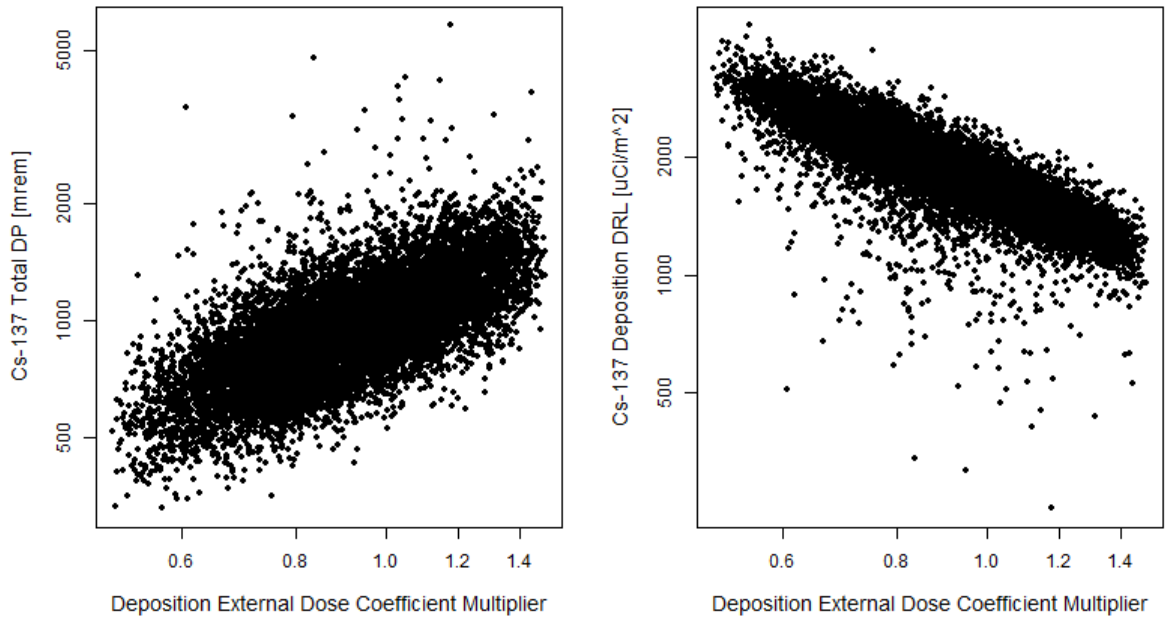

Figure 5-8. Scatter plots for the Cs-137 Total DP (left) and Cs-137 Deposition DRL (right) as a function of the deposition external dose coefficient multiplier for the single-radionuclide Early Phase (AD) In Situ scenario.

For the Early Phase (AD) time phase scenario when the source term consists of only Am-241, the resuspension coefficient multiplier is the most important input for both the Am-241 Deposition DRL (Table 5.2-7) and the Am-241 Total DP. Examining the scatter plots in Figure 5-9, the resuspension coefficient multiplier appears to be more heavily sampled to be less than the default of 1 despite the mean being 2.83, as documented in Table 5.1-1. This is due to the lognormal shape of the resuspension coefficient multiplier distribution. The left skew of the resuspension coefficient multiplier combined with its negative correlation with the Deposition DRL causes the Deposition DRL to be about three to four times greater on average than the default, as shown in Table 5.2-5.

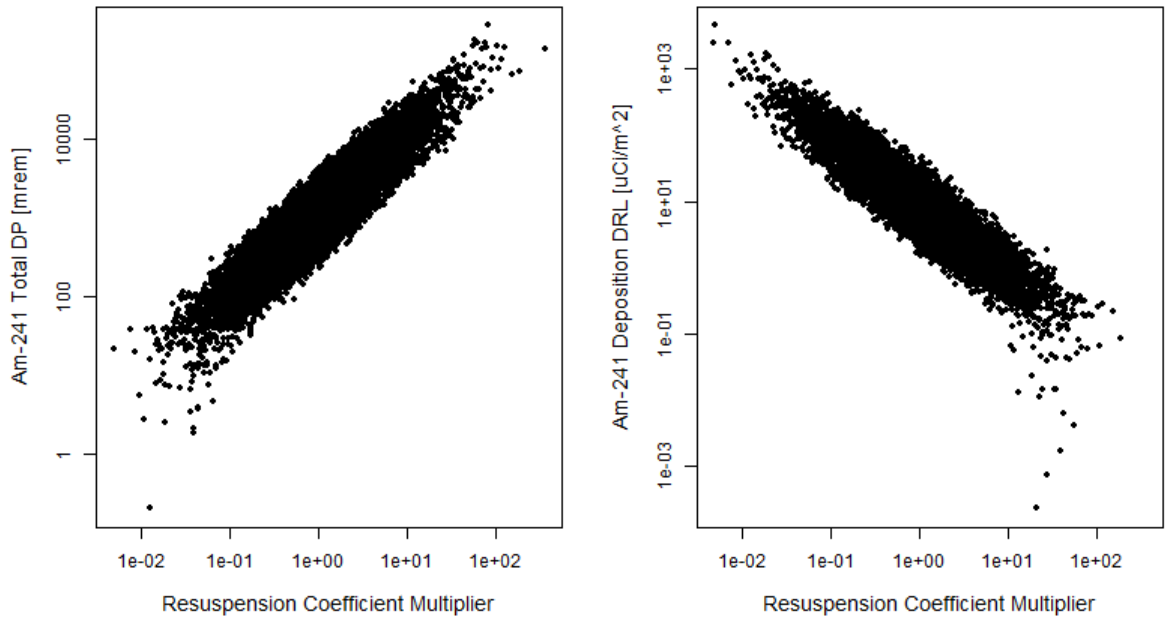

Figure 5-9. Scatter plots for the Am-241 Total DP (left) and Am-241 Deposition DRL (right) as a function of the resuspension coefficient multiplier for the single-radionuclide Early Phase (AD) In Situ scenario.

For the multiple-radionuclide scenarios based on In Situ, the sensitivity rankings for the DRLs are very similar to the Am-241-only results (for example, compare Table 5.3-5 and Table 5.3-7 to Table 5.2-8). This is because Am-241 drives the total dose in both scenarios and the measurement uncertainty associated with In Situ at the DRL is not large enough relative to the other inputs to play a significant role. However, this is not the case for the NARAC Complex results, for which the air concentration multiplier is an important contributor to DRL uncertainty (see Table 5.3-6 and Table 5.3-8). The scatter plots show that the air concentration multiplier is skewed such that is sampled to be greater than the default of 1, but with different relationships – the Cs-137 air concentration multiplier is positively correlated with the Cs-137 Deposition DRL and the Am-241 air concentration multiplier is negatively correlated with the Cs-137 Deposition DRL. The skew of the air concentration multiplier can also be seen in Figure 4-27. The skew of this input relative to the default causes Deposition DRL to be skewed to be greater than default on average.

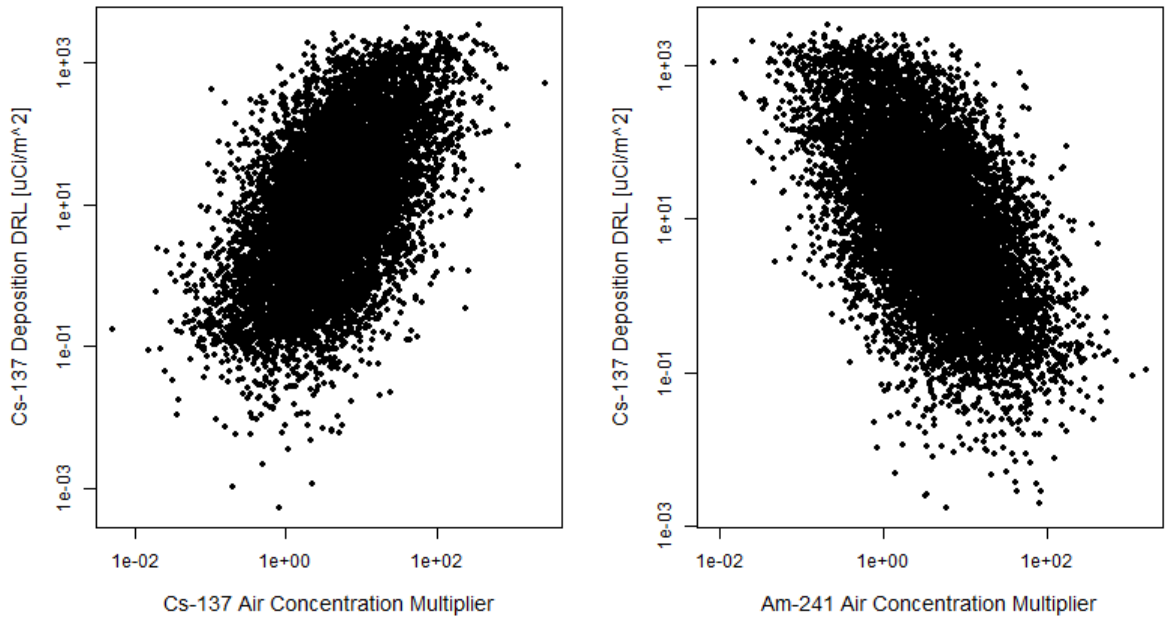

Figure 5-10. Scatter plots for the Cs-137 Deposition DRL as a function of the Cs-137 air concentration multiplier (left) and Am-241 air concentration multiplier (right) for the 1:1 Cs-137:Am-241 Early Phase (AD) scenario.

It is important to note that the consistent conservatism of the default Deposition DRL, a quantity frequently used for informing protective action decisions, has been observed only for the scenarios considered in this project. It is possible that a different combination of radionuclides in a different ratio could yield a case where the mean Deposition DRL does not show that the default once-through approach is conservative. Also, the distribution that was assigned to deposition velocity for this project is quite broad. A tailoring of this distribution for the scenario at hand, particularly with respect to particle size, could also cause different results. It is also important to note that the same "conservative" behavior was not always observed for the Integrated Air DRL results. However for sake of brevity and because these DRLs are less frequently used operationally, these results are not presented in this report.

Though CM might take comfort in the fact that the default once-through Deposition DRLs calculated today are often conservative compared to the mean DRLs from 10,000 simulations in the uncertainty analyses, it is important to consider more than just the radiological risk, i.e., there are potential risks associated with implementing a protective action such as evacuation. For this reason, choosing a conservative value, whether it is the default DRL or an extreme percentile of the distributions resulting from uncertainty analyses, might not be an appropriate value upon which to base protective action decisions.

5.5. Sampling Confidence Intervals

The table below shows the sampling CIs calculated about the mean for each output of interest for the NARAC Complex-based multiple-radionuclide Early Phase (AD) scenario. This scenario yielded the highest overall relative CI width for all simulations, meaning that this scenario represents the relatively worst case in terms of sampling CIs. The sample mean is also shown for reference for each output. The steps used to calculate the CIs are described in Section 3.3.3. These 95% CIs are interpreted as follows: 'there is a 95% confidence that the true value of the mean falls within this interval.'

The results given in Table 5.5-1 show that the estimate of the mean is well characterized by the 10,000 LHS samples used to quantify the uncertainty in each of the outputs of interest, even in this worst case scenario.

Table 5.5-1. Sampling CIs for the 1:1 Cs-137:Am-241 Early Phase (AD) NARAC Complex simulations.

Output Name	Lower Bound of 95% CI	Mean	Upper Bound of 95% CI
Dose Rate DRL [mrem/hr]	4.68E-01	4.93E-01	5.18E-01
Cs-137 Deposition DRL [μCi/m^2]	8.53E+01	8.99E+01	9.46E+01
Cs-137 Integrated Air DRL [μCi-s/m^3]	1.22E+04	1.32E+04	1.41E+04
Cs-137 Resuspension Inhalation DP [mrem]	1.44E+01	1.66E+01	1.90E+01
Cs-137 Groundshine DP [mrem]	2.17E+02	2.32E+02	2.51E+02
Cs-137 Total DP [mrem]	2.30E+02	2.49E+02	2.72E+02
Am-241 Deposition DRL [μCi/m^2]	2.19E+01	2.29E+01	2.41E+01
Am-241 Integrated Air DRL [μCi-s/m^3]	3.25E+03	3.49E+03	3.76E+03
Am-241 Resuspension Inhalation DP [mrem]	1.42E+05	1.67E+05	1.98E+05
Am-241 Groundshine DP [mrem]	8.62E+00	9.26E+00	9.99E+00
Am-241 Total DP [mrem]	1.44E+05	1.67E+05	2.00E+05
Mixture Total DP [mrem]	1.43E+05	1.68E+05	1.98E+05

6. SUMMARY

6.1. Summary of Overall Uncertainty Results

The results presented in this report show that the implementation of a probabilistic framework that can be used to characterize the uncertainty in CM data products was completed successfully for additional scenarios of interest. The inputs need to perform the analyses for the additional scenarios were assigned probability distributions that were based on data and/or expert opinion. These input distributions represent an attempt to broadly characterize input uncertainty and could be refined if needed using additional data or further expert input. The capability of the Dakota Error Analysis Tool in Turbo FRMAC© was expanded to allow Public Protection DRL calculations for any of the five default time phases and any mixture of radionuclides. Finally, statistical post-processing methods were used to characterize the uncertainty in the simulation results for the additional scenarios and to determine the sensitivity of uncertainty in simulation outputs to the uncertainty in the inputs.

The analyses for the additional scenarios confirmed that DRL calculations for single-radionuclide source terms are not influenced by the uncertainty associated with the activity per area or integrated air concentration assigned to the radionuclide of interest, and showed that this is not necessarily the case for calculations with multiple-radionuclide source terms.

The sensitivity analysis generally showed that deposition velocity is the most important contributor to DRL uncertainty in the case of a single-radionuclide source term DRL calculation that includes the plume. It is recommended that the uncertainty associated with particle size (assumed fixed for these analyses) be investigated further due to the importance of plume inhalation inputs to dose received in the Early Phase (TD) time phase. When the plume is not included, the DRL uncertainty is driven by the inputs to the primary dose pathway. For Cs-137, these are the groundshine inputs and for Am-241, these are the resuspension inhalation inputs. Because the resuspension inhalation inputs were assigned a broader probability distribution than the groundshine inputs, the Am-241 DRLs are more uncertain. These results can be used to motivate additional studies to better characterize these inputs and in turn reduce the overall uncertainty in the DRL results.

6.2. Incorporating Uncertainty Results in Data Products

Seven example data products were generated using the uncertainty analysis results. The products were generated using the following information:

- Source term of sufficient quantity to create an activity per area equal to the DRL at a hypothetical location downwind
- Real-world meteorology in the vicinity of terrain and spatially varying wind field
- Daytime population estimates

Each data product has a contour that corresponds to the 5th percentile (magenta), 95th percentile (yellow), and mean (orange) of the Deposition DRL distributions resulting from the uncertainty analyses. The default (red) contour is also included on each data product. The default is the result from a single Turbo FRMAC© simulation using FRMAC Assessment default values for the inputs (i.e., what is currently used for data products).

The data products can be interpreted as follows. Looking at the magenta contour for the 5th percentile, 95% of the simulation results have a Deposition DRL that is greater than the activity per area used for that contour. This means that 95% of the time, the contour could be drawn inside of the magenta shaded area if the contour was based on the DRL value calculated for a single simulation selected from the 10,000 samples. Further, 5% of the simulation results have a Deposition DRL that is less than the activity per area used for that contour. This means that 5% of the time the contour could be drawn outside the magenta shaded area if the contour was based on the DRL value calculated for a single simulation selected from the 10,000 samples. Decision makers may interpret this as meaning that there is a 5% chance that someone outside of the magenta shaded area could receive a dose that exceeds the PAG if a protective action is not taken.

Figure 6-1, Figure 6-2, and Figure 6-3 are data products for the Cs-137 only In Situ-based simulations for Early Phase (TD), Early Phase (AD), and First Year, respectively. Because the default Cs-137 Deposition DRL is smallest for the First Year, it results in the largest impacted area. Comparing the mean (orange) and default (red) contours on each data product, the default is more conservative than the mean because it impacts a larger area. However, the mean and default contours are significantly different for the Early Phase (TD), when the plume is included in the dose projection. In comparison, these contours results in about the same impacted area and population for the Early Phase (AD) and First Year time phases. Similarly, the contours for the tails of the Deposition DRL distribution (95th and 5th percentiles) are significantly different for the Early Phase (TD) data product compared to the products for the other two time phases. This reflects the results discussion included in Section 5.2, in which there is more uncertainty associated with a Cs-137 Deposition DRL that includes plume dose.

Figure 6-4, Figure 6-5, and Figure 6-6 are data products for the Am-241 only In Situ-based simulations for Early Phase (TD), Early Phase (AD), and First Year, respectively. The default Am-241 Deposition DRL is much smaller than the default Cs-137 Deposition DRL because it takes less activity of Am-241 to meet the PAG for a given time phase (see Table 2.5-1 for the default Deposition DRL values). This causes the impacted area from a dispersal of only Am-241 to be much larger than that from just Cs-137, regardless of uncertainty. Looking at the contours for the Am-241 data products, the default (red) is again conservative compared to the mean (orange), but by a much more significant amount than for the Cs-137 only scenarios. This is a visual demonstration of the distribution skewness described in Section 5.4. Additionally, the 5th percentile (magenta) contour in the Early Phase (AD) and First Year data products (Figure 6-4 and Figure 6-6) impacts an enormous area compared to any other contours on these data products. This demonstrates the breadth of the Am-241 Deposition DRL distribution, which is primarily due to uncertainty associated with the resuspension model, as discussed in Section 5.2. This breadth can also be seen by looking at the tails of the CDFs for the Early Phase (AD) and First Year time phases in Figure 5-2.

Figure 6-7 is a data product for the 1:1 Cs-137 and Am-241 In Situ based simulations for the Early Phase (TD) time phase. Essentially the same distribution resulted for the Cs-137 and Am-241 Deposition DRLs for this scenario, so each contour can be associated with either Cs-137 or Am-241. This data product looks very similar to the data product shown in Figure 6-4 for the Am-241 only scenario and vastly different from the data product shown in Figure 6-1 for the Cs-137 only scenario. The purpose of this comparison is to show how the presence of Am-241 in

a 1:1 ratio with Cs-137 not only drives down the Deposition DRL for Cs-137, but also increases the uncertainty associated with this DRL.

The data products included in this report illustrate the potential real-world implications of incorporating uncertainty analysis results into data products that inform protective action decisions. The location of a given percentile from a DRL distribution on a map, whether 5^{th}, 95^{th}, or some other meaningful statistical metric, differs significantly depending on scenario-specific source term and what is driving the total dose.

Example for Demonstration Only

CM Uncertainty Analysis Project
Cs-137 Early Phase (Total Dose) DRL

Hypothetical Surface Contamination from Deposited Radionuclides

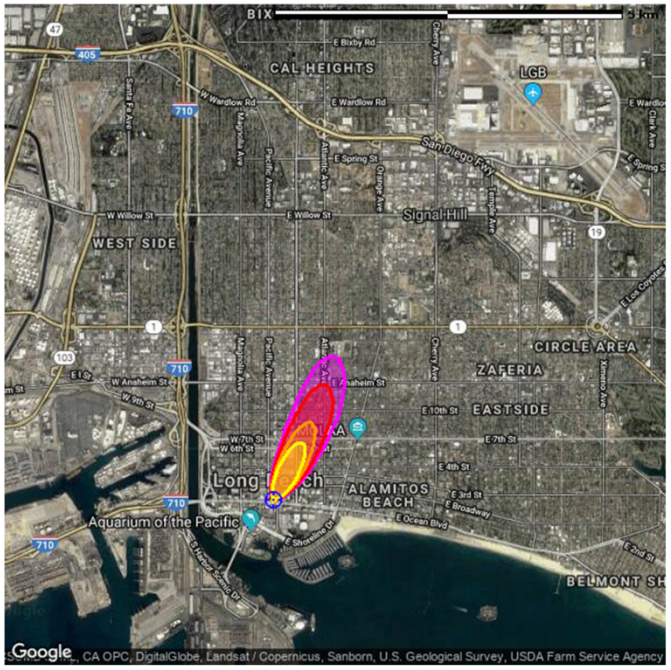

Effects and Actions

	Description	(uCi/m2) Extent Area	Population
	95th Percentile	>1,310 0.9km 0.2 km2	6,190
	Mean	>710 1.2km 0.3 km2	7,860
	Default	>330 1.8km 0.7 km2	14,000
	5th Percentile	>205 2.2km 1.1 km2	18,000

Areas and counts in the table are cumulative. Population Source = LandScan USA V1.0.

Effects or contamination at August 23, 2018 09:00 UTC
Release Location: 33.767536 N, 118.193010 W
Material: CS-137
Generated On: November 09, 2018 21:48 UTC
Model: ADAPT/PUFF/LODI
Comments: Hypothetical release starting at 08/22/2018 21:00:00 UTC for 1 sec met obs at 1 hr intervals from 08/22/2018 21:00:00 UTC to 08/23/2018 20:00:00 UTC

LLNL-MI-763469

Example for Demonstration Only

Figure 6-1. Data product displaying the Early Phase (TD) Cs-137 Deposition DRL distribution for In Situ single radionuclide simulations.

Example for Demonstration Only

CM Uncertainty Analysis Project
Cs-137 Early Phase (Avoidable Dose) DRL

Hypothetical Surface Contamination from Deposited Radionuclides

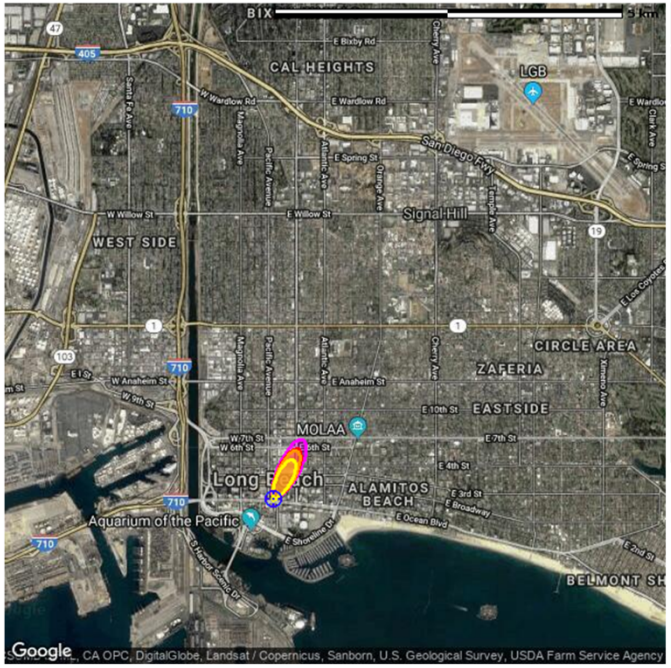

Effects and Actions

	Description	(uCi/m2) Extent Area	Population
	95th Percentile	>2,750 624m 106,741 m2	4,280
	Mean	>1,863 758m 143,686 m2	5,290
	Default	>1,700 793m 164,535 m2	5,580
	5th Percentile	>1,200 942m 222,412 m2	6,360

Areas and counts in the table are cumulative. Population Source = LandScan USA V1.0.

Effects or contamination at August 23, 2018 09:00 UTC
Release Location: 33.767536 N, 118.193010 W
Material: CS-137
Generated On: November 09, 2018 21:48 UTC
Model: ADAPT/PUFF/LODI
Comments: Hypothetical release starting at 08/22/2018 21:00:00 UTC for 1 sec
met obs at 1 hr intervals from 08/22/2018 21:00:00 UTC to 08/23/2018 20:00:00 UTC

LLNL-MI-763469

Example for Demonstration Only

Figure 6-2. Data product displaying the Early Phase (AD) Cs-137 Deposition DRL distribution for In Situ single radionuclide simulations.

Example for Demonstration Only

CM Uncertainty Analysis Project
Cs-137 First Year DRL

Hypothetical Surface Contamination from Deposited Radionuclides

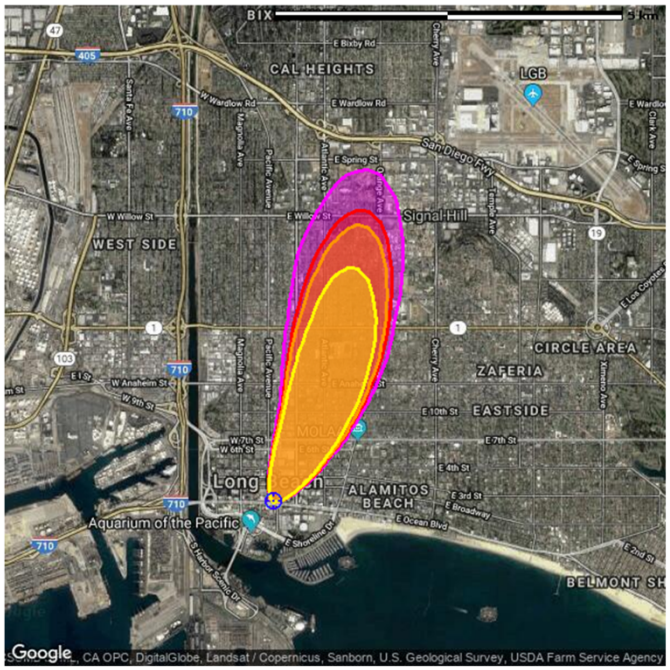

Effects and Actions

	Description	(uCi/m2) Extent Area	Population
	95th Percentile	>69.6 3.5km 2.8 km2	31,700
	Mean	>47.8 4.1km 3.9 km2	39,400
	Default	>42 4.4km 4.2 km2	40,800
	5th Percentile	>31.1 4.9km 5.7 km2	48,800

Areas and counts in the table are cumulative. Population Source = LandScan USA V1.0.

Effects or contamination at August 23, 2018 09:00 UTC
Release Location: 33.767536 N, 118.193010 W
Material: CS-137
Generated On: November 09, 2018 21:48 UTC
Model: ADAPT/PUFF/LODI
Comments: Hypothetical release starting at 08/22/2018 21:00:00 UTC for 1 sec
met obs at 1 hr intervals from 08/22/2018 21:00:00 UTC to 08/23/2018 20:00:00 UTC

LLNL-MI-763469

Example for Demonstration Only

Figure 6-3. Data product displaying the First Year Cs-137 Deposition DRL distribution for In Situ single radionuclide simulations.

Example for Demonstration Only

CM Uncertainty Analysis Project
Am-241 Early Phase (Total Dose) DRL

Hypothetical Surface Contamination from Deposited Radionuclides

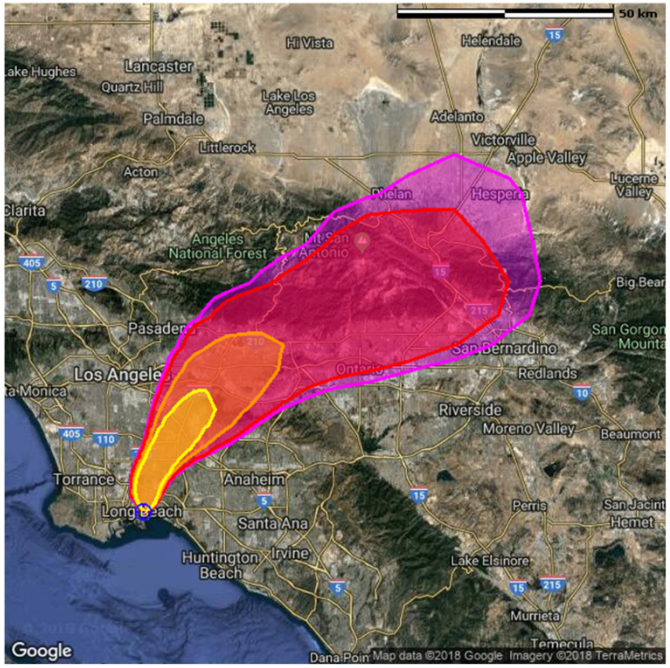

Effects and Actions

	Description	(uCi/m2) Extent Area	Population
	95th Percentile	>0.5 31.4km 211 km2	728,000
	Mean	>0.2 50.0km 621 km2	1.78E6
	Default	>0.05 99.8km 2,410 km2	3.10E6
	5th Percentile	>0.03 114km 3,331 km2	3.51E6

Areas and counts in the table are cumulative. Population Source = LandScan USA V1.0.

Effects or contamination at August 23, 2018 09:00 UTC
Release Location: 33.767536 N, 118.193010 W
Material: AM-241
Generated On: November 06, 2018 20:19 UTC
Model: ADAPT/PUFF/LODI
Comments: Hypothetical release starting at 08/22/2018 21:00:00 UTC for 1 sec met obs at 1 hr intervals from 08/22/2018 21:00:00 UTC to 08/23/2018 20:00:00 UTC

LLNL-MI-763469

Example for Demonstration Only

Figure 6-4. Data product displaying the Early Phase (TD) Am-241 Deposition DRL distribution for In Situ single radionuclide simulations.

Example for Demonstration Only

CM Uncertainty Analysis Project
Am-241 Early Phase (Avoidable Dose) DRL

Hypothetical Surface Contamination from Deposited Radionuclides

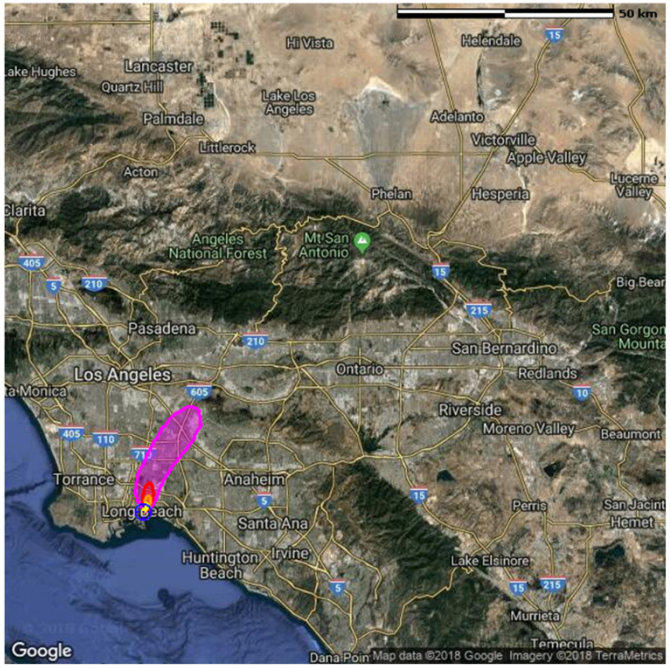

Effects and Actions

	Description	(uCi/m2) Extent Area	Population
	95th Percentile	>110 2.2km 1.1 km2	15,400
	Mean	>28.1 4.0km 3.7 km2	37,100
	Default	>8.7 6.9km 11.5 km2	90,700
	5th Percentile	>0.6 26.9km 152 km2	559,000

Areas and counts in the table are cumulative. Population Source = LandScan USA V1.0.

Effects or contamination at August 23, 2018 09:00 UTC
Release Location: 33.767536 N, 118.193010 W
Material: AM-241
Generated On: November 06, 2018 20:19 UTC
Model: ADAPT/PUFF/LODI
Comments: Hypothetical release starting at 08/22/2018 21:00:00 UTC for 1 sec met obs at 1 hr intervals from 08/22/2018 21:00:00 UTC to 08/23/2018 20:00:00 UTC

LLNL-MI-763469

Example for Demonstration Only

Figure 6-5. Data product displaying the Early Phase (AD) Am-241 Deposition DRL distribution for In Situ single radionuclide simulations.

Example for Demonstration Only

CM Uncertainty Analysis Project
Am-241 First Year DRL

Hypothetical Surface Contamination from Deposited Radionuclides

Effects and Actions

	Description	(uCi/m2) Extent Area	Population
	95th Percentile	>50.5 3.1km 2.1 km2	27,300
	Mean	>12.4 5.7km 7.2 km2	71,100
	Default	>4.2 10.7km 25.4 km2	140,000
	5th Percentile	>0.3 39.2km 350 km2	1.08E6

Areas and counts in the table are cumulative. Population Source = LandScan USA V1.0.

Effects or contamination at August 23, 2018 09:00 UTC
Release Location: 33.767536 N, 118.193010 W
Material: AM-241
Generated On: November 06, 2018 20:19 UTC
Model: ADAPT/PUFF/LODI
Comments: Hypothetical release starting at 08/22/2018 21:00:00 UTC for 1 sec met obs at 1 hr intervals from 08/22/2018 21:00:00 UTC to 08/23/2018 20:00:00 UTC

LLNL-MI-763469

Example for Demonstration Only

Figure 6-6. Data product displaying the First Year Am-241 Deposition DRL distribution for In Situ single radionuclide simulations.

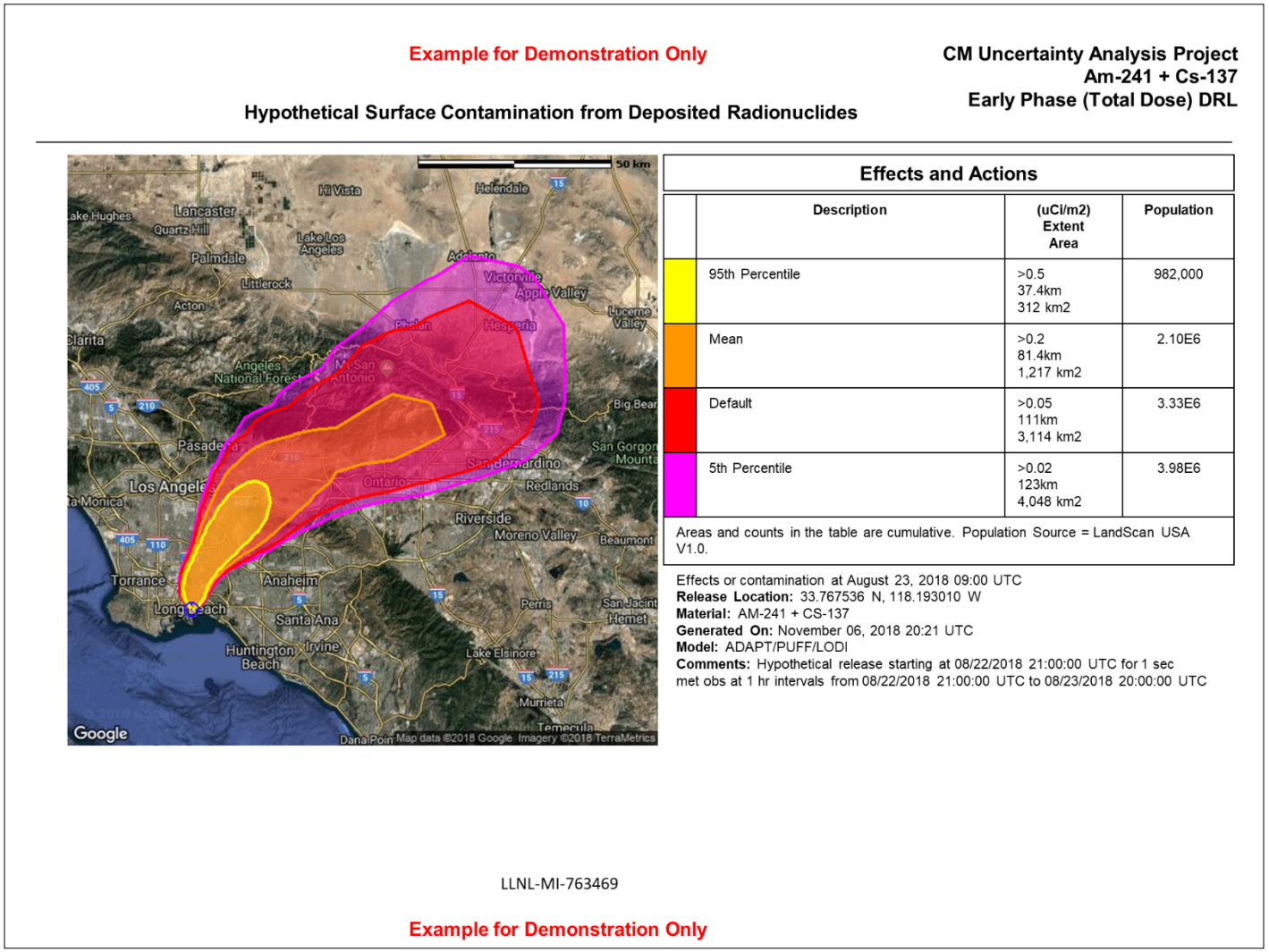

Figure 6-7. Data product displaying the Early Phase (TD) Deposition DRL distribution for 1:1 Cs-137:Am-241 In Situ simulations.

6.3. Implications & Future Work

The probabilistic framework developed for this project in FY17 was used to analyze additional scenarios of interest in FY18 in an effort to better understand uncertainty analysis results and their potential impact on informing protective action decisions. As the scope of the project is focused on the development of methods for characterizing uncertainty in CM data products, the explanations provided that link uncertainty analysis results to the physics of the problem could be further expanded in future work.

The FY18 analyses for the scenarios that considered a 1:1 mixture of Cs-137 and Am-241 showed that when multiple radionuclides are included in a source term, the associated measurement or modeled uncertainty can be very important to the resulting uncertainty in the DRL. These results can be used to motivate future studies to better understand measurement uncertainty, including characterizing this uncertainty for complex mixtures, determining thresholds at which measurement uncertainties contribute significantly to overall uncertainty in DRL calculations, and recommending monitoring measurements or sample collections and analyses that will reduce these uncertainties.

The statistical methods and tools used to both generate simulation inputs and to perform uncertainty and sensitivity analyses may need to be adapted to adequately analyze the results of increasingly complex scenarios and data products. Additional sampling techniques, such as importance sampling, may be useful if more information is needed in portions of the input space or output space (i.e., extreme high or low percentiles of input or output distributions). As the uncertainties in the inputs and the relationships between these uncertainties and the uncertainties in the outputs become more complex, additional regression techniques that capture additional types of input/output relationships, as well as conjoint relationships between inputs, may need to be added to the suite of tools used to complete the sensitivity analysis portion of the post-processing. This will be explored further in FY19.

The potential for implementation of uncertainty quantification calculations in a real-world response must also be studied further. The current implementation of these calculations in Turbo FRMAC© executes the simulation for each sample one after the other; parallelization of these calculations would help to increase the calculation speed for a probabilistic analysis of a given scenario. However, the bulk of the effort required to run a comprehensive probabilistic analysis is in the definition of the input distributions that will be used to generate input samples. These input distributions may need to be changed based on the release scenario, information and data collected in the field as a response is happening, etc. A feasibility study will be performed in FY19 to investigate the level of effort required to provide these input distributions for users. Because current functionality requires operation of separate statistical pre- and post-processing tools to perform full uncertainty analyses, the feasibility study will also investigate the effort required to integrate these tools into Turbo FRMAC© in the future. The result of the feasibility study will inform the path forward for integrating uncertainty capabilities and results into the public protection decision-making process.

The FY17-18 project demonstrated that probabilistic dose assessment calculations made for scenarios with increased complexity using CM tools are possible; however, the interpretation and use of uncertainty analysis results in the operational public protection context still needs to be addressed. The probabilistic framework developed for this project enables CM to generate DRL

values for any percentile of interest for use as contours on CM data products. It is yet to be determined what is considered an acceptable amount of uncertainty in the DRLs used to inform protective action decisions. Additionally, it would be prudent to consider the non-radiological hazards and socioeconomic risks associated with implementing protective actions such as evacuation and relocation. The discussions needed to determine a proposed default approach for using uncertainty analysis results in the public protection decision-making process are also planned for FY19.

7. REFERENCES

[1] *Uncertainty Analysis of Consequence Management (CM) Data Products,* SAND2018-0329, Sandia National Laboratories, Albuquerque, NM, 2018.

[2] *PAG Manual: Protective Action Guides and Planning Guidance for Radiological Incidents*, EPA-400/R-17/001, U.S. Environmental Protection Agency, Washington, DC, January 2017.

[3] Fulton, J., et al., "Turbo FRMAC© Assessment Software Package," Sandia National Laboratories, Albuquerque, NM, 2018.

[4] *Federal Radiological Monitoring and Assessment Center (FRMAC) Assessment Manual, Volume 1 Overview and Methods*, SAND2017-7122 R, Sandia National Laboratories, Albuquerque, NM, 2017.

[5] Metropolis, N., and S. M. Ulam, "The Monte Carlo Method," *Journal of the American Statistical Association*, Vol. 44, pp. 335-341, 1949.

[6] Helton, J.C, Johnson, J.D., Sallaberry, C.J., and Storlie, C.B. "*Survey of Sampling-Based Methods for Uncertainty and Sensitivity Analysis."* Sandia Report, SAND2006-2901, 2006.

[7] Adams, B.M., Bauman, L.E., Bohnhoff, W.J., Dalbey, K.R., Eddy, J.P., Ebeida, M.S., Eldred, M.S., Hough, P.D., Hu, K.T., Jakeman, J.D., Swiler, L.P., Stephens, J.A., Vigil, D.M., and Wildey, T.M, "*DAKOTA, A Multilevel Parallel Object-Oriented Framework for Design Optimization, Parameter Estimation, Uncertainty Quantification, and Sensitivity Analysis: Version 6.0 User's Manual,*" Sandia Technical Report SAND2014-4633, May 2014.

[8] R Core Team. "R: A Language and Environment for Statistical Computing." R Foundation for Statistical Computing. Vienna, Austria. URL http://www.R-project.org/. 2017.

[9] Efron, B., and Tibshirani, R. J. *An Introduction to the Bootstrap.* CRC Press, 1994.

[10] Eckerman, K., *Radiation Dose and Health Risk Estimation: Technical Basis for the State-of-the-Art Reactor Consequence Analysis Project*, Oak Ridge National Laboratory, Oak Ridge, TN, 2012.

[11] Taylor, B. N., & E., K. C., "Guidelines for Evaluating and Expressing the Uncertainty of NIST Measurement Results", Technical Note 1297, National Institute of Standards and Technology, 1994.

[12] Thuillier, R.H., "Evaluation of a Puff Dispersion Model in Complex Terrain" in *Journal of the Air & Waste Management Association*, 42:3, 290-297, 1992.

[13] Lucas, D.D., Simpson, M., Cameron-Smith, P., and Baskett, R.L., "Bayesian Inverse Modeling of the Atmospheric Transport and Emissions of a Controlled Tracer Release from a Nuclear Power Plant" in *Atmospheric Chemistry and Physics*, 17, 13521-13543, 2017.

[14] Molenkamp, C.R., *Prognostic Prediction of the Tracer Dispersion for the Diablo Canyon Experiments on August 31, September 2, and September 4, 1986*, UCRL-ID-136692, Lawrence Livermore National Laboratory, Livermore, CA, 1999.

[15] Skamarock, W.C., et al., *A Description of the Advanced Research WRF Version 3*, NCAR Technical Note NCAR/TN-475+STR, 2008.

[16] Ermak, D.L., and Nasstrom, J.S., "A Lagrangian Stochastic Diffusion Method for Inhomogeneous Turbulence, *Atmospheric Environment*, 34, 1059-1068, 2000.

[17] Nasstrom, J.S., Sugiyama, G., Leone, Jr., J.M., and Ermak, D.L., "A Real-Time Atmospheric Dispersion Modeling System," *Eleventh Joint Conference on the Applications of Air Pollution Meteorology*, Long Beach, CA, Jan. 9-14, 2000. American Meteorological Society, Boston, MA, 84-89.

[18] Larsen, S., Fischer, K, Walker, H., Foster, C., and Pobanz, B. *Rapid processing and utilization of field measurement data.* UCRL-ID-408227, Lawrence Livermore National Laboratory, Livermore, CA, 2008.

[19] Perice, B. "Criterion for the rejection of doubtful observations" in *The Astronomical Journal*, 45, 2, 161-165, 1852.

[20] Gould, B.A., "On Peirce's criterion for the rejection of doubtful observations, with tables for facilitating its application," in *The Astronomical Journal*, 83, 4, 81-87, 1855.

[21] Ross, S.M., "Peirce's criterion for the elimination of suspect experimental data," in *Journal of Engineering Technology*, 2003.

[22] Dardis, C. "Package 'Peirce'". https://r-forge.r-project.org/scm/viewvc.php /*checkout*/pkg/Peirce/Peirce-manual.pdf?root=peirce. September 7. 2012. Accessed July 25, 2018.

DISTRIBUTION

1 Lawrence Livermore National Laboratory
Attn: Jessica Osuna
P.O. Box 808, L-103
Livermore, CA 94551

1 Remote Sensing Laboratory – Nellis
Attn: Colin Okada
P.O. Box 98521
M/S RSL-47
Las Vegas, NV 89193-8521

1	MS0828	Aubrey Eckert-Gallup	1544
1	MS0828	Angel Urbina	1544
1	MS0791	Lainy Cochran	6631
1	MS0791	Brian Hunt	6631
1	MS0791	Terry Kraus	6631
1	MS0791	Art Shanks	6631
1	MS0899	Technical Library	9536 (electronic copy)


Sandia National Laboratories